A Dissertation for the Degree of Doctor of Philosophy

The role of IL-1 and MyD88 signal for protective immunity against pathogenic bacteria infection

병원성 세균 감염시 방어면역을 위한 IL-1 과 MyD88 신호의 역할

2013년 2월

서울대학교 대학원

수의학과 해부세포생물학 전공

양 형 준

The role of IL-1 and MyD88 signal for protective immunity against pathogenic bacteria infection

By

Hyungjun Yang

February 2013

The College of Veterinary Medicine

The Graduate School

Seoul National University

The role of IL-1 and MyD88 signal for protective immunity against pathogenic bacteria infection

By

Hyungjun Yang

Advisor: Prof. Je Kyung Seong, DVM, MS, PhD

A dissertation submitted to the faculty of Graduate School of Seoul National University in partial fulfillment of the requirements for the degree of Ph. D.

February 2013

The College of Veterinary Medicine

The Graduate School

Seoul National University

The role of IL-1 and MyD88 signal for protective immunity against pathogenic bacteria infection

Hyungjun Yang

(Supervised by Prof. Je Kyung Seong)

Abstract

Every organism has armed itself with the immune system for the protection against the infection of various pathogens. The host tried to recognize and to distinguish non-self organism for the initiation of protective immunity. The representative innate sensor is Interleukin 1 receptor (IL-1R)/ Toll-like receptor (TLR) superfamily whish is primitive signal for the induction of immune responses when the host is infected with various pathogens. In this study, I aimed to clarify the role of innate signal in the protective immunity against bacterial infection.

In the first part of this study, interleukin (IL)-1 is a well-known cytokine for the initiation of innate immunity together with TNF-α in bacterial infection. However, the underlying mechanism of IL-1 on the respiratory infection is not fully elucidated. It was studied how IL-1 signal contributes to the host defense pathway against *Streptococcus (S.) pneumoniae* in a mouse model. IL-1R$^{-/-}$ mice showed high mortality, local cytokine storm, and substantial infiltrates in the lower respiratory tract after intratracheal challenge with *S. pneumoniae*. The IL-1-

deficient condition did not suppress the propagation of bacteria in the lung, although the recruitment and the bacteria-killing ability of neutrophils ($CD11b^{+}Ly6C^{+}Ly6G^{+}$) were not defective compared with wild-type mice. Unexpectedly, it was found that the transcription of fibrinogen alpha and gamma genes were highly activated in the lungs of wild-type mice after *S. pneumoniae* infection while no significant changes were found in IL-$1R^{-/-}$ mice. Of note, synthesis of fibrinogen, which is crucial for clotting, in the lung in *S. pneumoniae* infection, was dependent on the IL-1-IL-6-Stat3 cascade. Treatment with recombinant fibrinogen improved survival and bacterial propagation in the IL-$1R^{-/-}$ mice and blockade of the coagulation pathway increased the susceptibility of wild-type mice to pneumococcal pneumonia. These findings suggest that IL-1 signaling leads to the synthesis of fibrinogen in the lung after *S. pneumoniae* infection and is followed by coagulation, which contributes to the control of bacterial infection in the pulmonary tract.

For the second part, the role of TLR signaling to link innate and adaptive immune systems has been one of controversial issues remained to be resolved. Here, it was determined whether MyD88-dependent TLR signals are required for the generation of B-cell responses during chronic *Salmonella* infection. Oral administration of recombinant attenuated *Salmonella* Typhimurium vaccine (RASV) strain in $MyD88^{-/-}$ mice resulted in chronic infection. Infection was accompanied by enlarged germinal centers and hypergammaglobulinemia with anti-double-stranded DNA (dsDNA)-specific Ab in sera, and the deposition of immune complexes in the kidneys, suggesting onset of autoimmunity. $CD4^{+}$ T cells expressing PD-1, CXCR5, ICOS, and IL-21 were dramatically increased in chronically-infected mice, indicating the expansion of follicular helper T (Tfh)-like cells. Of note, the depletion of $CD4^{+}$ T cells completely blocked the generation of polyclonal IgG Ab in sera after oral RASV challenge. Inflammatory myeloid cells expressing CD11b and Gr-1 accumulated in high numbers in the spleen of $MyD88^{-}$

$^{/-}$ mice. Interestingly, the blockade of PD-1 or ICOS significantly reduced the hypergammaglobulinemia and dsDNA-specific autoantibody production. Overall, these results suggest that Tfh-like cells in chronic bacterial infection trigger autoimmune hypergammaglobulinemia in a PD-1- and ICOS-dependent manner.

Keywords: IL-1, *S. pneumoniae*, pneumonia, innate immunity, coagulation, MyD88, *Salmonella*, Tfh, adaptive immunity, chronic infection, autoantibody, hypergammaglobulinemia

Student number: 2010-30458

CONTENTS

Summary of Abbreviation

ACRONYM	FULL NAME
Ab	Antibody
AIDS	Acquired immune deficiency syndrome
BAFF	B-cell activating factor
BALF	Bronchoalveolar lavage fluid
BSA	Bovine serum albumin
B6	C57BL/6
B. burgdorferi	*Borrelia burgdorferi*
CD	Cluster of differentiation
CFU	Colony-forming unit
CXCL	C-X-C chemokine ligand
CXCR	C-X-C chemokine receptor
(c)DNA	(complementary) Deoxyribonucleic acid
dsDNA	Double stranded DNA
ELISA	Enzyme-linked immunosorbent assay
FACS	Fluorescence-activated cell sorting
FBS	Fetal bovine serum
Fga	Fibrinogen α gene
Fgb	Fibrinogen β gene
Fg g	Fibrinogen γ gene
GAS	Group A Streptococcus
GC	Germinal center

GM-CSF	Granulocyte-macrophage colony-stimulating factor
HRP	Horseradish peroxidase
H&E	Hematoxylin and eosin
IFN	Interferon
Ig	Immunoglobulin
IL	Interleukin
IL-1RAcp	IL-1 receptor accessory protein
IL-1Rrp2	IL-1 receptor-related protein-2
IL-1R$^{-/-}$	IL-1 receptor knockout mice
IRAK	IL-1 receptor-associated kinase
i.p.	Intraperitoneal(ly)
i.t.	Intratracheal(ly)
LPS	Lipopolysaccharide
LRR	Leucine-rich repeat
MACS	Magnetic-activated cell sorting
MCP-1	Monocyte chemotactic protein 1
MHC	Major histocompatibility complex
MIP-2	Macrophage inflammatory protein 2
MLN	Mesenteric lymph node
MyD88	Myeloid differentiation factor 88
NFkB	Nuclear factor kappa B
NLR	NOD-like receptor
NOD	Nucleotide-binding oligomerization domain-containing protein
PAMP	Pathogen-associated molecular pattern

PBS	Phosphate buffered saline
PCR	Polymerase chain reaction
PD-1(L)	Programmed cell death protein 1 (ligand)
PMN	Polymorphonuclear leukocytes
PP	Peyer's patches
PRR	Pattern recognition receptor
RASV	Recombinant attenuated *Salmonella* Typhimurium vaccine
(m)RNA	(messenger) Ribonucleic acid
RPMI	Roswell Park Memorial Institute medium
RT-PCR	Real-time polymerase chain reaction
SP	Spleen
S. pneumoniae	*Streptococcus pneumoniae*
Stat3	Signal transducer and activator of transcription 3
Tfh	Follicular helper T cell
TGFβ	Tumor growth factor β
Th	T helper
THY	Todd-Hewitt broth plus yeast extract
TIR	Toll/IL-1 receptor
TLR	Toll-like receptor
TNF	Tumor necrosis factor
TNFR1, 2	TNF receptor type 1, 2
TRIF	TIR domain-containing adapter-inducing interferon-β
trpG	Tryptophan G
WT	Wild type

Literature Review

I. Bacterial pathogenesis

1. *Streptococcus pneumoniae*

Streptococcus pneumoniae (*S. pneumoniae*) is a gram-positive, anaerobic bacterium. It is the common cause of bacterial pneumonia and bacterial meningitis [1]. Pneumococci consist of diverse serotype. Some of them are invasive and others are not [2]. The other strains employ the phase variation. They are usually colonized in nasopharynx of healthy people as commensal bacteria. When the hosts are in the immunocompromised status such as virus infection, they secrete more capsular components and invade into lower respiratory tract [3].

The pneumococcus can easily colonize in the nose. One third of children have one serotype of pneumococcus. Also they are detectable in over 10% of the population including healthy adults who can act as a carrier to spread the bacteria in the community. Therefore the pneumococcus is classified as a community-acquired bacterium [4, 5].

Healthy hosts easily clear *S. pneumoniae* and they only experienced runny nose and sniffing. But unhealthy or certain condition such as baby, old, aging, AIDS. Cancer therapy can make this pathogen virulent and they can invade into the low respiratory tract such as lung [4, 6].

The hosts have the machinery to recognize the pneumococcus. One of the well-known pattern recognition receptors (PRRs) is the toll-like receptors (TLRs). TLR2 binds to bacterial cell wall. TLR4 can detect the pneumolysin which bursts by autolysis of bacteria and attaches the host cell membrane to form the pore. TLR9 also has important role on detection of the infection by recognition of bacterial DNA [7]. These TLR signaling pathway has common adapter molecule which is myeloid differentiation

factor 88 (MyD88). MyD88 signal activates NFκB and initiates the inflammation [8] (Fig. 1).

In the inflammation against to pneumococci, there are crucial cells which are alveolar macrophage and neutrophils. Alveolar macrophages are tissue resident macrophages and they recognize the bacteria at the initiatory stage and kill them by phagocytosis [9]. Neutrophils are subsequently recruited into the lung. They are major phagocytes to clear the pneumococci [10].

2. *Salmonella* Typhi (-murium)

Salmonella Typhi (-murium) is Gram-negative intracellular bacteria. It is the cause of typhoid fever. It is very common in the developing countries. It causes an epidemic because contaminated water can inflict illness to those who drink this water. Epidemiologist calculated the typhoid fever occurred over 21 million illnesses and 216,510 deaths in 2000[11]. *Salmonella* Typhi is restricted to human. For animal study, *Salmonella* Typhimurium strain was discovered and it is an adaptive strain for mice and has similar pathogenesis to *Salmonella* Typhi in human. They invade from intestinal rumen to the host through M cells which are abundant in Peyer's patches (PP) and also located in solitary intestinal lymphoid tissues on the intestinal epithelia using type III/IV secretion system [12, 13]. Then they move to mesenteric lymph node (MLN), which is the draining lymph node for the intestine, as freely by itself or with DC containing bacteria. They spread systemically to spleen, liver or kidney. Thus the major features in salmonellosis are fever and splenomegaly [14]. The infected host can induce immune responses sensing bacterial components. TLR-2, -4, -5, -9 recognized lipoprotein, lipopolysaccharide (LPS), flagellin and bacterial DNA, respectively [8]. In addition, S. Typhi can exist in the cytosolic compartment of the cell and it can activate the

Nucleotide-binding oligomerization domain-containing protein 1 (NOD1) and NOD2, which can recognize the bacterial components such as peptidoglycan [15] (Fig. 2).

II. IL-1R/TLR superfamily

1. IL-1R/TLR superfamily

The term of "Interleukin-1 receptor (IL-1R)/ Toll-like receptor (TLR) superfamily" was defined in 1998 [16]. Both IL-1Rs and TLRs have an important role in the innate immunity. They are different of extracellular domains. IL-1R family has three immunoglobulin domains in the extracellular part. TLR family has leucine-rich repeats (LRRs). However, both receptor families have homologous cytosolic domain which is Toll/IL-1 Receptor (TIR) domain [16]. Furthermore, IL-1R and TLRs except TLR3 share the signaling adaptor molecule, which is myeloid differentiation factor 88 (MyD88) [17]. Therefore, the signal transduction of both receptors activate nuclear factor-κB (NFκB) through IL-1 receptor-associated kinase 4 (IRAK4) and IRAK1 [18]. Finally, NFκB induce the expression of numerous genes for the initiation of inflammation-associated genes (Fig. 3).

2. IL-1 and IL-1 receptor family

IL-1 was first isolated about thirty years ago from macrophages [19]. It has been studied as the initiative factor for inflammation. Recently, IL-1 arose as a hot issue in the immunology field followed by the discovery of inflammasome, which is a machinery to transform the inactive form of pro-IL-1β to active form of IL-1 β and IL-18 also [20]. There are two forms of IL-1, IL-1α and IL-1 β, which share the receptor and activities [21]. IL-1 is produced mainly by macrophages and by other myeloid cells. However, it signals to almost all kinds of cell types including lymphocytes and epithelia through

heterodimeric receptor consisted of type I IL-1 receptor (IL-1RI) and IL-1 receptor accessory protein (IL-1RAcP) [21, 22]. There are other cytokines which are homologous to IL-1, IL-18 and IL-33. IL-18 and IL-33 are recognized by IL-1R-like receptors, IL-18 receptor and IL-1 receptor-related protein-2 (IL-1Rrp2; which is also known as T1/ST2), respectively (Fig. 3) [23]. The roles of IL-18 and IL-33 are different from IL-1. IL-18 is important in cell-mediated immunity like Th1 type immunity [24]. And IL-33 is known as Th2 type immunity for B cell responses [25].

3. TLR and MyD88

For recent several decades, immunologists were concerned about how the pathogens can be recognized separating the host cells. Someone looked for the bacterial specific sensory machinery to identify pathogen-associated molecular pattern (PAMP). Others insisted the host derived danger signals which emitted by damaged host cells. The various sensors, also called as pattern recognition receptors (PRRs) are discovered. Toll-like receptor family (TLR) is the most well-defined PRR.

TLR2 is a key receptor to recognize the bacterial cell wall which is first combined with CD14 [26]. TLR2 acts as homodimer or heterodimer together with TLR1 or TLR6. TLR4 is homodimeric receptor specific to LPS. TLR5 is a plasma membrane receptor and specific to flagellin [8]. There are endosomal receptors that are TLR3, 7(8) and 9 [27]. These endosomal TLRs recognize bacterial or viral amino acids such as viral dsRNA, viral ssRNA and CpG DNA, respectively. MyD88 is a common adaptor molecule for TLRs except TLR3. TLR3 has TIR-domain-containing adapter-inducing interferon-β (TRIF) as an adaptor molecule. TLR4 has both adaptor molecules MyD88 and TRIF [8].

III. Helper T cell

1. Subsets of helper T cell

T cell lineage is classified according to the type of T cell receptor (TCR). For instance, αβT cells have a heterodimeric receptor which consists of α and β chain. Likewise, γ and δ chain make γδT cells. The αβT cells are categorized by the expression of CD4 or CD8 that are co-receptors for major histocompatibility complex (MHC) molecules. $CD4^+$ T cells are named helper T cells (Th) because they help other type of cells such as B cells. Naïve Th cells are activated and progress clonal expansion when they encounter DC presenting peptide MHC class II complex which binds to T cell receptor (TCR). Activated Th cells are differentiated into various subsets which are determined by costimulatory molecules and cytokines from antigen presenting cells (APCs). Type I helper T cells (Th1) are developed by IL-12 and IFN-γ. The transcription factor, T-bet leads Th1 to produce IFN-γ for helping protective immunity against intracellular pathogen [28, 29]. Type II helper T cells (Th2) are induced by the Th2 master regulator GATA-3. Th2 cells secrete IL-4, IL-5, IL-13 and support B cells to produce antibodies for extracellular pathogens [30]. The master regulators T-bet for Th1 and GATA-3 for Th2 inhibit reciprocally to solidify the direction of development [31]. Th17 is recently defined as a subset of Th cells [32]. Th17 is termed according to the production of IL-17. TGF-β and IL-6 induce the differentiation of Th17. Particularly, IL-6 promotes RORγt which is distinct transcription factor for Th17 [33]. For immune homeostasis, the initiation of inflammation is not only important, but the regulation of immune responses is also necessary. Regulatory T cells (Treg) exist to suppress other effector cells by inhibitory molecules and the production of IL-10. Treg cells are generated by TGF-β signal. The characteristic transcription factor of Treg is Foxp3 which blocks RORγt for Th17 and vice versa (Fig. 4) [34, 35].

2. Follicular helper T cell

Follicular helper T cell (Tfh) is a recently defined subset of helper T cell lineage [36]. The distinctive character of Tfh is its location in B cell region, not in extrafollicular T cell region. The translocation of Tfh is responsive to CXCL13, which is abundant in B cell follicles, through the expression of CXCR5 that is the receptor for CXCL13 and expressed on B cells and Tfh cells [31, 37]. The development of antigen-specific Tfh is strongly dependent on IL-6 and IL-21. IL-6 is able to produce IL-21through Stat3 in Th cells [38]. Induced IL-21 acts as an autocrine way to enhance the differentiation of naïve Th cells to Tfh [39, 40]. The distinguishable transcription factor of Tfh from other Th cell lineage such as Th1, Th2, Th17 and Treg is bcl-6 [41]. The function of Tfh is primarily to help B cell immunity for production of antibodies. For cognate interaction with B cells, Tfh cells express ICOS, OX40 and PD-1 on their surface. Those molecules bind to ICOSL, OX40L and PD-1L on B cells, respectively [42-45]. In addition, there are a number of evidences that Tfh is indispensable to germinal center formation. The inhibition of Tfh decreased the number of B cell follicles and germinal centers (Fig. 4) [31, 46, 47].

IV. Coagulation vs bacteria

1. Host

Coagulation system primarily exists to prevent of leakage of blood when injury of blood vessels occurs. Several factors from factor I to factor XII and tissue factor are associated in clotting formation. Those factors finally activate prothrombinase complex which cleaves the active form of thrombin. Thrombin acts as enzyme to cleave fibrinogen to make fibrin [48]. Coagulation does not involve in blood clotting only, but in the immune system also. Fibrin networks in the clot can entrap bacteria to prevent the spread of invaded pathogen [49]. Fibrinogen also plays important roles in the

inflammatory response. It is able to alter leukocyte functions, including cell adhesion, migration, and cytokine expression [48]. Mice lacking the fibrinogen binding motif ($\alpha_M\beta_2$/Mac-1) have severely compromised inflammatory responses to bacterial infection that is by caused by their inability to inhibit the binding of leukocytes to fibrinogen [50]. Further, the formation of complexes between fibrinogen and bacteria activate neutrophil recruitment, which may induce vascular leakage [51].

2. Bacteria

As the host has equipped itself with defense system against pathogens, bacteria too have developed means to circumvent host immunity. Group A Streptococcus (GAS) is known to have various weapons to escape host clotting [48]. For example, streptokinase produced by streptococcus activates plasminogen, which transforms to plasmin for fibrinolysis [52, 53]. Further, the M protein produced by GAS forms complexes with the host fibrinogen enabling resistance to phagocytosis [54]. Other bacteria, including *Staphylococcus aureus* and *E. coli*, also can escape the host coagulation system by using staphylokinase or flagella, respectively [55, 56]. However, *S. pneumoniae* has not been reported to avoid blood clotting despite its phylogenetic similarity to GAS and *S. aureus*. The efficacy of coagulation is thought to be pathogen-dependent and the murine pneumococcal pneumonia model is ideal for studying the relationship between bacteria and host coagulation in the respiratory tract.

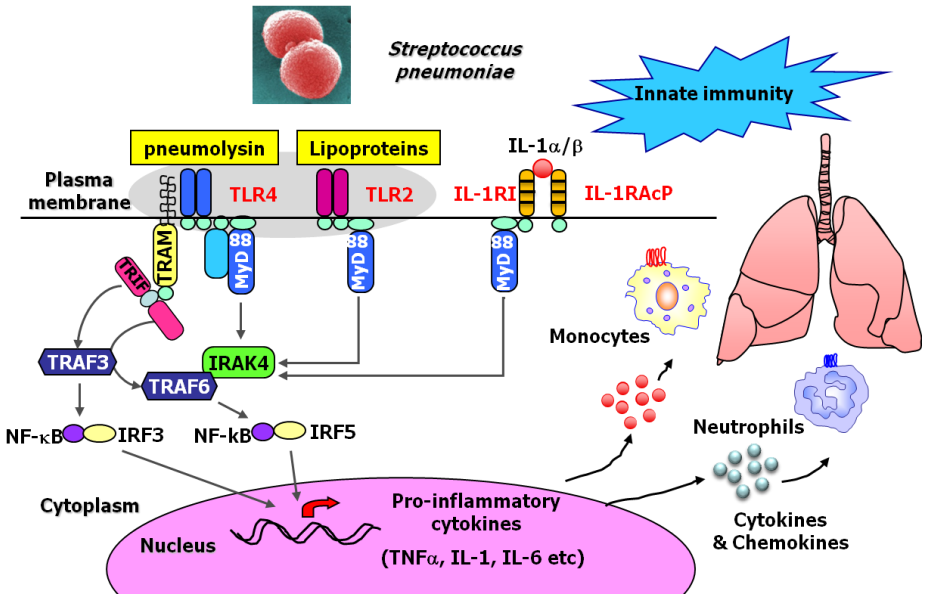

Figure 1. Bacterial cell wall components (e.g. lipoproteins) and pneumolysin of *Streptococcus pneumoniae* are recognized by TLR2 and TLR4, respectively. The activated TLR signals through the adaptor molecules, MyD88 or TRIF. The signaling pathways activate NFκB and translocation of NFκB into the nucleus NFκB acts as a transcription factor for pro-inflammatory genes including IL-1. IL-1 signaling also conducts the activation of NFκB. Produced inflammatory cytokines recruit neutrophils and monocytes into the infected site (e.g. lung).

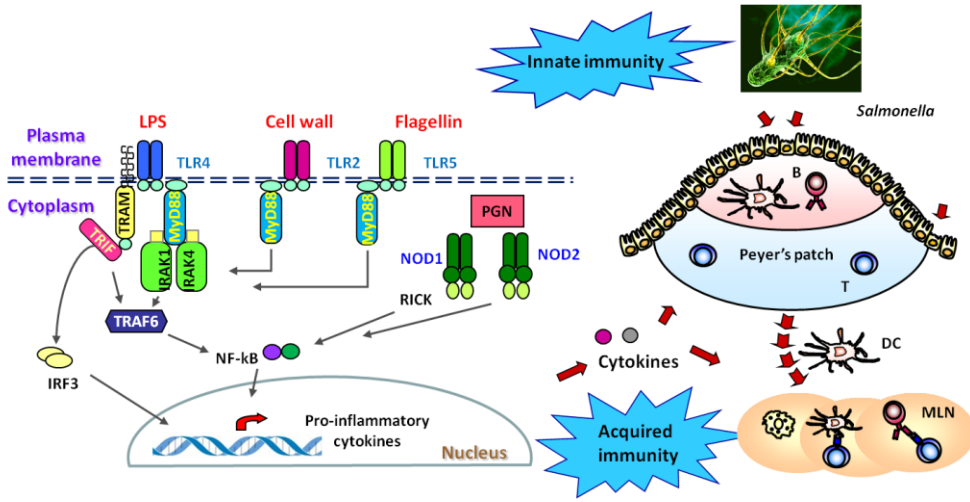

Figure 2. *Salmonella* invades by M cells in the gut. Several components of *Salmonella* bind to TLRs and other pattern recognition receptors (PRRs) such as NOD. Those PRRs induce pro-inflammatory cytokines. Dendritic cells (DCs) encountered *Salmonella* move to secondary lymph nodes and then create acquired immunity by presenting antigen to T and B cells in PP and MLN.

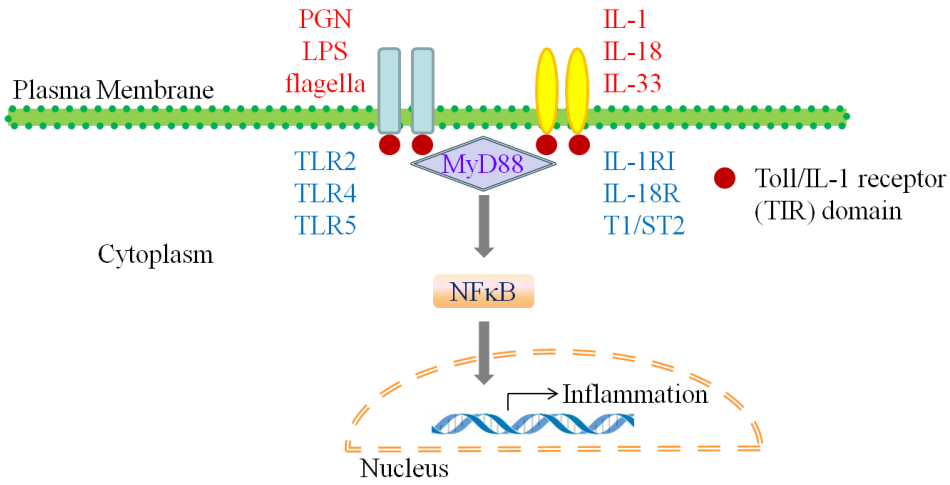

Figure 3. TLRs and IL-1R families have TIR domain in intracellular compartment of those receptors. MyD88 is a universal adaptor molecule of the IL-1R/TLR superfamily. MyD88 delivers the signal to activate NFκB. Active form of NFκB moves to nucleus and act as a transcription factor for inflammatory genes.

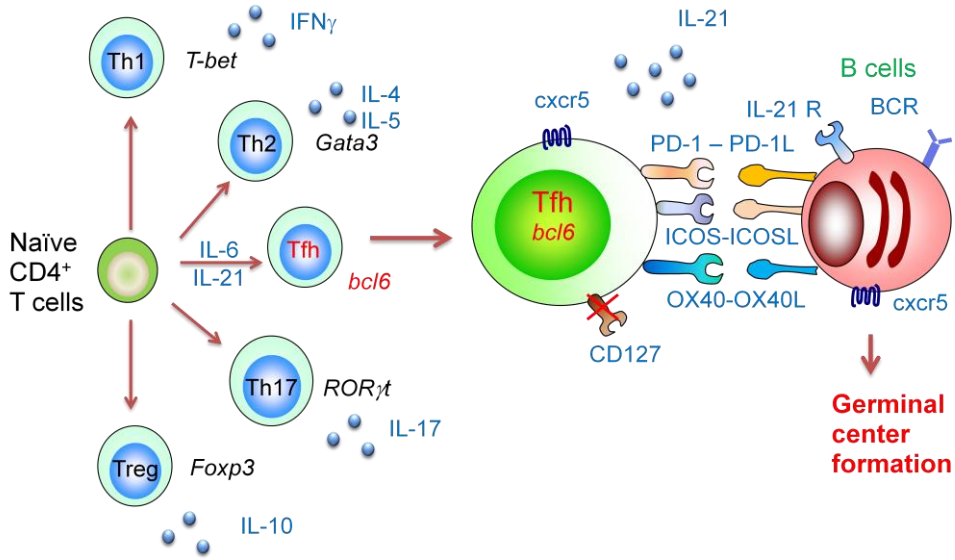

Figure 4. Tfh cells are differentiated by the cytokines (IL-6 and IL-21) and transcriptional repressor (bcl-6). The hallmarks of Tfh are the expression of CXCR5, PD-1, ICOS and OX40 and the loss of CD127. Tfh also secretes IL-21. Those features are important in the function of Tfh to activate B cells and to generate germinal centers.

General introduction

A normal person experiences numerous pathogens such as viruses, bacteria, fungi and parasites in his life. The host combats these invaders to keep sanitary and to protect the cells and tissues from destruction. Primary factors to overcome the infection are mechanisms to sense the pathogens. Toll-like receptor (TLR) is a representative receptor family in the series of pattern recognition receptors (PRRs). Thirteen different TLRs are reported currently in human and mouse. TLRs consisting of homodimer or heterodimer recognize various pathogen-associated molecular patterns (PAMPs). TLR signaling except TLR3 mainly conducts the universal adaptor molecule; Myeloid differentiation factor 88 (MyD88). The signals by MyD88 express inflammatory genes dependent on NFκB as a transcription factor. TNF-α and IL-1β are regarded as initiative cytokines for induction of inflammation. One of them, IL-1 signal, also accompanies MyD88 same as TLR signals. Therefore, IL-1 signal seems to mimic TLR signals to alert other cells that did not encounter pathogen. In the chapter I, the role of IL-1 signal for the protective immunity is clarified in the pulmonary infection with *Streptococcus pneumoniae*. Especially the highly conserved and primitive coagulation pathway is proposed to be a new member of innate immune responses in the bacterial pneumonia.

Innate and adaptive immune responses are defined separately by several features such as responsive time, participating cells and their products. However, they are certainly connected bidirectionally in some aspects. The sensory machineries in innate immunity are important to activate antigen presenting cells (APC) such as dendritic cells (DC). In reverse, Th17 cells play a role in the recruitment of neutrophils which are considered as an innate compartment. Another example is antibody-mediated

complement system which is called as classical pathway. In the chapter II, another possibility is suggested in which chronic infection of *salmonella* in the innate immune-deficient condition can affect the fate of adaptive immune responses. Additionally, the follicular helper T cell (Tfh) is implied as the underlying mechanism of autoantibody production in autoimmune diseases.

Chapter I.

Interleukin-1 promotes coagulation which is necessary for protective immunity in the lung against *Streptococcus pneumoniae* infection

I. Introduction

Streptococcus pneumoniae, a gram-positive anaerobic bacterium, is arguably the most common cause of pneumonia in the world. It has been described as "the captain of all the men of death" [6, 57]. Colonization with pneumococcus typically induces mild symptoms that are easily cleared in healthy people; however, when risk factors weaken the protective immunity (e.g., the patient's age, diabetes, and HIV infection) pneumococcus can cause serious diseases [6]. Pneumococcal pneumonia frequently arises after infection by a secondary pathogen such as influenza [58]. For instance, more than half of those who died during the 1918 Spanish flu pandemic (H1N1 influenza A) died after of secondary infection with pneumococcus [59]. Moreover, the more recent emergence of antibiotic-resistant pneumococci, termed 'superbacteria', makes patient treatment more difficult [60]. Therefore, alternative therapies are needed to enhance the immune system.

The recognition of *S. pneumoniae* by the host is mediated by various ways. For instance, pattern recognition receptors such as toll-like receptors (TLRs) are expressed on airway epithelia and alveolar macrophages [8]. The bacterial cell wall component is recognized by TLR2 and the pneumococcal toxin pneumolysin depends on TLR4 [61]. These TLRs trigger the activation of NFκB which, in turn, mediates the signaling pathways from IL-1 and the TNF receptor super families [8]. The nuclear translocation of NFκB is sufficient for the recruitment of neutrophils that are crucial for the clearance of pneumococcus [62]. In addition, natural IgM antibodies bind to the bacterial surface and increase resistance to pneumococcal pneumonia [57].

Coagulation systems are important for innate immunity in invertebrates and vertebrates ranging from drosophila to humans [49]. Fibrinogen, the source of clot formation, is synthesized in the liver and circulates in blood vessels in the natural state [63]. Studies of several infectious diseases of the skin and liver reveal that coagulation

is the early innate response to bacterial infection and that bacteria are trapped and killed by fibrin formation [49, 64]. Thus, regulation of the coagulation system has become a topic of interest in regard to host response to bacterial infection. However, the contribution of coagulation in other tissues such as lung has been poorly established.

Here is shown that IL-1 receptor-mediated signal plays an indispensable role in protection against pneumococcal pneumonia. Unexpectedly, fibrinogen synthesis in the lung after S. *pneumoniae* infection was significantly down-regulated in IL-1R$^{-/-}$ mice, unlike findings in wild-type mice. Moreover, the inhibition of coagulation in wild-type mice increased their mortality and bacterial burden. In vivo intratracheal treatment with mouse fibrinogen reinstated the susceptibility of IL-1R$^{-/-}$ mice to *S. pneumoniae* infection. Overall, these findings imply that IL-1 signal can activate fibrinogen synthesis in the lung and that coagulation is an important mechanism for protection during pneumococcal pneumonia.

II. Materials and Methods

1. Ethics Statement

All animal experiments were approved by the Institutional Animal Care and Use Committee of the International Vaccine Institute (Approval No: PN 2010-003), and all experiments were carried out in strict accordance with the Guide for the Care and Use of Laboratory Animals, Institute of Laboratory Animal Resources Commission on Life Sciences National Research Council, USA. All experiments were performed under anesthesia with a mixture of ketamine (100 mg/kg) and xylazine (20 mg/kg), and all efforts were made to minimize suffering.

2. Mice

Wild-type C57BL/6 (B6) and IL-1R$^{-/-}$ mice were purchased from Charles River Laboratories (Orient Bio, Inc., Korea) and Jackson Laboratories (Bar Harbor, ME), respectively. All mice used in experiments were between 6 and 12 weeks of age. Mice were maintained under pathogen-free conditions in the experimental facility at the International Vaccine Institute (Seoul, Korea), where they received sterilized food and water *ad libitum*. The experiments were approved by the Institutional Animal Care and Use Committee of the International Vaccine Institute.

3. Bacteria strain and infection

S. pneumoniae virulent capsular serotype 3 strain WU2 was cloned on trypticase soy agar containing 5% sheep blood (BD Biosciences, San Jose, CA) and cultured in Todd-Hewitt broth (BD Biosciences) plus 0.5% yeast extract (THY medium, BD Biosciences). WU2 strain was grown in 50 ml of THY medium until O.D.=0.4, adjusted with 15% glycerol, and frozen in 1-ml aliquots. For inoculation, a fresh aliquot was thawed and appropriately diluted in PBS. The actual number of colony-

forming units (CFU) injected was confirmed by plating on 5% sheep blood (BD Biosciences) as described previously [65]. After mice were anesthetized, they were given 5×10^5 colony-forming units (CFU) or 5×10^3 CFU/30 μl of *S. pneumoniae* diluted in PBS intranasally. All bacteria used in this study, WU2 strain, wild-type *S. pneumoniae* TIGR4 strain (AC535), and the mutant strain (AC1142) attenuated by suppression of tryptophan biosynthesis were kindly provided by Prof. David Briles (Department of Microbiology, Univ. of Alabama at Birmingham, USA) [66].

4. Treatment in vivo

Six hours after the IL-1R$^{-/-}$ mice were infected with WU2 ($5x10^5$ CFU), they were injected intraperitoneally (i.p.) with penicillin (1 mg/mouse). For the blockade of IL-6 signal, wild-type B6 mice were treated i.t. with PBS, anti-IL-6Ra antibody (Ab) (0.1 mg/mouse), or NSC 74859 (10 μg/mouse; SellecBio.com, Houston, TX). Anti-IL-6Ra Ab was kindly provided by Prof. Tadamitsu Kishimoto (Osaka Univ., Japan). For the regulation of clotting cascade, IL-1R$^{-/-}$ mice were treated i.t. with PBS or mouse fibrinogen (0.1 mg/mouse; Haematologic Technologies, Inc., Essex Junction, VT) at 0 and 1 day post-infection (dpi). Warfarin (10 μg/mouse; DAE HWA Pharmaceutical Co., Ltd., Korea) was administered orally to wild-type B6 mice every day beginning 1 day before infection.

5. Preparation of bronchoalveolar lavage fluid (BALF)

To obtain BALF, tracheas were cannulated after exsanguination and lungs were washed twice with 0.5 ml of PBS. BALF samples were centrifuged (800g, 5 min) to isolate cells and supernatant was centrifuged again (13,000g, 1 min) to completely remove remaining cells as described previously [67].

6. Cytokine and fibrinogen detection

The levels of MCP-1, IL-6, TNF-α, and IFN-γ were determined by BD™ Cytometric Bead Array Mouse Inflammation Kit (BD Biosciences). The levels of KC and IL-6 were measured by DuoSet Mouse ELISA Kit (R&D Systems, Minneapolis, MN) and ELISA MAX™ Standard Sets (Biolegend, Inc., San Diego, CA), respectively. The mouse fibrinogen was quantified by Mouse Fibrinogen ELISA (Immunology Consultants Laboratory, Inc., Newberg, OR). All experiments were performed according to each manufacturer's instructions.

7. Histology

The lungs were removed and washed in PBS before being fixed with 4% formaldehyde. The tissues were embedded in paraffin and stained with hematoxylin and eosin (H&E). Histopathological score was assessed by a pathologist using a blind test as previously described [68]. A 20-point scoring system was used to evaluate the level of lung tissue destruction, epithelial cell layer damage, polymorphonuclear (PMN) cell infiltration into the site, and alveolitis. For a confocal microscopy study, bacteria were stained with PKH26 Red Fluorescent General Cell Linker Kit (Sigma, St. Louis, MO) before infection according to the manufacturer's instructions. Lungs were embedded in OCT compound (Sakura Finetec, Tokyo, Japan). Cryo sections (5 μm) were fixed in ice-cold acetone.

8. Determination of bacterial load

Lungs were removed and homogenized in 1 ml of 0.2% Triton X-100 in PBS. Samples were serially diluted in PBS and plated onto TSA II™ (BD Biosciences, San Jose, CA) for CFU determination.

9. Flow cytometry

Cells were collected from the BALF and stained with CD11b (M1/70), Ly6C (AL-21), and Ly6G (1A8), which were purchased from BD Biosciences.

10. Neutrophil killing assay in vitro

To determine the neutrophil killing ability in vitro, the experiment was performed as previously described [69]. Peritoneal cells were obtained by peritoneal wash with 10 ml of 2% FBS-RPMI medium at 4.5 hr following i.p. injection with 2 ml of 3% Brewer thioglycollate medium (Sigma-Aldrich, St. Louis, MO). The $Ly6G^{+}$ peritoneal neutrophils were purified by MACS (Miltenyi Biotec, Bergisch Gladbach, Germany) and resuspended in 2% FBS-RPMI medium. For negative control, sorted neutrophils were heat-killed at 55℃ for 30 min. *S. pneumoniae* were resuspended in 2% FBS-RPMI medium and then added to a siliconized plate containing suspended neutrophils at a multiplicity of infection of 0.1 bacteria per cell. An aliquot of each well (25 µl) was diluted and immediately plated on TSA II™ (BD Biosciences) for counting (time = 0). The plate was placed under rotation at 37℃, and 25-µl aliquots were diluted and plated at each time point.

11. Microarray analysis

Whole lung tissues from B6 and $IL\text{-}1R^{-/-}$ mice were obtained 4 hr post-infection after perfusion. The lungs were then homogenized and RNA was extracted (RNA Isolation Kit, Qiagen, Valencia, CA). The cDNA microarray analysis was performed using a MouseRef-8 v2 Expression Beadchip Kit (Illumina, Inc., San Diego, CA).

12. Real-Time RT-PCR

Total RNA was isolated from the whole lung. Reverse transcription was performed using SuperScript™ II Reverse Transcriptase (Invitrogen, Grand Island, NY) according to the manufacturer's instructions. For real-time PCR analysis, the cDNA was serially diluted 10-fold and amplified using the 7500 Real Time PCR System (Applied Biosystems, Grand Island, NY) with Power SYBR® Green PCR Master Mix (Applied Biosystems). After the first denaturation step (95℃ for 10 min), amplification was performed for 40 cycles at 95℃ for 15 s, 55℃ for 15 s, and 72℃ for 40 s. The final cycle was followed by the dissociation stage. The following primers were used: Fga— (forward) ACC AGG AGA CTC GCG GGG AG and (reverse) CCG TGG TCC CAG GGT TCC GA and Fgg—(forward) ACC TGT CGC CTA CTG GCA CCA and (reverse) TCG AAG GCA TCC CCG GCA TCT.

13. Thrombin activity

Thrombin activity in BALF collected from wild-type B6 or IL-1R$^{-/-}$ mice at 0 or 1 dpi was determined by SensoLyte® AFC Thrombin Activity Assay Kit (AnaSpec, Inc., Fremont, CA). The experiment was performed according to the manufacturer's instructions.

14. Statistics

To compare differences between two experimental groups, a paired two-sample t-test was used for analysis, except for survival data for which Kaplan-Meier analysis was used. *$p<0.05$, **$p<0.01$, and ***$p<0.001$ were assumed to be statistically significant.

III. Results

1. IL-1R$^{-/-}$ mice are more susceptible to pulmonary *S. pneumoniae* infection than wild-type mice

In order to clarify the role of IL-1 on bacterial infection of the lung, both wild-type B6 and IL-1R$^{-/-}$ mice were infected intratracheally with sublethal doses of *S. pneumoniae* WU2 mouse virulent serotype 3 strain ($5x10^5$ or $5x10^3$ CFU). All IL-1R$^{-/-}$ mice died within 7 days post-infection when given $5x10^5$ CFU of WU2 strain while all B6 mice survived (Fig. 1A). Even the lower dose ($5x10^3$ CFU) killed about 80% of the IL-1R$^{-/-}$ mice (Fig. 1A). Treatment of B6 mice with anakinra, an IL-1 receptor antagonist, before and after infection with WU2 ($5x10^5$ CFU) resulted in deaths in half the mice but all mice that were not treated survived (Fig. 1B). In general, the amount of total protein in the BALF is representative of the severity of lung inflammation. In the kinetic study, total protein in the BALF of IL-1R$^{-/-}$ mice was much higher at 3 days post-infection with $5x10^5$ CFU of WU2 strain than found in the wild-type mice (Fig. 2A). To clarify why IL-1R$^{-/-}$ mice are susceptible to *S. pneumoniae* infection, the level of pro-inflammatory cytokines were compared in BALF at 3 days post-infection in IL-1R$^{-/-}$ and wild-type B6 mice. It was found that the pro-inflammatory cytokines (e.g., TNF-α, IFN-γ, IL-6, and MCP-1) were significantly higher in the BALF of IL-1R$^{-/-}$ mice than in the wild-type B6 mice (Fig. 2B). In a histologic study, the lungs of IL-1R$^{-/-}$ mice were not intrinsically different from those of B6 mice, but they had many more infiltrated polymorphonuclear cells and their alveolar spaces were filled with exudates at 3 days post-infection with $5x10^5$ CFU of WU2 strain (Fig. 3). In addition, tissue destruction, epithelial cell layer damage, and alveolitis were much more severe in the IL-1R$^{-/-}$ mice, resulting in a significantly higher clinical score than in the B6 mice (Fig. 3). When viewed together, these results indicate that IL-1R$^{-/-}$ mice were

susceptible to sublethal intratracheal challenge with pneumococcus because of severe inflammation in the lung.

2. Bacterial proliferation is not restrained in IL-1R$^{-/-}$ mice

Next, the relationship between severe inflammation and bacterial load in the IL-1R$^{-/-}$ mice was assessed. There were significantly more bacteria (CFU) in the lungs of IL-1R$^{-/-}$ mice at 4 hr after infection with $5x10^5$ CFU of WU2 than in the B6 mice; however, bacteria colonies gradually declined in the lungs of wild-type B6 mice by 1 day post-infection (Fig. 4A). Further, confocal microscopy at 1 day post-infection showed more red fluorescence-labeled WU2 strain in the lungs of IL-1R$^{-/-}$ mice than in wild-type B6 mice (Fig. 4B). It was speculated that the severe inflammation in IL-1R$^{-/-}$ mice might be caused by uncontrolled bacterial propagation. To further examine this hypothesis, two experiments to control the propagation of bacteria were performed. First, the IL-1R$^{-/-}$ mice were challenged intratracheally with TIGR4 ΔtrpG strain, which has a defect in tryptophan G synthesis and therefore is invasive but cannot proliferate. IL-1R$^{-/-}$ mice were infected with either the TIGR4 ΔtrpG or the mother TIGR4 strain as a control and determined bacterial load in the lung and survival rate. When pneumococcal propagation was suppressed, the IL-1R$^{-/-}$ mice survived (Fig. 5A). Next, IL-1R$^{-/-}$ mice were treated with penicillin, an antibiotic for gram-positive bacteria, 6 hr after infection with $5x10^5$ CFU with WU2. Penicillin treatment led to total clearance of pneumoniae by 1 day post-infection and survival of the IL-1R$^{-/-}$ mice (Fig. 5B). These results suggest that the lethal effects of pneumococcal infection in IL-1R$^{-/-}$ mice might be driven by uncontrolled bacterial propagation in the lung in the IL-1 signaling-deficient condition.

3. Normal neutrophil recruitment was detected in the IL-1-deficient condition

Because the role of neutrophils in the susceptibility of bacterial infection in the IL-1-deficient condition is controversial [62, 70], the characteristics of neutrophils in the lungs of IL-1R$^{-/-}$ mice were assessed following intratracheal infection with 5x10^5 CFU of WU2. As shown in Fig. 6A and B, at 1 day post-infection the lungs of IL-1R$^{-/-}$ and B6 mice had comparable numbers of CD11b$^+$Ly6C$^+$Ly6G$^+$ neutrophils. Moreover, at 3 days post-infection, there were significantly more CD11b$^+$Ly6C$^+$Ly6G$^+$ neutrophils in the lungs of IL-1R$^{-/-}$ mice than in B6 mice (Fig. 6A and B). The level of KC, the chemokine that recruits neutrophils, in the BALF of B6 and IL-1R$^{-/-}$ mice was similar at 1 day post-infection but was substantially enhanced in IL-1R$^{-/-}$ mice at 3 days post-infection following intratracheal infection with 5x10^5 CFU of WU2 (Fig. 6C). Moreover, the bactericidal activity of peritoneal neutrophils from IL-1R$^{-/-}$ and wild-type B6 mice was similar (Fig. 7A). An earlier study showed that phagocytosis by alveolar macrophages also plays a critical role in clearing bacteria from the lung [9], therefore, the phagocytosis of alveolar macrophages in both B6 and IL-1R$^{-/-}$ mice was compared at 1 day post-infection using red fluorescence-labeled WU2 strain. The CD11b$^+$CD11c$^+$ alveolar macrophages captured red fluorescence-labeled WU2 strain in a normal way in both wild-type B6 and IL-1R$^{-/-}$ mice (Fig. 7B). Overall, any defects were not found of infiltration or killing ability of neutrophils and phagocytosis of alveolar macrophages in IL-1R$^{-/-}$ mice. Thus, there may be other underlying mechanisms that affect the control of bacterial propagation in IL-1R$^{-/-}$ mice.

4. Fibrinogen synthesis in the lung is down-regulated in the IL-1 signal-deficient condition

To determine which genes are regulated by IL-1 signaling, at 4 hr after intratracheal infection with $5x10^5$ CFU of WU2, microarray analysis was conducted to assess gene expression patterns in the lungs of B6 and IL-$1R^{-/-}$ mice and compared the results to those of mice given PBS. Among approximately 50,000 genes, the SMAD signal, protein folding, and apoptosis-related genes were highly expressed in the lungs of IL-$1R^{-/-}$ mice as compared with those of B6 mice (Fig. 8). Both Fos and Jun are transcription factors induced by TGFβ and SMAD proteins during pneumocystis pneumonia [71]. A recent study showed that pneumonia infection enhances endoplasmic reticulum stress and induces the protein folding-related genes [72]. In addition, apoptosis is a well-known feature of *S. pneumoniae* infection [73]. It was unexpectedly found that there were little expressions of fga and fgg mRNA in the lungs of IL-$1R^{-/-}$, whereas mRNA expression of fga and fgg were significantly enhanced in the lungs of wild-type B6 mice 4 hr after infection with WU2 (Fig. 8 and Table. 1). To confirm this result, quantitative PCR of fga and fgg was performed. It was found that mRNA expression levels of fga and fgg were greatly increased in the lungs of wild-type B6 mice after infection but there were no significant changes in the IL-$1R^{-/-}$ mice (Fig. 9A). Likewise, protein levels of fibrinogen were significantly higher in BALF of B6 mice at 1 day post-infection than at 4 hr post infection but no changes were observed in the IL-$1R^{-/-}$ mice (Fig. 9B). On the other hand, fibrinogen levels in blood of both B6 and IL-$1R^{-/-}$ mice increased in a time-dependent manner after infection (Fig. 9C). These results demonstrate that fibrinogen can be expressed in both mucosal (mainly lung) as well as systemic tissues (mainly liver) after pulmonary pneumococcal infection and that local synthesis of fibrinogen might be induced in the lung in an IL-1-dependent manner.

5. Fibrinogen synthesis is activated by IL-1- dependent IL-6 signal

Next, it was sought how IL-1 signal transduction induced the synthesis of fibrinogen in the lung after *S. pneumoniae* infection. Previous studies demonstrated that IL-6 leads to the transcription of the fibrinogen genes in lung epithelium [74] and that IL-6 is regulated by IL-1 receptor-mediated NFκB activation [75]. Therefore, the IL-6 levels were examined in the BALF from wild-type and IL-1R$^{-/-}$ mice 4 hours after infection. The IL-6 levels were increased in both wild-type and IL-1R$^{-/-}$ mice, although the amount of IL-6 in IL-1R$^{-/-}$ mice was significantly less than in wild-type mice (Fig. 10A). The IL-6 signaling pathway activates Stat3, which acts as a transcription factor and binds to the IL-6 motif on human fibrinogen gamma promoter [76]. Thus, it was investigated the alteration of fibrinogen production by the blockade of IL-6 or Stat3 activation using anti-IL-6Ra Ab or Stat3 inhibitor (i.e., NSC 74859), respectively [77]. The transcriptional levels of fga and fgg genes were significantly reduced in wild-type mice treated with anti-IL-6 Ab or Stat3 inhibitor (Fig. 10B). Likewise, the fibrinogen levels in the BALF of wild-type mice decreased after in vivo treatment with anti-IL-6 Ab or Stat3 inhibitor (Fig. 11A). The reduced fibrinogen levels after treatment were similar to those of non-treated IL-1R$^{-/-}$ mice at 1 day post-infection (Fig. 11A). In addition, the thrombin activity, which cleaves the fibrinogen to fibrin for the initiation of clotting, was also down-regulated in BALF of IL-1R$^{-/-}$ mice compared with wild-type mice (Fig. 11B). Overall, the results clearly indicate that the synthesis of fibrinogen in lungs with bacterial infections is tightly regulated by the IL-1-IL-6-Stat3 cascade.

6. Coagulation in the lung is critical to control bacterial propagation

Next, it was addressed whether the defect in the lung coagulation system, especially fibrinogen synthesis in the lung of IL-1R$^{-/-}$ mice after pneumococcal infection, has a direct relationship to controlling bacteria. First, recombinant mouse fibrinogen was administered in vivo by intratracheal injection after infection with $5x10^5$ CFU of WU2 in IL-1R$^{-/-}$ mice and then monitored survival and bacterial propagation. Survival significantly improved with fibrinogen treatment (Fig. 12A), and at 2 days post-infection, bacterial burden in the lung had declined in the fibrinogen-treated IL-1R$^{-/-}$ mice but not in those given PBS (Fig. 12A). Next, wild-type B6 mice were orally treated with warfarin to inhibit coagulation. When warfarin-treated mice were infected intratracheally with $5x10^5$ CFU WU2, approximately 60% died within 14 days post-infection and bacterial load in the lung significantly increased (Fig. 12B). Overall, it was found that fibrinogen in the lung played an indispensable role in the control of pneumococcus in IL-1R$^{-/-}$ mice and that treatment with an anti-coagulant drug exacerbated pneumococcal pneumonia in B6 mice.

IV. Discussion

Innate immunity is the immediate host defense against infections [8]. IL-1, consisting of α and β subtypes, is the initial cytokine that accompanies TNF-α to induce inflammation [78]. In the murine pneumococcal pneumonia model, high levels of IL-1, TNF-α, and IL-6 were determined in lung exudates within 4 hr of infection [79, 80]. IL-1, which is mainly produced by resident alveolar macrophages, binds to the heterodimeric receptor made of IL-1RI and IL-1R accessory proteins on pulmonary epithelial cells [24, 81]. The IL-1 deficient condition has been presumed to be vulnerable in infectious diseases. In a previous study, the lack of IL-1 impaired bacterial clearance and induced high mortality in pneumococcal meningitis [82]. IL-1$\beta^{-/-}$ and IL-1$\alpha/\beta^{-/-}$ mice are particularly susceptible to pneumococcal infection, but not IL-1$\alpha^{-/-}$ and IL-1R antagonist$^{-/-}$ mice [83]. Recently, caspase-1-independent IL-1β production but not TLR signaling was shown to be critical for host resistance to *Mycobacterium tuberculosis* or *Chlamydia pneumoniae* [84, 85]. Here was demonstrated that IL-1R$^{-/-}$ mice have higher mortality and more severe inflammation than wild-type mice when infected i.t. with *S. pneumoniae*. These results suggest that IL-1 is critical for protection against pneumococcal infection and that deficiency of IL-1 signal gives rise to the weakness of the host in fighting infectious diseases.

In this study, IL-1R$^{-/-}$ mice had large amounts of inflammatory cytokines in the BALF and predominant propagation of *S. pneumoniae* in the lung. The enhanced inflammatory responses and subsequent increased bacterial propagation in the IL-1-deficient condition have been reported elsewhere[82-85]. The severity of inflammatory responses is thought to be correlated with the uncontrolled proliferation of the invader. When bacterial propagation was inhibited by using the mutant *S. pneumoniae* strain or antibiotic treatment, IL-1R$^{-/-}$ mice were rescued from the inflammation. Hence, severe inflammation and tissue damage in the IL-1-

deficient condition might be caused by the breakdown of a mechanism that controls *S. pneumoniae* in the lung.

Neutrophils are thought to be the first innate immune cells recruited after infection. Within a few hours of infection, they give rise to powerful protective immunity, especially against extracellular bacteria [86]. The depletion of neutrophils after treatment with the anti-Gr-1 mAb or the blockade of neutrophil recruitment in the $CXCR2^{-/-}$ mice demonstrates the failure of bacterial clearance in murine pneumonia models [87, 88]. Several reports have suggested that insufficient recruitment of neutrophils may explain the susceptibility of IL-1-deficient mice [70, 83]. A recent study noted that IL-1β and its related signaling pathways play a central role in the production of CXCL8, a potent neutrophil chemoattractant, in rhinovirus infection [89]. However, it seems likely that IL-1R signals are activated via MyD88, a common adaptor molecule of TLRs, and that activation of MyD88-mediated NFκB is a general transcription factor for the induction of inflammation that can also be activated by TNF-α [90]. Others propose that TNF-α can compensate for IL-1-mediated NFκB activation [62, 91]. There are no differences in the recruitment of neutrophils in the absence of IL-1 or TNF-α alone, but triple-mutant mice deficient in TNFR1, TNFR2, and IL-1RI are defective in the production of KC and MIP-2 and in the recruitment of neutrophils [62, 91]. In this study, it was wondered why the number of $CD11b^{+}Ly6C^{+}Ly6G^{+}$ neutrophils recruited into the lung was similar or even higher in $IL\text{-}1R^{-/-}$ mice than in wild-type mice. Further, bacterial killing ability of peritoneal neutrophils from $IL\text{-}1R^{-/-}$ mice was identical to those of wild-type mice. Overall, the bactericidal ability of neutrophils in the $IL\text{-}1R^{-/-}$ mice in this study seemed to operate normally.

Inasmuch as uncontrolled proliferation of pneumococcus cannot be fully explained by the recruitment and killing ability of neutrophils in the $IL\text{-}1R^{-/-}$ mice, microarray analysis was used to investigate another factor that might be altered in an IL-1-dependent manner after pneumococcal infection. It was found the

coagulation factors, transcripts of fga and fgg genes, were down-regulated in lung tissue from IL-1R$^{-/-}$ mice compared with wild-type mice at 4 hr after infection. Fibrinogen consists of two sets of three different chains (α, β, and γ) and is cleaved to fibrin by thrombin during coagulation [92]. The fibrinogen is usually synthesized in the liver and is abundant in circulating blood [63, 93]. However, previous studies indicated that constitutive expression of the three fibrinogen genes (fga, fgb, and fgg) were found in cultured pulmonary epithelial cells and lung epithelium [94, 95]. Importantly, fibrinogen can be induced in the lung epithelium by respiratory infection such as pneumocystis pneumonia or inflammatory cytokines such as IL-6 [95-97]. A recent study suggested a scenario in which phosphorylated Stat3, by IL-6 signaling cascade, binds to IL-6 motifs on the promoter region of fibrinogen genes and expresses three fibrinogen chains [98]. In this study, it was found less IL-6 secretion was induced in IL-1R$^{-/-}$ mice than in wild-type mice at early time points after infection. This was followed by lack of fibrinogen in the BALF. Likewise, blockade of IL-6 or Stat3 reduced the secretion of fibrinogen in the lungs of infected wild-type mice. It is therefore suggested that IL-6 secretion induced by IL-1 signal plays an indispensable role in the synthesis of fibrinogen in the pulmonary epithelium against pneumococcal infection.

Since fibrinogen plays a key role in producing blood clots, the relationship between coagulation and pulmonary infection was investigated in vivo. Coagulation is one of the serine protease cascades and the ancestral innate immune system [99]. Coagulation not only contributes to arresting hemorrhage but also participates in controlling bacterial growth in the skin, vascular system, and liver [100, 101]. Moreover, when coagulation is prevented by treatment with an anticoagulant or as seen in fibrinogen-deficient mice, the propagation of the pathogen is not limited and mice have higher mortality [102]. In this study, thrombin activity in the BALF of infected IL-1R$^{-/-}$ mice was reduced compared with wild-type mice as were decreased fibrinogen levels. In vivo treatment of

exogenous fibrinogen decreased the bacterial burden and delayed death. In addition, oral administration of warfarin dramatically decreased survival and escalated the bacterial burden in the lung following *S. pneumoniae* infection. This result supports the notion that coagulation plays an indispensable role in regulation of bacterial growth in the lung.

IL-1 might also regulate coagulation via neutrophil activation. Administration of IL-1α in baboons after lethal challenge with *Escherichia coli* induced the formation of thrombin and treatment of IL-1 receptor antagonist attenuated the release of neutrophil elastase [103]. A recent study revealed that neutrophil serine proteases promote tissue factor- and factor XII-dependent coagulation and help retain GAS in blood vessels [64]. Hence, it was hypothesized that IL-1 might have various means to regulate coagulation: These include induction of fibrinogen directly and activation of neutrophil serine proteases for enhancing thrombus formation indirectly. If so, the diminished thrombin activity in IL-1R$^{-/-}$ mice could be caused by the impaired activation of neutrophil serine proteases but this requires further study.

As for application to clinical cases, IL-1R$^{-/-}$ mice mimic humans treated with anakinra. Patients given anakinra or other IL-1 antagonist drugs are thought to be more vulnerable to infectious diseases [104]. In addition, treatment with anti-coagulants such as warfarin also increases susceptibility to infection [101]. The treatment with fibrinogen ameliorates the resistance to illness.

In summary, IL-1R$^{-/-}$ mice are highly susceptible to pulmonary infection with *S. pneumoniae*. In this study, the bacterial burden in the lung could not be controlled in the IL-1-deficient condition even though the recruitment and the bacteria-killing function of CD11b^{+}Ly6C^{+}Ly6G^{+} neutrophils were normal. Of note, fibrinogen was synthesized locally in the lung after pneumococcal infection in an IL-1 signal-dependent manner and restricted the proliferation of pathogen; however, the blockade of coagulation failed to overcome the pneumococcal

pneumonia. Taken together, these findings indicate that IL-1 might be involved in activating the coagulation pathway that is critical for protecting the lung against *S. pneumoniae* infection (Fig. 13).

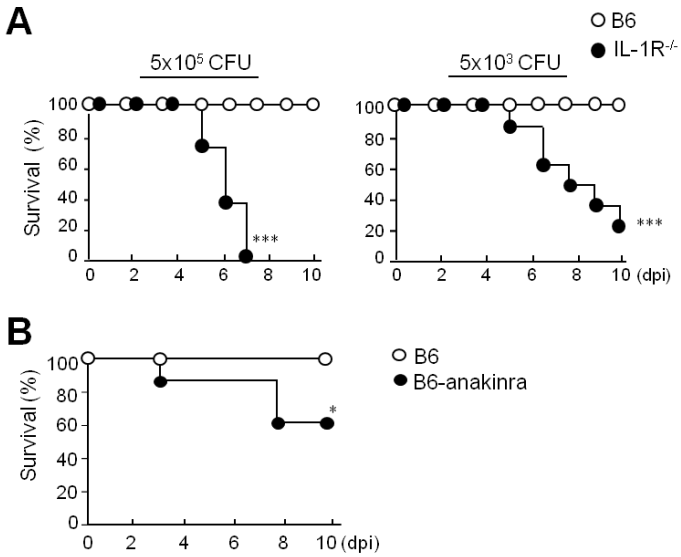

Figure 1. A. Wild-type and IL-1R$^{-/-}$ mice of B6 background were infected intratracheally with S. pneumoniae WU2 ($5x10^5$ or $5x10^3$ CFU) and monitored daily for survival (n=8 mice per group). B. Wild-type mice were treated intraperitoneally with anakinra (0.5 mg/mouse) (Amgen, Thousand Oaks, CA), antagonist for IL-1, or PBS every 3 days starting 1 day before infection (dpi) with *S. pneumoniae* WU2 ($5x10^5$ CFU) (n=8 mice per group) *, $p<0.05$; ***, $p<0.001$ (Kaplan-Meier analysis).

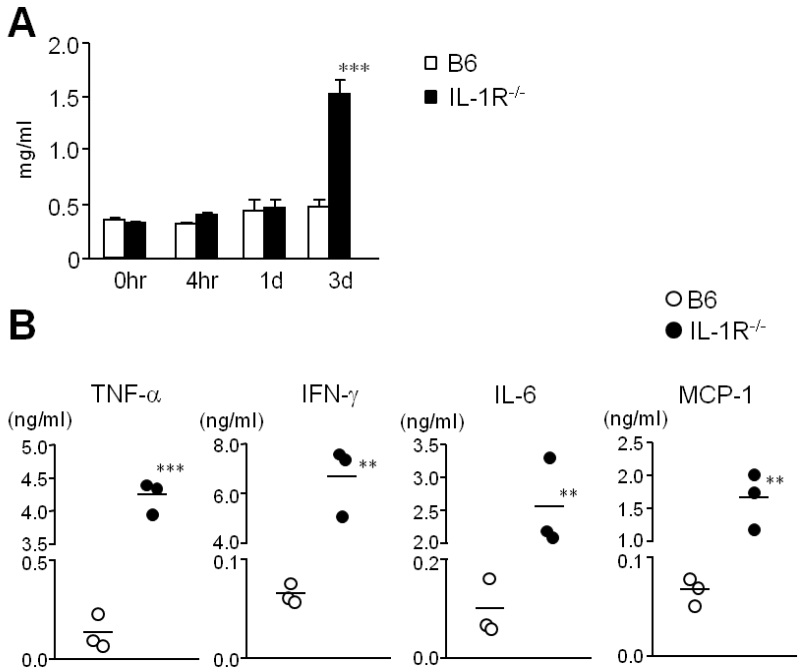

Figure. 2. A. Total protein levels in BALF of wild-type B6 and IL-1R$^{-/-}$ mice at 0 and 4 hr and 1 and 3 dpi. Values are mean ± SD and results are representative of three independent experiments with n=5 per group. B. Proinflammatory cytokine levels in the BALF of wild-type and IL-1R$^{-/-}$ mice were measured 3 days post infection. Data are representative of three experiments. **, $p<0.01$; ***, $p<0.001$. (t-test).

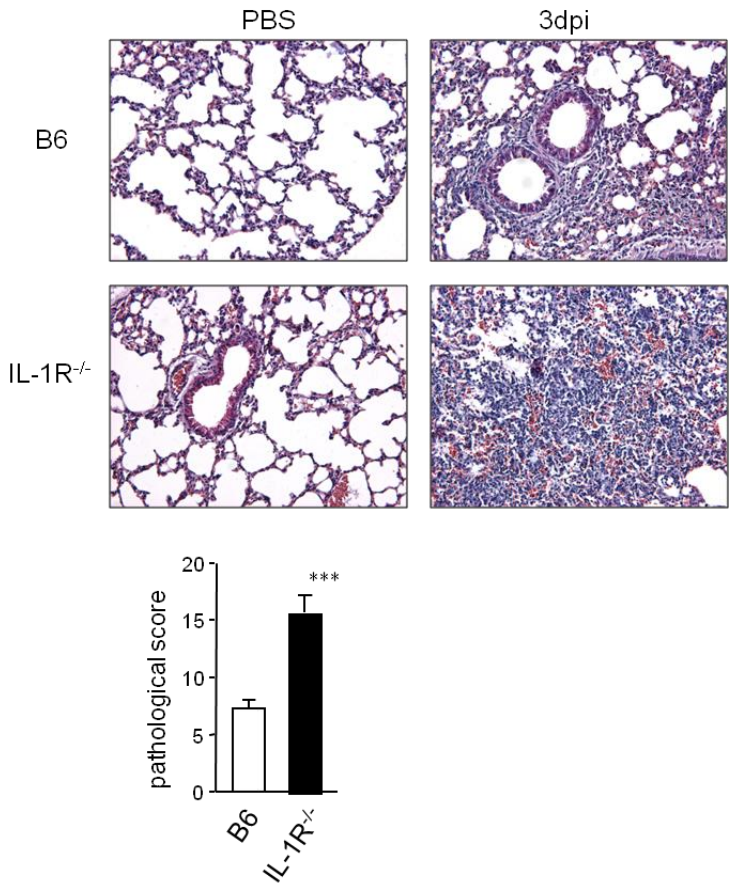

Figure 3. Pathophysiologic study of the lung was done at 3 days post-infection by H&E staining. Representative pictures and histopathological scores are shown as mean ± SD of mice per group (n=10). Data are representative of three experiments. ***, $p<0.001$.

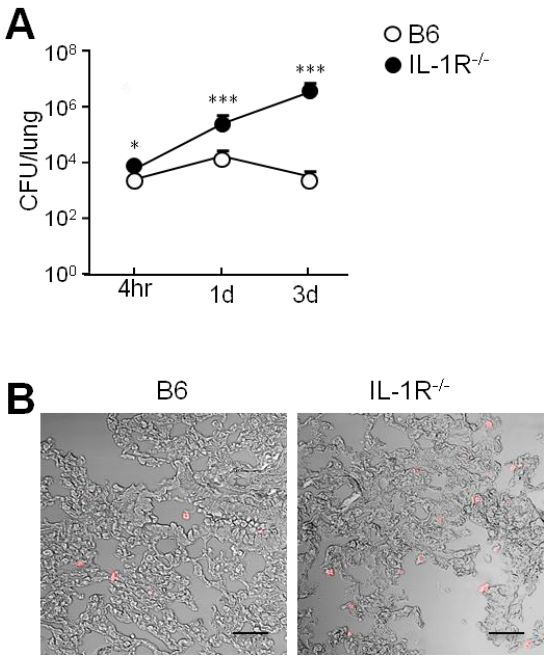

Figure 4. A. Lung bacterial load was determined at 4 hr and 1 and 3 days after intratracheal challenge with *S. pneumoniae* WU2 strain ($5x10^5$ CFU). Lung homogenates were serially diluted in PBS and plated onto blood agar plates to measure colony-forming units (CFU). B. Increased numbers of red fluorescence-labeled WU2 in the lungs of IL-$1R^{-/-}$ mice at 1 day post infection. Scale bar: 50μm.

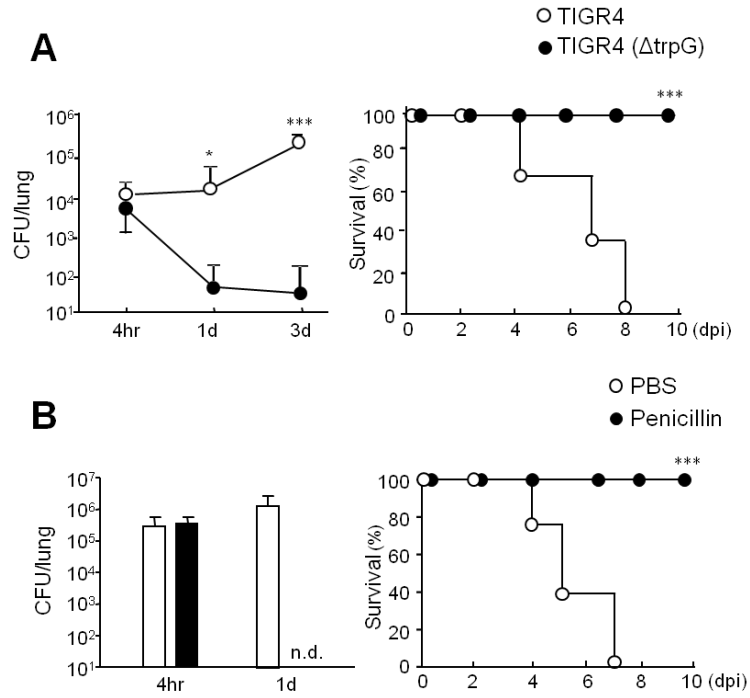

Figure 5. A. Bacterial load and survival rate of IL-1R$^{-/-}$ mice after intratracheal challenge with *S. pneumoniae* TIGR4 and its tryptophan mutant (ΔtrpG). B. Role of antibiotics on bacterial load and survival rate of IL-1R$^{-/-}$ mice after intratracheal challenge with *S. pneumoniae* WU2 strain. Each mouse received 1 mg of penicillin 6 hr after infection. CFU data are mean ± SD (n=4 mice per group) and survival rate (n=8 mice per group). Data are from three independent experiments. *, $p<0.05$; ***, $p<0.001$. n.d., not detectable.

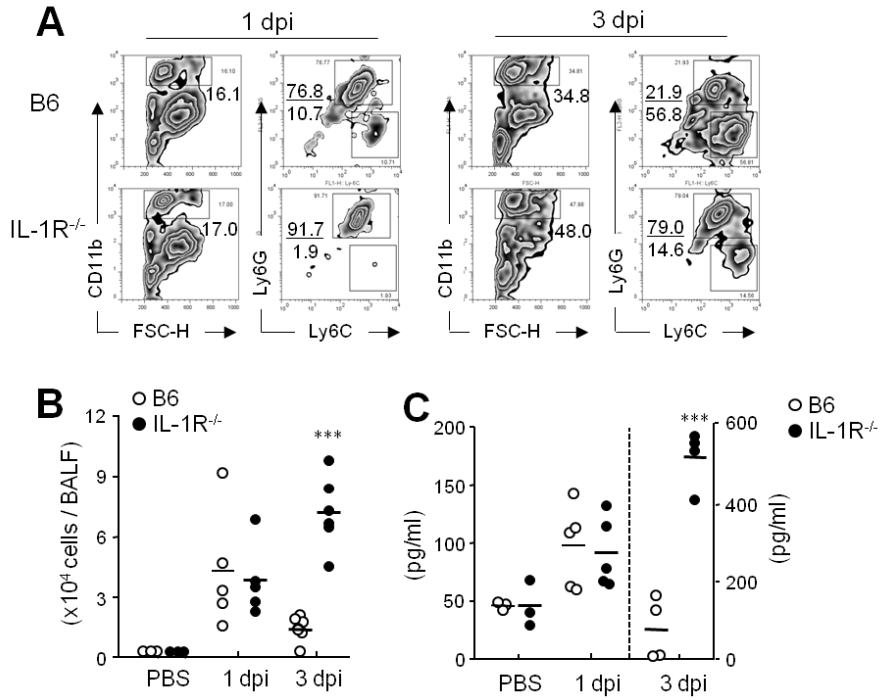

Figure 6. A. Cells were obtained from BALF at days 0, 1, and 3 after intratracheal infection with *S. pneumoniae* WU2 strain ($5x10^5$ CFU). Cellular composition was determined by flow cytometry. Numbers in boxes are percentages of each cell population. Absolute recovered cells (B) and KC levels (C) in the BALF of wild-type B6 and IL-$1R^{-/-}$ mice are shown before and after infection. Data represent three independent experiments. ***, $p<0.001$.

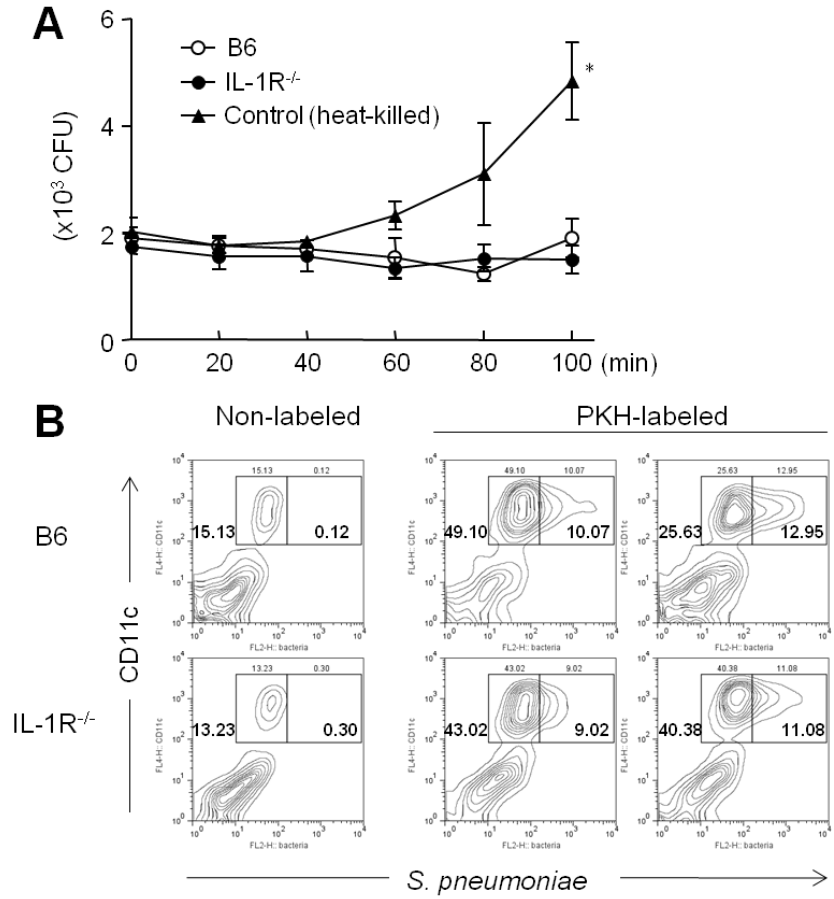

Figure 7. A. No significant difference was found between wild-type B6 and IL-1R$^{-/-}$ mice in neutrophil killing ability in vitro. Numbers of bacteria are shown as mean ± SEM (n=4 mice per group). *, $p<0.05$; ***, $p<0.001$. B. Wild-type B6 and IL-1R$^{-/-}$ mice were infected with $5x10^5$ CFU of PKH-labeled or non-labeled *S. pneumoniae* WU2. Phagocytosis in the cells in BALF was analyzed by flow cytometry 1 day after infection. Numbers indicate percentages of gated cells. Results are representative of three independent experiments.

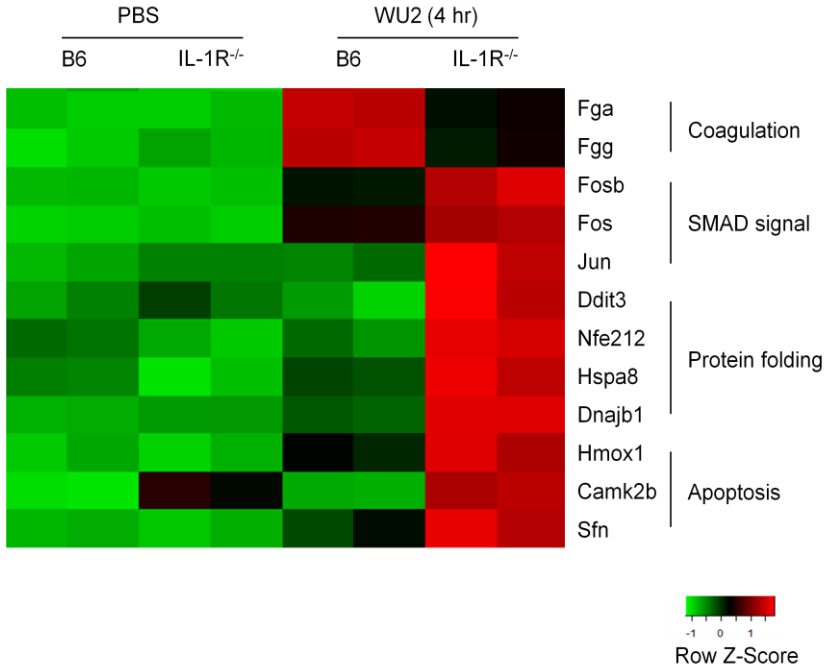

Figure 8. Total RNA of the whole lung tissue was extracted and gene expression profiles were addressed by microarray analysis. Wild-type B6 and IL-1R$^{-/-}$ mice were infected intratracheally with *S. pneumoniae* WU2 strain (5x10^5 CFU). Lung tissue samples were taken at 0 and 4 hr after infection. Data are representative of two independent experiments.

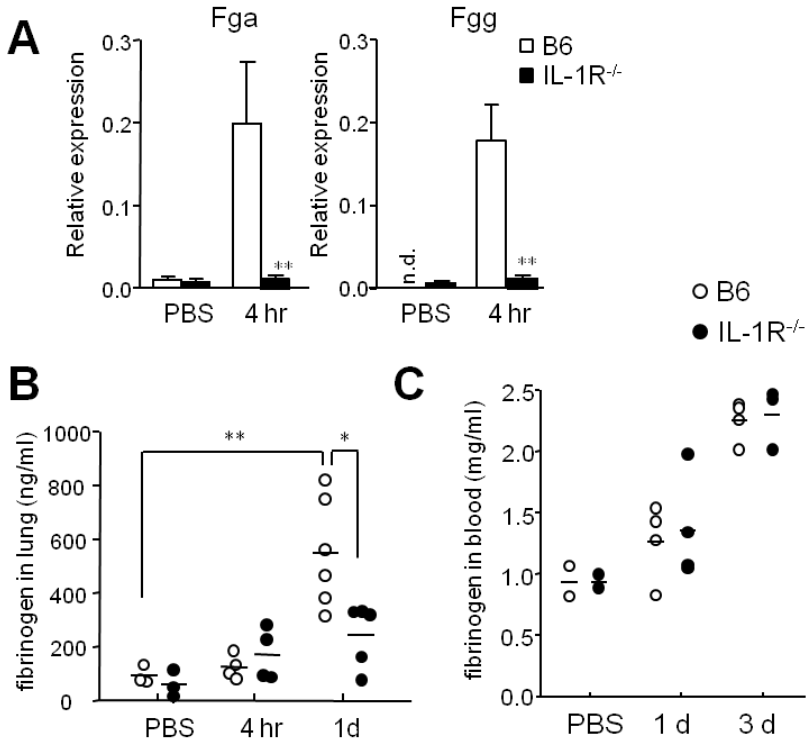

Figure 9. A. Quantitative PCR for mRNA levels of fibrinogen alpha (Fga) and gamma (Fgg) in the lung was done to confirm the microarray analysis results. The mRNA expression levels were adjusted to the expression levels of β-actin. Values are mean + SD of three independent experiments carried out in triplicate. B. The protein level of fibrinogen was determined by ELISA in BALF at 0 and 4 hr and 1 day after infection. C. The level of fibrinogen in peripheral blood was determined by ELISA at days 0, 1 and 3 after infection with *S. pneumoniae* WU2 ($5x10^5$ CFU). Results are representative of three independent experiments. *, $p<0.05$; **, $p<0.01$. n.d., not detectable.

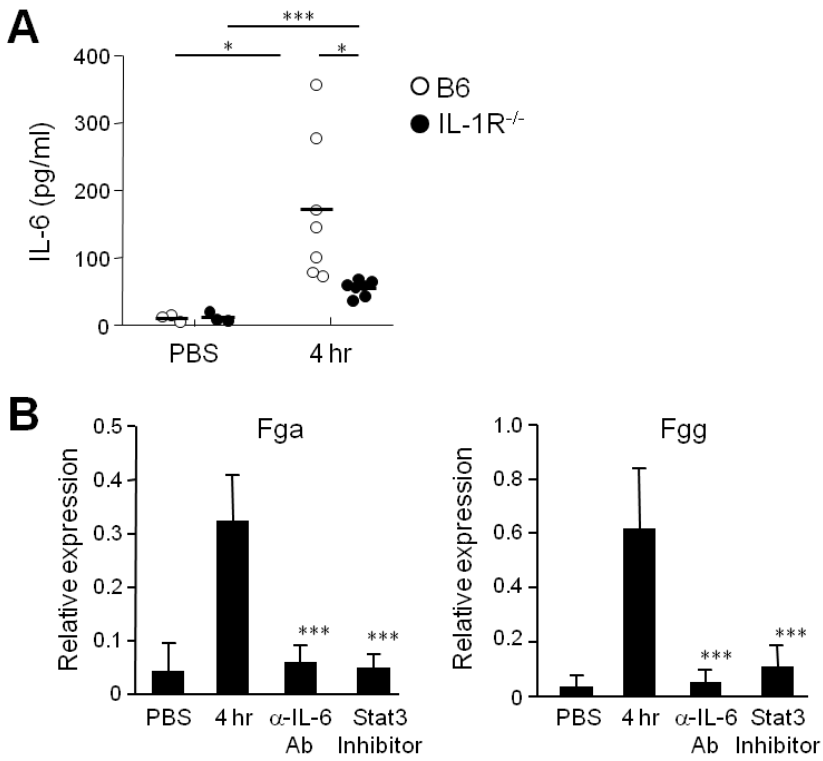

Figure 10. A. IL-6 levels in BALF from wild-type or IL-1R$^{-/-}$ mice were measured by ELISA at 0 and 4 hr after infection with *S. pneumoniae* WU2 (5x10^5 CFU). B. Wild-type B6 mice were treated intratracheally with PBS, anti-IL-6 Ab (0.1 mg/mouse), or Stat3 inhibitor (NSC 74859; 10 μg/mouse) following infection. Quantitative PCR was used to determine mRNA levels of fibrinogen alpha (Fga) and gamma (Fgg) in the lung 4 hr after infection. The mRNA expression levels were adjusted to the expression levels of β-actin. Values are mean + SD of three independent experiments carried out in triplicate. Data are representative of three independent experiments. ***, $p<0.001$.

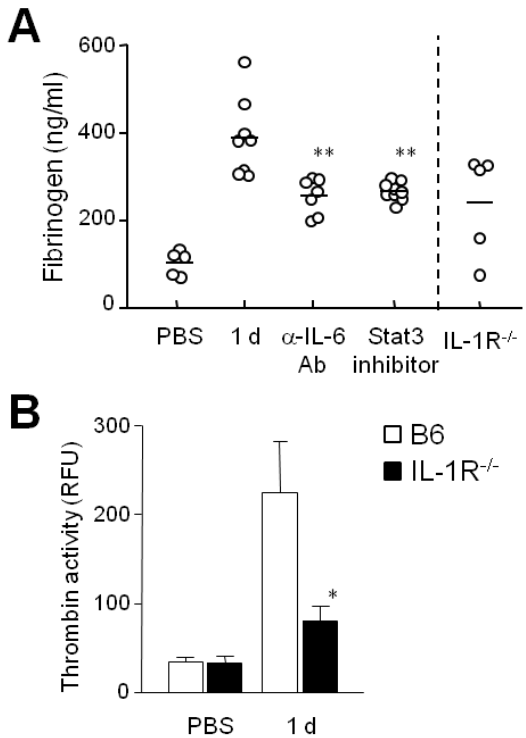

Figure 11. A. Fibrinogen levels measured in BALF by ELISA at days 0 and 1 day post-infection. Significance is versus 1 day post-infection. Data are representative of three independent experiments. B. Thrombin activity in BALF at 0 and 1 day post-infection. Values are mean relative fluorescence units (RFU) + SED of five mice per group. Data are representative of three independent experiments. *, $p<0.05$; **, $p<0.01$

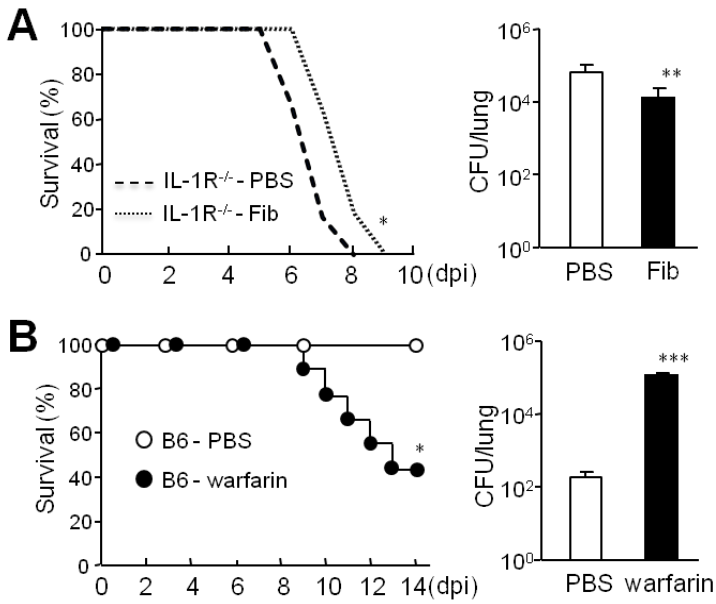

Figure 12. A. Survival plots of IL-1R$^{-/-}$ mice treated intratracheally with PBS or mouse fibrinogen (Fib.; 0.1 mg/mouse) at days 0 and 1 post-infection with *S. pneumoniae* WU2 ($5x10^5$ CFU). Lung bacterial load was determined at 2 days post-infection (n=8 per group). Graphs for bacterial CFU are shown as mean ± SD (n=4 per group). Data are representative of three independent experiments. B. Survival plots for wild-type B6 mice treated intragastrically with PBS or warfarin (10 μg/mouse) every day from 1 day before infection with WU2 ($5x10^5$ CFU). Lung bacterial load was determined at 5 days post-infection (n=9 per group). Graphs for bacterial CFU are shown as mean ± SD (n=4 per group). Data are representative of three independent experiments. *, $p<0.05$; **, $p<0.01$; ***; $p<0.001$.

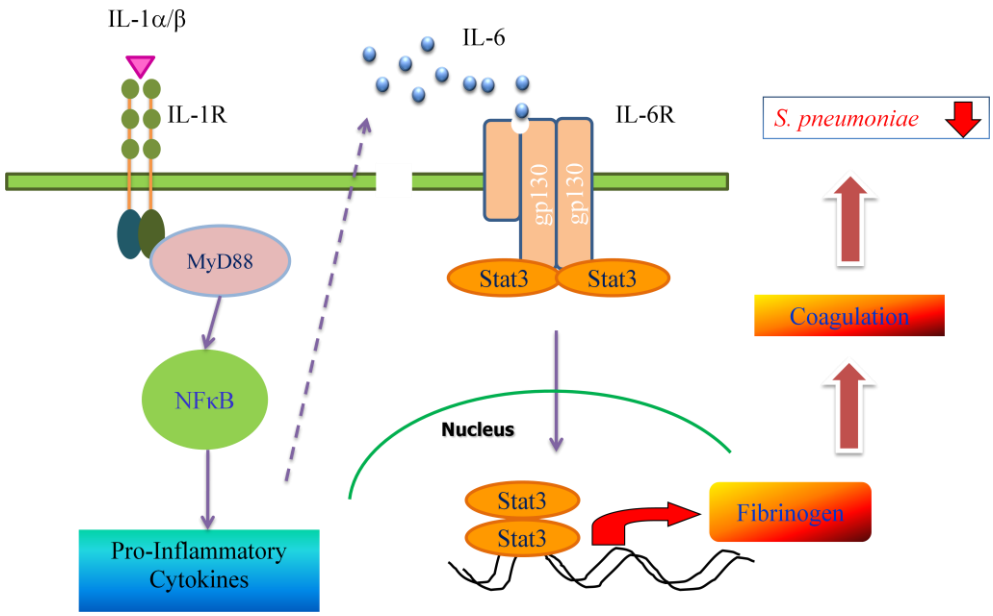

Figure 13. Graphic summary. *Streptococcus pneumoniae* infection induces the production of IL-1α and β cytokines which bind to IL-1 receptors. IL-1 signals through its adaptor molecule, MyD88, to activate NFκB. The activated NFκB is translocated in nucleus and expresses proinflammtory genes such as IL-6. The secreted IL-6 signals to Stat3 in pulmonary epithelia. The activated Stat3 moves into nucleus and binds on the promoter of fibrinogen gene. The produced fibrinogen acts as a source of coagulation. The enhanced coagulation inhibits the proliferation of invaded pneumococcus.

Probe ID	Gene Symbol	WT0 mean(SD)	KO0 mean(SD)	WT4 mean(SD)	KO4 mean(SD)	KO4 / WT4 FC(*P*)
ILMN_2832105	Fgg	8.05(0.08)	8.27(0.08)	10.22(0.05)	9.16(0.17)	-2.08(0.00)
ILMN_2624363	Fga	7.64(0.11)	7.49(0.02)	10.02(0.03)	8.78(0.13)	-2.35(0.00)
ILMN_2883961	Sybl1	12.44(0.05)	11.52(0.07)	12.50(0.10)	11.26(0.22)	-2.37(0.00)
ILMN_1226472	Retnla	13.13(0.06)	13.11(0.07)	14.31(0.06)	13.04(0.03)	-2.40(0.00)
ILMN_2811154	Cxcl2	7.27(0.03)	7.14(0.12)	9.49(0.04)	8.21(0.03)	-2.42(0.00)
ILMN_1242829	Prdx2	8.66(0.00)	7.55(0.07)	8.66(0.04)	7.36(0.11)	-2.47(0.00)
ILMN_1255006	Rpe	9.72(0.01)	7.86(0.15)	9.74(0.05)	7.96(0.07)	-3.43(0.00)
ILMN_2878542	Myl1	10.04(0.10)	8.76(0.03)	10.78(0.02)	8.83(0.08)	-3.87(0.00)
ILMN_2690676	Clca3	10.72(0.10)	10.11(0.04)	11.78(0.00)	9.24(0.06)	-5.80(0.00)
ILMN_2619408	Atf3	8.17(0.05)	8.42(0.08)	9.23(0.01)	13.31(0.17)	16.81(0.00)
ILMN_2829594	Hspa1a	8.41(0.07)	8.56(0.05)	11.51(0.03)	14.82(0.03)	9.91(0.00)
ILMN_2617468	Chac1	10.01(0.02)	9.97(0.00)	11.59(0.01)	14.15(0.06)	5.91(0.00)
ILMN_1240323	Dnajb1	12.10(0.02)	12.26(0.01)	12.73(0.07)	15.29(0.02)	5.89(0.00)
ILMN_3161547	Nppa	10.53(0.08)	12.98(0.05)	10.90(0.03)	12.93(0.03)	4.09(0.00)
ILMN_2645780	Osgin1	9.33(0.10)	9.36(0.05)	10.43(0.05)	12.23(0.11)	3.47(0.00)
ILMN_2824002	Frat2	8.88(0.03)	8.96(0.03)	9.20(0.06)	10.99(0.13)	3.45(0.00)
ILMN_2735350	Gdf15	7.61(0.09)	7.66(0.06)	8.87(0.09)	10.55(0.20)	3.21(0.00)
ILMN_2619330	Plk3	8.18(0.05)	8.42(0.06)	8.94(0.00)	10.61(0.08)	3.18(0.00)
ILMN_2662926	Egr1	12.18(0.14)	12.03(0.03)	13.71(0.06)	15.24(0.22)	2.89(0.00)
ILMN_2646625	Jun	10.61(0.06)	10.81(0.00)	10.85(0.09)	12.37(0.21)	2.86(0.00)
ILMN_2809443	EG638695	8.21(0.03)	8.64(0.23)	8.48(0.05)	9.95(0.02)	2.76(0.00)
ILMN_2716098	Hsp105	11.00(0.01)	11.00(0.12)	11.36(0.00)	12.79(0.14)	2.71(0.00)
ILMN_1228031	Dusp8	8.65(0.01)	8.99(0.22)	8.76(0.03)	10.18(0.08)	2.66(0.00)
ILMN_2596979	Nrarp	11.49(0.05)	11.78(0.05)	11.12(0.04)	12.51(0.03)	2.61(0.00)
ILMN_2918479	Hspa8	11.52(0.03)	11.14(0.12)	11.77(0.05)	13.14(0.17)	2.58(0.00)
ILMN_2648169	Sfn	7.70(0.04)	7.65(0.09)	8.42(0.24)	9.76(0.20)	2.54(0.00)
ILMN_2617858	Ovol1	7.72(0.06)	7.66(0.07)	8.01(0.00)	9.35(0.23)	2.53(0.00)
ILMN_3137552	Mtap2	8.93(0.08)	10.51(0.10)	8.95(0.00)	10.26(0.12)	2.48(0.00)
ILMN_2788073	Hmox1	9.40(0.15)	9.34(0.14)	10.37(0.14)	11.67(0.21)	2.48(0.00)
ILMN_2750515	Fos	10.22(0.05)	10.32(0.10)	12.44(0.04)	13.73(0.09)	2.45(0.00)
ILMN_1247691	Hes1	10.96(0.01)	10.59(0.01)	11.03(0.01)	12.32(0.08)	2.43(0.00)
ILMN_3147944	Ap2b1	9.97(0.06)	10.01(0.18)	8.82(0.07)	10.08(0.11)	2.39(0.00)
ILMN_2639036	Hspd1	9.78(0.01)	9.54(0.01)	9.65(0.04)	10.89(0.08)	2.35(0.00)
ILMN_1238547	Areg	9.97(0.11)	10.04(0.05)	11.50(0.09)	12.70(0.14)	2.30(0.00)
ILMN_2754985	Phlda1	12.83(0.06)	12.51(0.06)	13.07(0.07)	14.22(0.03)	2.23(0.00)
ILMN_1224128	Nfe2l2	9.78(0.02)	9.54(0.07)	9.72(0.09)	10.83(0.04)	2.16(0.00)
ILMN_2993109	Ddit4	9.14(0.18)	9.27(0.09)	9.69(0.09)	10.79(0.18)	2.14(0.00)
ILMN_2622983	Dusp1	13.38(0.01)	13.92(0.03)	13.86(0.04)	14.95(0.14)	2.13(0.00)
ILMN_1220516	Wnt3a	11.52(0.05)	11.73(0.00)	9.19(0.00)	10.27(0.17)	2.12(0.00)
ILMN_2706269	Hspb1	11.27(0.07)	11.59(0.08)	12.05(0.02)	13.12(0.01)	2.09(0.00)
ILMN_1236009	Camk2b	8.02(0.02)	8.74(0.11)	8.18(0.01)	9.24(0.04)	2.08(0.00)
ILMN_1225528	Trib3	9.59(0.00)	9.47(0.00)	10.28(0.07)	11.34(0.07)	2.08(0.00)
ILMN_2751505	Brd2	12.65(0.01)	12.70(0.08)	12.78(0.05)	13.82(0.10)	2.06(0.00)
ILMN_2613878	Prg2	8.67(0.06)	9.07(0.00)	8.32(0.02)	9.36(0.08)	2.06(0.00)
ILMN_2691780	Myl3	9.27(0.02)	11.21(0.13)	10.15(0.10)	11.19(0.17)	2.05(0.00)
ILMN_1213615	Gpr182	10.15(0.03)	10.42(0.14)	9.13(0.18)	10.17(0.05)	2.05(0.00)
ILMN_1224637	Foxq1	10.20(0.11)	10.11(0.09)	11.26(0.01)	12.29(0.05)	2.04(0.00)
ILMN_2652909	Ddit3	9.55(0.06)	9.69(0.10)	9.46(0.10)	10.49(0.12)	2.04(0.00)
ILMN_2857086	Tra2a	11.60(0.07)	11.81(0.11)	11.18(0.10)	12.20(0.09)	2.03(0.00)
ILMN_2765378	Gpr182	9.70(0.02)	10.00(0.08)	8.74(0.09)	9.75(0.17)	2.02(0.00)
ILMN_2778279	Fosb	7.85(0.00)	7.79(0.04)	8.58(0.02)	9.59(0.13)	2.01(0.00)

Table 1. Differentially expressed genes in WT versus IL-1R$^{-/-}$ ($|FC| \geq 2$)

SD, standard deviation; *P*, adjusted p-value; FC, fold change; Statistical significance determined by Local Pooled Error(LPE) test.

Chapter II.

Expansion of Tfh-like cells during chronic *Salmonella* exposure mediates the generation of autoimmune hypergamma-globulinemia in MyD88-deficient mice

I. Introduction

Bacterial persistence leads to polyclonal B-cell proliferation and hypergammaglobulinemia [105]. Although the mechanism underlying nonspecific B-cell activation in chronic infection is uncertain, possible explanations include direct activation by B-cell mitogens and bystander activation by cytokines from helper T cells [105-107]. In several studies using MyD88$^{-/-}$ mice, the activation of B cells through Toll-like receptor (TLRs) is regarded as a key factor [105]. Furthermore, MyD88 signaling in innate cells may contribute to autoantibody production in B cell-activating factor of the tumor necrosis factor family (BAFF) transgenic mice [108]. Also, T cell-independent activation of autoreactive B cells is known to be elicited in a MyD88-dependent manner [109]. However, another recent study found that mice deficient in MyD88 still elicit hypergammaglobulinemia and autoantibody production after chronic infection by *Borrelia burgdorferi* [110], suggesting there might be other stimulators for B-cell activation in chronic bacterial infection.

Although B cells can be activated in a T cell-independent manner, T cells provide a milieu for efficient B-cell proliferation, somatic hypermutation, and class-switch recombination of immunoglobulin [111, 112]. Follicular helper T (Tfh) cells, which were recently characterized as a new subset of CD4$^+$ helper T cells, are now regarded as critical for the regulation of humoral responses, including the germinal center (GC) reaction [39, 40]. Tfh cells express ICOS, CD40L, PD-1, and CXCR5 on the cell surface, but their function has not been fully elucidated. ICOS-ICOSL interaction, IL-21 and IL-6, but not IL-4, IFN-γ, and TGF-β, are important for the generation of Tfh cells, suggesting that Tfh cells are a distinct subset of CD4$^+$ helper T cells, independent of Th1, Th2, and Th17 cells [39, 40, 113]. Further, PD-1 expressed on Tfh was recently found to be important for the survival and selection of B cells in the GC [43].

In this study, it was sought whether MyD88-dependent TLR signals are required for the generation of B cell responses in the course of *Salmonella* infection at the late chronic stage. Unexpectedly, $MyD88^{-/-}$ mice given oral recombinant attenuated *Salmonella* Typhimurium vaccine (RASV) strain exhibited autoimmune hypergammaglobulinemia with an enhanced GC reaction; however, wild-type mice had no significant changes. Further, it was found that the enhanced B-cell responses in the MyD88-deficient condition was directly due to the aberrant generation of Tfh ($CD4^+ICOS^+PD\text{-}1^+CXCR5^+$) and extrafollicular helper T cells ($CD4^+ICOS^+PD\text{-}1^+ CXCR5^-$) during chronic inflammation, and that inflammatory $CD11b^+Gr\text{-}1^+$ myeloid cells accumulated adjacent to $CD4^+$ T cells. Collectively, the enhanced generation and activation of Tfh-like cells triggered hypergammaglobulinemia with autoimmunity in the MyD88-deficient condition with persistent *Salmonella* exposure.

II. Materials and Methods

1. Mice

Wild-type BALB/c and C57BL/6 (B6) mice were purchased from Charles River Laboratories (Orient Bio Inc., Korea). MyD88$^{-/-}$ mice were kindly provided by Shizuo Akira (Research Institute for Microbial Diseases, Osaka Univ., Osaka, Japan). All mice used in the experiments were between 6 and 12 weeks of age. Mice were maintained under pathogen-free conditions in the experimental facility at the IVI (Seoul, Korea), where they received sterilized food and water ad libitum. The experiments were approved by the Institutional Animal Care and Use Committee of the IVI.

2. Bacteria strain

Recombinant attenuated *Salmonella* vaccine strain (RASV), *S.* Typhimurium *χ*9241 [*ΔpabA1516 ΔpabB232 ΔasdA16 ΔaraBAD23 Δrel*A198:: *ara*CP_{BAD}*lacI* (ATG)TT, containing pYA3620] (RASV), was used in this study [65, 114]. The strain was grown at 37℃ in Luria-Bertani broth without shaking. The actual administered bacterial dose was confirmed by plating serial dilutions onto MacConkey agar plates (Becton Dickinson, Sparks, MD).

3. Ab for flow cytometric analysis

All Abs were from BD Biosciences (San Jose, CA) except for anti-OX40L (RM134L; eBioscience, San Diego, CA) and anti-F4/80 (BM8; Invitrogen, Camarillo, CA).

4. Cytokine detection

BD™ CBA (Cytokine Bead Assay) Mouse Inflammation kit and Th1/Th2/Th17 kit (BD Biosciences) were used to assess the amount of cytokines in the serum. The splenocyte was restimulated with PMA (50 ng/ml) and ionomycin (750 ng/ml) in the medium containing BD GolgiStop™ for 4 hr in vitro. Multicolor staining for surface Ags and intracellular IL-21 was performed by BD Cytofix/Cytoperm™ according to the manufacturer's protocol.

5. ELISA

NUNC-Immuno MaxiSorp plates (NUNC, Denmark) were coated with 2 μg/ml goat F(ab')2 anti-mouse Ig-UNLB, human adsorbed (Southern Biotechnology Associates, Birmingham, AL) in 50 mM sodium bicarbonate and incubated overnight at 4℃ as described elsewhere [115]. After blocking with 1% BSA in PBS, 100 μl/well serum serial dilutions or standard dilutions in 1% BSA in PBS were added to the plates for 2 hr at 37℃. HRP-conjugated goat anti-mouse IgG, IgA, and IgM Abs (Southern Biotechnology Associates) (1:3000 anti-mouse immunoglobulin Ab except for IgM (1:10000) in 0.1% BSA in PBS plus 0.1% Tween 20) was added to each well at 37℃. For color development, the substrate solution (TMB; Moss, Pasadena, MD) was added. Color development was stopped by adding 0.5 N HCl and measured at 450 nm on an ELISA reader (Microplate spectrophotometer; Molecular Devices, Sunnyvale, CA).

6. Anti-double-stranded DNA assay

Anti–double-stranded (ds) DNA Ab were detected using NUNC-Immuno MaxiSorp plates (NUNC A/S). Plates were coated overnight at 4℃, first with 100 μg/ml methylated BSA (Calbiochem, San Diego, CA) and then with 50 μg/ml of grade I calf thymus DNA (Sigma Chemical, St. Louis, MO), which was previously

sheared by sonication, and finally digested with S1 nuclease. After blocking, serial dilutions of the serum samples were added and incubated at room temperature for 2 hr. Autoantibodies were detected with goat anti–mouse IgG-HRP (Sigma) and developed as previously described [116].

7. Neutralizing Ab treatment

Anti-CD4 Ab purified from GK1.5 hybridoma (ATCC, Rockville, MD) was used for depletion of $CD4^+$ T cells (200 μg/mouse). Purified anti-ICOS Ab and anti-PD-1 Ab from eBioscience were injected i.p. for the neutralization of ICOS and PD-1 on $CD4^+$ T cells, respectively. Mice were injected i.p. with 200 μg of Ab or isotype control rat IgG (Sigma) Ab 1 day before vaccination and every 3 or 4 days thereafter.

8. Histopathological analysis

For the IgG and IgA staining, kidneys were fixed in 4% paraformaldehyde and embedded in paraffin. Tissues were cut into 5-μm sections and stained with anti-mouse-IgG-HRP and anti-mouse-IgA-HRP. The peroxidase activity was determined using DAB substrate kit (Vector Labs, Burlingame, CA). The sections were mounted and viewed under x20 optics using a digital light microscope. For the immunohistochemical study, freshly obtained spleens were rapidly frozen in OCT embedding medium (Tissue-Tek, Sakura Finetek, Japan) after sucrose gradient dehydration procedures and stored at -80˚C until processing. Cryostat sections (5 μm) were fixed in cold acetone (-20˚C). Tissues were stained with PE-conjugated CD4, PE- or FITC-conjugated B220 (all BD Pharmingen) and biotin-conjugated peanut agglutinin (PNA) (Vector Labs) and then visualized with Alexa Fluor® 488-conjugated streptavidin (Molecular Probes, Eugene, OR). The sections were mounted with PermaFluor mounting medium (Thermo, Cheshire, UK) and viewed under a confocal scanning laser microscope (Zeiss, Germany).

9. Real-Time RT-PCR

Total splenocytes were obtained from Balb/c background MyD88$^{-/-}$ mice 4 weeks after infection with RASV. Total RNA was isolated from CD4^{+} T cells sorted by MACS (Miltenyi Biotec, Bergisch Gladbach, Germany). Reverse transcription was performed using SuperScript™ II Reverse Transcriptase (Invitrogen) according to the manufacturer's instructions. For real-time PCR analysis, the cDNA was serially diluted 10-fold and amplified using the 7500 Real Time PCR System (Applied Biosystems) with Power SYBR® Green PCR Master Mix (Applied Biosystems). After the first denaturation step (95℃ for 10 min), amplification was performed for 40 cycles at 95℃ for 15 s, 55℃ for 15 s, and 72℃ for 40 s. The final cycle was followed by the dissociation stage. The following primers were used for RT-PCR: T-bet: 5'-CCT GGA CCC AAC TGT CAA CT-3' (forward) and 5'-AAC TGT GTT CCC GAG GTG TC-3' (reverse); GATA3: 5'-CTG GAG GAG GAA CGC TAA TG-3' (forward) and 5'-CAG GGA TGA CAT GTG TCT GG-3' (reverse); BCL-6: 5'-CTG CAG ATG GAG CAT GTT GT-3' (forward) and 5'-CAC CCG GGA GTA TTT CTC AG-3' (reverse); IL-21: 5'-GAG GAC CCT TGT CTG TCT GG-3' (forward) and 5'-TCA CAG GAA GGG CAT TTA GC-3' (reverse); and CXCR5: 5'-CGA CAT CAG ACA GTG ACC AGC C-3' (forward) and 5'-GTC CTG TAG GGG AAT CTC CGT G-3' (reverse) [117, 118].

10. Isolation of myeloid cells

Splenocytes were prepared from RASV-infected MyD88$^{-/-}$ mice and Gr-1-positive cells were isolated using biotinylated anti-Gr-1 Ab (RB6-8C5) and anti-biotin microbeads (Miltenyi Biotec). The purity of Gr-1^{+} cells was more than 90% in total viable cells and most of the Gr-1^{+} cells were CD11b positive (data not shown).

11. In vitro T cell suppression

OT-II $CD4^+$ T cells (5×10^5/well) were stimulated with OVA (grade V; Sigma)-pulsed splenocytes and cocultured for 3 days with $Gr\text{-}1^+$ or $Gr\text{-}1^-$ cells from $MyD88^{-/-}$ mice administered RASV. For the final 24 hr, 1 μCi/well of ^3H-thymidine was added and cultured cells were harvested by FilterMate™ Cell Harvester (PerkinElmer®, Downers Grove, IL). ^3H-thymidine incorporation into divided cells was detected by using MicroBeta® TriLux (Wallac, Turku, Finland).

12. Data and statistical analysis

The Student's t-test was used to compare differences between two experimental groups. To compare multiple groups, one-way ANOVA was carried out followed by the Tukey-HSD post hoc test. Each experiment was repeated three times. *P* values of <0.05, <0.01, and <0.001 were considered statistically significant.

III. Results

1. Persistent *Salmonella* exposure in MyD88$^{-/-}$ mice results in systemic inflammation with autoimmune hypergamma-globulinemia

It was previously found that TLR signaling via MyD88 is not essential for generation of antigen-specific B cell responses, but adoptive transfer of MyD88$^{-/-}$ B220^{+} cells to μMT mice led to significant defects of antigen-specific Ab production after oral administration with recombinant attenuated *Salmonella* Typhimurium vaccine (RASV) strains [115]. In the current study, it was attempted to determine which factors contribute to B cell responses in MyD88$^{-/-}$ mice given the attenuated vaccine strain RASV χ9241 (ΔpabA ΔpabB ΔasdA) strain that has been used extensively as a multivalent vector expressing heterologous antigens. RASV is able to invade and transiently persist in lymphoid tissues including Peyer's patches, spleen, and liver. It stimulates immune responses but causes no disease symptoms in wild-type mice. Unexpectedly, in this study, oral administration of RASV provoked significantly increased total IgG and IgA levels in the sera of MyD88$^{-/-}$ mice as compared with levels found in wild-type mice of BALB/c and B6 background (Fig.1A and B); however, IgM levels were similar in both wild-type and MyD88$^{-/-}$ mice after RASV administration (Fig. 1A). In addition to the increase of total IgG in the sera of MyD88$^{-/-}$ mice, *Salmonella*-specific IgG Ab were also elevated (Fig. 2A). These data are supported by the findings in the previous studies in which anti-LPS or anti-PspA specific Ab was determined [65, 115]. Next, it was investigated whether the hypergammaglobulinemia in MyD88$^{-/-}$ mice after RASV administration, especially with increased serum IgG levels, could be related to autoimmunity. Surprisingly, anti-dsDNA autoantibodies were detected in sera obtained from MyD88$^{-/-}$ mice at 4

weeks after oral RASV challenge (Fig. 2B). Moreover, the deposition of immune complex was observed in kidneys of RASV-administered MyD88$^{-/-}$ mice (Fig. 2C). In addition, MyD88$^{-/-}$ mice had increased levels of serum pro-inflammatory cytokines including IL-6, TNF-α, MCP-1, and IFN-γ, but not IL-4 and IL-5 at 2 weeks after oral RASV challenge (Fig. 3A). Further, significant numbers of *Salmonella* were found persisting in polymorphonuclear cells of MyD88$^{-/-}$ mice, but not in wild-type mice, at 4 weeks after oral administration of RASV (Fig. 3B). These findings suggest that MyD88$^{-/-}$ mice failed to eradicate *Salmonella* even though the production of inflammatory cytokines and *Salmonella*-specific Ab was elevated. Taken together, MyD88$^{-/-}$ mice orally infected with attenuated *Salmonella* showed autoimmune hyper-IgG responses with systemic inflammation in the chronic stage.

2. Expansion of B cell compartment is accompanied by augmentation of CD4^{+} T cells and CD11b^{+}Gr-1^{+} myeloid cells

In accordance with hyper-IgG responses, MyD88$^{-/-}$ mice administered oral RASV had enlarged spleens, mesenteric and cervical lymph nodes, and Peyer's patches (Fig. 4A). Of interest, total recovered CD4^{+} T cells, CD11b^{+}Gr-1^{+} inflammatory myeloid cells, as well as CD19^{+} B cells were significantly increased in spleens of MyD88$^{-/-}$ mice compared with wild-type mice after oral RASV challenge (Fig. 4B). Previous studies suggested that GC formation was delayed until 1 month after attenuated *Salmonella* infection in wild-type mice [119, 120]. Further, extrafollicular Ab responses to attenuated *Salmonella* were IL-21-independent [119, 120], whereas GC B cell responses were regulated by IL-21 produced by T cells [121]. In the present study with MyD88$^{-/-}$ mice, however, significantly increased GC formation in MyD88$^{-/-}$ mice was found than in wild-type mice 4 weeks after oral RASV challenge (Fig. 5A and B). A previous study found the phenotype of GC B cells is B220^{+}CD19^{+}GL7^{high} [122]. Thus, GL7

staining was used to further confirm the acceleration of GC formation in MyD88$^{-/-}$ mice following oral RASV administration. Expanded CD19^{+} B cells in the spleens of RASV-administered MyD88$^{-/-}$ mice significantly co-expressed high levels of GL7 on their surfaces unlike those of wild-type mice (Fig. 5C and Fig. 6). These finding suggest that B cells are highly proliferative and generate GC under the MyD88-deficient condition caused by chronic *Salmonella* infection. To clarify the cross-talk among the expanded cell populations in RASV-administered MyD88$^{-/-}$ mice, the distribution of each cell population in the spleen was determined by immunofluorescence confocal microscopy. Two-color staining of spleen sections of RASV-administered MyD88$^{-/-}$ mice produced overviews of cell population locations in which extrafollicular CD4^{+} T cells (red) were adjacent to Gr-1^{+} cells (green) (Fig. 7A). Further, some CD4^{+} T cells (red) were located in the B cell follicles (green) (Fig. 7B). These results suggest the possibility of cross-talk between CD4^{+} T cells by CD11b^{+}Gr-1^{+} inflammatory myeloid cells as well as the activation of B cells by CD4^{+} T cells inside the B cell follicles.

3. Hypergammaglobulinemia is CD4^{+} T cell-dependent and Tfh-like cells accumulate in MyD88$^{-/-}$ mice after RASV challenge

Since the role of CD4^{+} T cells was important for efficient B cell response, the need for CD4^{+} T cells for hypergammaglobulinemia was assessed by depleting CD4^{+} T cells with anti-CD4 mAb in groups of mice orally administered RASV. In both wild-type and MyD88$^{-/-}$ mice, the depletion of CD4^{+} T cells completely blocked the generation of polyclonal IgG Ab in sera after oral RASV challenge (Fig. 8A). Since the induction of several cell surface molecules on CD4^{+} T cells have been suggested to be closely related to hypergammaglobulinemia [123], the expression of PD-1, CD62L, GITR, and CD25 on splenic CD4^{+} T cells was

determined after RASV challenge. It was found that the expression of PD-1 was drastically increased in the splenic $CD4^+$ T cells of $MyD88^{-/-}$ mice compared with those of wild-type mice after oral RASV challenge (Fig. 8B). Further, the phenotypes of $CD4^+PD\text{-}1^+$ T cells were addressed using other Tfh cell markers including CXCR5, ICOS, OX40, and CD127 [39, 40]. It was found that more than half of the $CD4^+PD\text{-}1^+$ cells expressed ICOS and OX40 and lost CD127 expression, a well-known phenotype for Tfh cells [39, 40, 124]. In addition, 14.3($\pm$2.5)% of $CD4^+$ T cells from $MyD88^{-/-}$ mice had the phenotypes of Tfh cells, expressing both CXCR5 and PD-1, compared with only 3.1($\pm$1.1)% of $CD4^+$ T cells from wild-type mice at 4 weeks after RASV administration (Fig. 9A). Approximately 35% of $CD4^+PD\text{-}1^+$ T cells expressed CXCR5 as did more than 55% of $ICOS^+$ cells in $CD4^+PD\text{-}1^+$ T cells in the spleens of RASV-infected $MyD88^{-/-}$ mice (Fig. 9A). ICOS expression was assessed in splenic $CD4^+$ T cells before and after RASV administration. There were dramatically higher levels of $ICOS^+CD4^+$ T cells in RASV-administered $MyD88^{-/-}$ mice than in wild-type mice but identical numbers of $ICOS^+CD4^+$ T cells at the steady-state condition (Fig. 9B). The ICOS expression on splenic $CD4^+$ T cells of $MyD88^{-/-}$ mice increased 2 weeks after RASV administration (Fig. 9C), which correlated with the increased kinetics of serum IgG (Fig. 1B). Of most importance, the expanded $CD4^+ICOS^+$ cells from RASV-infected $MyD88^{-/-}$ mice produced IL-21; however, $MyD88^{-/-}$ mice had more IL-21-secreting cells than the RASV-infected wild-type mice (Fig. 10A). Further the RASV-administered $MyD88^{-/-}$ mice had significantly increased transcriptional levels of bcl-6, IL-21, and CXCR5, but not of t-bet and gata-3 (Fig. 10B), suggesting the transcriptional patterns of Tfh cells [31]. Of note, many $ICOS^+$ cells (stained red) were located inside the B cell follicles (green) in $MyD88^{-/-}$ mice after oral RASV challenge (Fig. 10C). Overall, these data suggest that the induction of hypergammaglobulinemia was $CD4^+$ T cell-dependent and that Tfh-like cells, including Tfh cells ($CD4^+ICOS^+PD\text{-}1^+CXCR5^+$) and extrafollicular helper T cells

($CD4^+ICOS^+PD\text{-}1^+CXCR5^-$), were highly accumulated in $MyD88^{-/-}$ mice after RASV administration.

4. Characteristics of $CD11b^+Gr\text{-}1^+$ inflammatory myeloid cells accumulated in $MyD88^{-/-}$ mice after oral RASV challenge

Next focus was on the role of $CD11b^+Gr\text{-}1^+$ myeloid cells, which were dramatically expanded in $MyD88^{-/-}$ mice after RASV administration (Fig. 4B and Fig. 11). The expansion of $CD11b^+Gr\text{-}1^+$ cells could be ascribable to the increased levels of serum GM-CSF [125] in the $MyD88^{-/-}$ mice after RASV administration, which occurred in a time-dependent manner (Fig. 11B). Analysis of the cell surface phenotypes showed expanded $CD11b^+Gr\text{-}1^+$ cells in both wild-type and $MyD88^{-/-}$ mice highly expressed MHC class II, CD40, CD80, and CD86 together with low expression of CD11c on their surfaces after oral RASV challenge (Fig. 12). They also expressed PD-L1 and ICOS-L, suggesting possible cross-signaling between Tfh-like cells and $CD11b^+Gr\text{-}1^+$ cells (Fig. 12). In addition, accumulated $CD11b^+Gr\text{-}1^+$ cells in the spleens of $MyD88^{-/-}$ mice after oral RASV administration mainly consisted of $Ly\text{-}6C^{int}Ly6G^{high}$, $Ly\text{-}6C^{int}Ly\text{-}6G^{low}$, and $Ly\text{-}6C^{high}Ly\text{-}6G^{low}$ cells (Fig. 13A) [126]. Further analysis of the cell surface phenotypes showed that most $CD11b^+Gr\text{-}1^+$ cells highly expressed MHC class II and that $Ly\text{-}6C^{high}Ly\text{-}6G^{low}$ cells in particular expressed CD40, CD80, and CD86 but had low expression of CD11c on their surfaces (Fig. 13B). Of interest, $CD11b^+Gr\text{-}1^+$ cells isolated from RASV-administered wild-type and $MyD88^{-/-}$ mice were the main cell population producing high levels of IL-6 after restimulation with RASV *in vitro* (Fig. 14). This finding might be important for B cell activation by inducing Tfh-like cells. Collectively, these data indicate that aberrantly expanded $CD11b^+Gr\text{-}1^+$ inflammatory myeloid cells in $MyD88^{-/-}$ mice could influence $CD4^+$ T cells to

regulate Tfh-like cell differentiation after RASV challenge in the chronic inflammatory condition.

5. Blockade of $CD4^+$ Tfh-like cells by anti-ICOS or anti-PD-1 Ab treatment ameliorates the induction of hypergammaglobulinemia in RASV-administered $MyD88^{-/-}$ mice

Next, to assess whether the expanded $CD4^+$ Tfh-like cells could induce B cell class switching to IgG, the function of $CD4^+$ Tfh-like cells was blocked by anti-ICOS or anti-PD-1 Ab treatment in $MyD88^{-/-}$ mice after oral RASV administration and checked to see if they could prevent the induction of hypergammaglobulinemia in chronic inflammation caused by persistent *Salmonella* infection. It was found that blockade of ICOS costimulation reduced the increment of total serum IgG production in the $MyD88^{-/-}$ mice (Fig. 15A). In addition, blocking of PD-1 signaling significantly reduced the induction of hypergammaglobulinemia in the $MyD88^{-/-}$ mice (Fig. 15B). The blockade of ICOS or PD-1 signaling also decreased anti-dsDNA specific autoantibodies in the RASV-administered $MyD88^{-/-}$ mice (Fig. 15C). Taken together, ICOS- and PD-1-expressing Tfh-like cells, which expand in $MyD88^{-/-}$ mice after chronic *Salmonella* infection, are crucial for aberrant induction of serum IgG Ab and the blockade of ICOS and PD-1 ameliorate the induction of autoimmune hypergammaglobulinemia in chronic inflammation.

IV. Discussion

Although the activation of autoreactive B cells during infection has long been considered to result from non-specific bystander activation of polyclonal B cells, the mechanisms of hypergammaglobulinemia in the infected host remain uncertain [106]. Chronic infection with *B. burgdorferi* in self-reactive B cell transgenic mice breaks the immunologically ignorant status of autoreactive B cells and causes hypergammaglobulinemia in a $CD4^+$ T cell-dependent manner, in which *in vitro* B cell proliferation against *B. burgdorferi* is completely dependent on MyD88-mediated TLR signaling [105]. In contrast, $MyD88^{-/-}$ mice show significant B cell hyperplasia accompanying autoantibody production and hypergamma-globulinemia in the same *B. burgdorferi* infection model [110]. Thus, the suppressive role of MyD88 on B cells has been proposed as a control mechanism against autoreactive B cell activation. Similarly, MyD88 has been postulated to provide a negative signal for Th2 cell development via TLR signaling in dendritic cells [127, 128]. However, in a model of polymicrobial sepsis, the MyD88-dependent accumulation of $Gr\text{-}1^+CD11b^+$ cells in the spleen mediated Th2 cell-dependent hyper-B cell responses [129]. Thus, the role of MyD88-dependent innate signaling for the regulation of B cell responses in the inflammatory condition remains controversial, especially the role of $CD11b^+Gr\text{-}1^+$ myeloid cells. In this regard, it was previously shown that in mice vaccinated with attenuated *Salmonella,* MyD88 is not essential for generation of antigen-specific B cell responses. However, adoptive transfer of $MyD88^{-/-}$ $B220^+$ cells to μMT mice led to significant defects of antigen-specific Ab production after oral vaccination with attenuated *Salmonella* strains, suggesting that there might be other stimulators for B cell activation in $MyD88^{-/-}$ mice chronically infected with bacteria [115]. In the present study, persistent *Salmonella* infection resulted in the generation of Tfh-like cells expressing ICOS, PD-1, and IL-21, which are responsible for hyper-B cell responses.

During analysis of expanded cell populations in RASV-administered MyD88$^{-/-}$ mice, significant expansion of splenic ICOS^{+}CD4^{+} T cells was detected, which resembled Tfh cells, and typically express PD-1, CXCR5, BCL-6, and IL-21 [39, 40]. Tfh cells are a subset of activated CD4^{+} T cells and are specialized to regulate B cell-mediated humoral immunity [113, 130]. Furthermore, a recent study suggested that persistent infection of virus could drive the differentiation of helper T cells to Tfh cells [131]. Although Tfh cells are linked to GC B cell survival and the formation of long-lived plasma cells [43, 132], their role in chronic inflammatory condition, especially related to persistent bacteria, has not been reported.

ICOS has been considered an inducible T cell costimulatory molecule important for CD40-mediated Ab class switching [133]; however, recent studies of uncontrolled expression of ICOS in several gene-modified mice showing lupus-like pathology provide insight for the close relationship between ICOS-expressing CD4^{+} T cells and autoimmunity [123, 134]. In the present study, blockade of ICOS using neutralizing Ab significantly reduced the production of total IgG in RASV-administered MyD88$^{-/-}$ mice, suggesting possible cross-talk between Tfh-like cells and B cells via ICOS-ICOSL interaction for hypergammaglobulinemia.

The results of current study suggest that extra-follicular helper T cells assist in the production of autoantibodies in an IL-21-dependent manner similar to Tfh cells, but that they do not express CXCR5 and that they are located outside the B cell follicles [123]. Further, dysregulation of Tfh cells or extrafollicular helper T cells has been linked with development of autoimmunity in several murine models of human lupus and rheumatoid arthritis [123, 135, 136]. In the present study, CD4^{+}ICOS^{+}PD-1^{+} T cells expanded in RASV-administered MyD88$^{-/-}$ mice were found to be a mixed population of both Tfh cells (CXCR5^{+}) and extrafollicular helper T cells (CXCR5^{-}) (Fig. 9A). Thus, it is possible that both Tfh and extrafollicular helper T cells are involved in the development of hypergammaglobulinemia.

PD-1 is a well-known marker for $CD8^+$ T cell exhaustion [137] and recently the blockade of PD-1 has been reported to enhance Ab production in response to helminth infection [138]. However, PD-1 was also found to be involved in GC B cell survival and formation of long-lived plasma cells [43]. PD-1 was blocked using anti-PD-1 Ab in RASV-infected $MyD88^{-/-}$ mice, thereby ameliorating the induction of hypergammaglobulinemia in those mice. When these findings are considered together, the persistent presence of attenuated *Salmonella* strain might trigger $CD4^+$ T cell differentiation into intra- and extrafollicular helper T cells, resulting in aberrant activation of B cell response in RASV-administered $MyD88^{-/-}$ mice.

Interestingly, a recent study showed that CTLA4-Ig, a promising treatment for rheumatoid arthritis, significantly reduced the upregulation of PD-1 and ICOS on Tfh cells in a murine model of arthritis [135, 139], providing evidence for the relationship between abnormal Tfh cell activation and autoimmunity. Further, CTLA4-Ig treatment reduced GC B cell responses and prevented breach of B cell tolerance [135], suggesting that CD28-dependent signaling is also required for optimal Tfh cell generation and that regulation of Tfh cell generation is important to prevent the onset of autoimmunity including autoantibody production.

To determine the specific factors in RASV-infected $MyD88^{-/-}$ mice responsible for Tfh-like cell generation, cells neighboring $CD4^+$ T cells in the spleen were analyzed. Findings of co-localization of $CD4^+$ T cells and $Gr\text{-}1^+$ cells in spleens of RASV-administered $MyD88^{-/-}$ mice (Fig. 7A) suggest that $CD11b^+Gr\text{-}1^+$ inflammatory myeloid cells might regulate the generation of $CD4^+$ Tfh-like cells. Further, $CD11b^+Gr\text{-}1^+$ inflammatory myeloid cells produced IL-6, one candidate cytokine for Tfh cell differentiation [140, 141], and also expressed ICOSL and PD-L1. However, the requirement of IL-6 for Tfh cell development in vivo is still controversial [141], and IL-6 might influence B cell activation T cell-independent manner. Collectively, expanded $CD11b^+Gr\text{-}1^+$ inflammatory myeloid

cells may modulate Tfh-like cells in the chronic inflammatory condition. Previously, the expansion of myeloid-derived suppressor cells (i.e., MDSCs) was reported in mice infected with aroA mutant and wild-type *Salmonella* and these MDSCs inhibited antigen-specific $CD4^+$ T cell proliferation [142]. Likewise, $CD11b^+Gr\text{-}1^+$ inflammatory myeloid cells obtained from RASV-infected $MyD88^{-/-}$ mice showed suppression against OT-II $CD4^+$ cell proliferation when there were equivalent numbers of myeloid cells and $CD4^+$ T cells (Fig. 16). However, proliferation of OT-II $CD4^+$ T cells rose as the numbers of $CD11b^+Gr\text{-}1^+$ myeloid cells declined, suggesting the divergent regulation of $CD4^+$ T cells by $CD11b^+Gr\text{-}1^+$ myeloid cells under different conditions. In addition, although the accumulation of $Gr\text{-}1^+$ myeloid cells with high titers of *Salmonella*-specific Ab was previously reported in mice, there was no significant alteration in splenic $CD4^+$ T cells [143]. Thus, the role of MyD88 for the protection of aberrant $CD4^+$ T cell activation linked with autoimmunity is an intriguing question that warrants further investigation.

Among the $CD11b^+Gr\text{-}1^+$ inflammatory myeloid cells, $Ly6C^{high}Ly6G^{low}$ cells, which have the characteristics of activated macrophages, could be the candidate for Tfh cells differentiation in chronic infection. They highly expressed MHC class II molecules and costimulatory molecules such as CD40, CD80, and CD86. However, direct generation of antigen-specific Tfh cells in vitro by the subset of $CD11b^+Gr\text{-}1^+$ inflammatory myeloid cells was unsuccessful (data not shown). Further studies will be needed to elucidate the mechanism for the differentiation of the Tfh-like cells in the persistent exposure of attenuated *Salmonella*. Another possibility for uncontrolled B cell activation in $MyD88^{-/-}$ mice after RASV infection is failure in the feedback regulation of Tfh cell generation and function by plasma cells. Recently, plasma cells were reported to regulate Tfh cells in an antigen-specific manner and mice deficient in plasma cells showed lack of negative feedback regulation for Tfh cell activity [144, 145].

Collectively, systemic hyper-IgG Ab response to persistent bacterial exposure might be initiated as a danger signal to provoke immune responses but fail to control the infection due to the lack of proper defense by the MyD88 molecule. This could result in chronic inflammation and possibly autoimmunity. Depletion of $CD4^+$ T cells as well as blockade of PD-1 and ICOS in Tfh-like cells prevents aberrant increases of total serum IgG, suggesting that Tfh-like cells expanded in chronic bacterial infection can be considered as targets for the treatment of Ab-mediated immune diseases (Fig. 17).

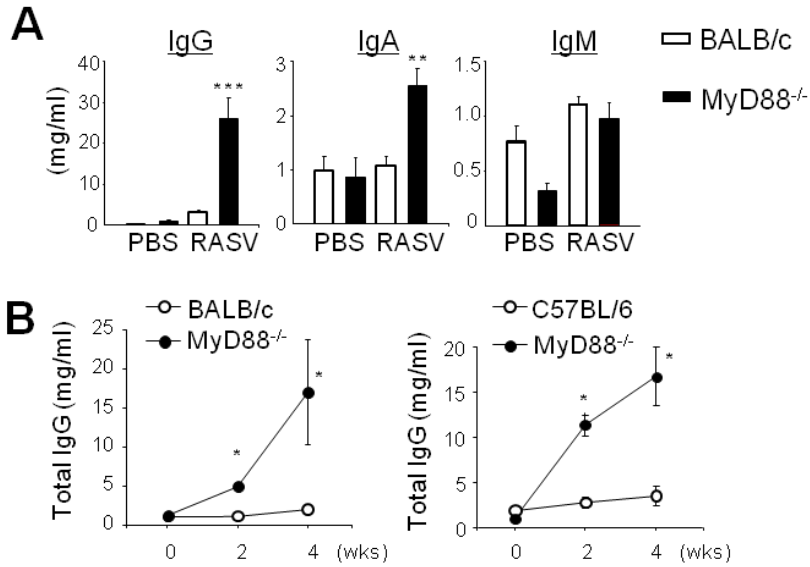

Figure 1. A. Sera from BALB/c and MyD88$^{-/-}$ mice were analyzed for IgM, IgG, and IgA levels 4 weeks after oral administration of RASV ($1x10^9$ cfu). Data are shown as mean +SD of n=4-8 mice per group. B. Serum IgG Ab at weeks 0, 2, and 4 after oral RASV administration in both BALB/c and B6-background wild-type and MyD88$^{-/-}$ mice (n=4~6 mice/group). *$p<0.05$ and **$p<0.01$ (Student *t*-test).

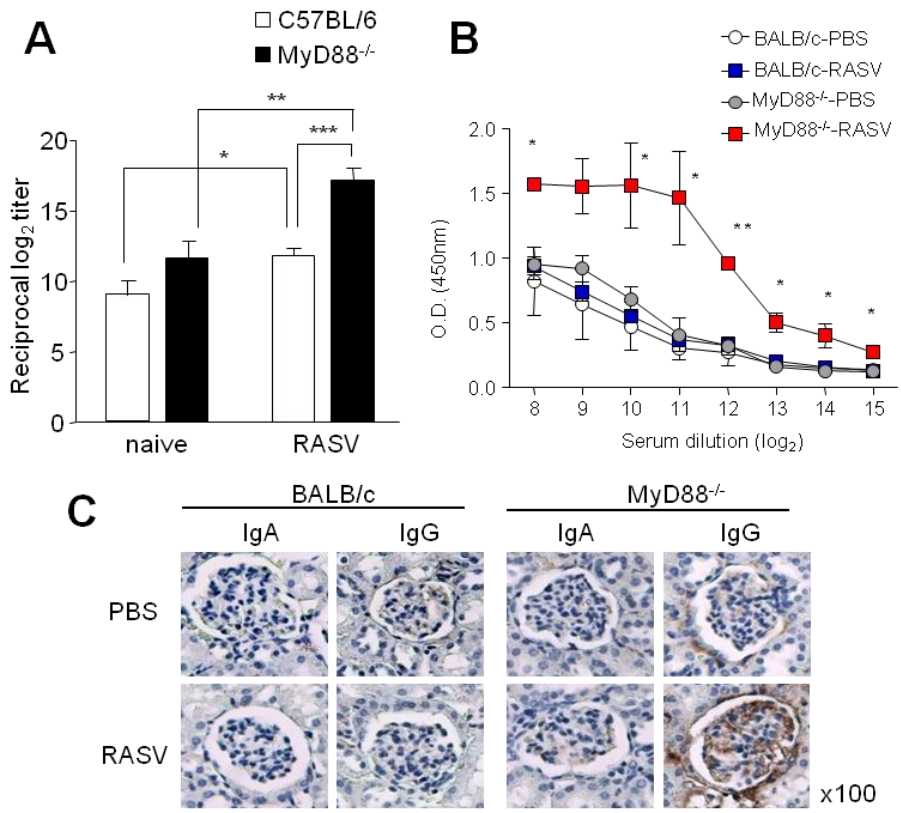

Figure 2. A. Reciprocal titration of anti-*Salmonella* specific IgG Ab in serum at 0 and 4 weeks after RASV administration in wild-type and MyD88$^{-/-}$ mice. Lysate of RASV strain were prepared by freezing and thawing the harvested cells in the lysis buffer (50 mM Tris-HCl (pH 8.0), 1 mM DTT, 0.1% Triton X-100, and protease inhibitor) followed by sonication. Supernatant was then coated for ELISA (n=4 or 5 mice/group). *p<0.05, **p<0.01, ***p<0.001 (Student *t*-test). B. Anti-dsDNA-specific serum IgG Ab were analyzed by ELISA 4 weeks after BALB/c and MyD88$^{-/-}$ mice were orally administered RASV. Data are shown as mean ± SD of n=4 mice per group. *p<0.05 and **p<0.01, ANOVA. C. Kidney sections of BALB/c and MyD88$^{-/-}$ mice 4 weeks after oral RASV administration stained with anti-IgA or anti-IgG Ab. Magnification 100×. Data are representative of five independent experiments

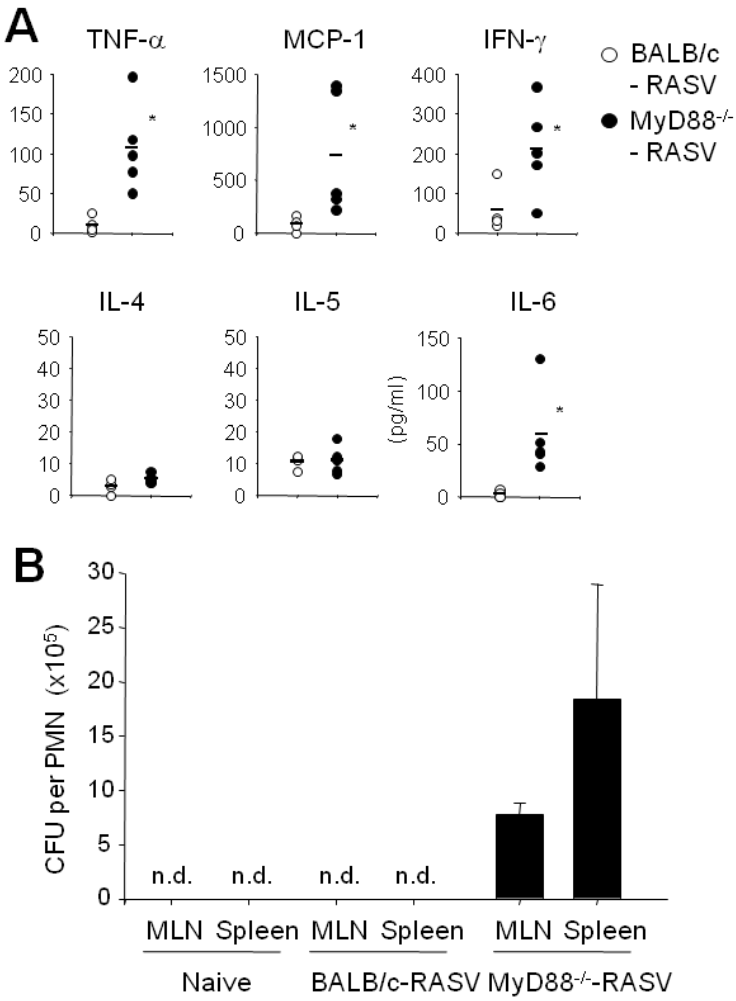

Figure 3. A. Serum cytokine levels including TNF-α, MCP-1, IFN-γ, IL-4, IL-5, and IL-6 at 2 weeks after RASV challenge (n=5 mice/group). *$p<0.05$, Student's *t*-test. B. Intracellular survival of RASV strain as determined by PMN isolated from mesenteric lymph node (MLN) and spleens of wild-type and MyD88$^{-/-}$ mice of BALB/c background 4 weeks after oral administration of RASV (10^9 cfu/head). CFU were counted using *Salmonella-Shigella* agar containing 0.05% arabinose and 0.1% mannose. n.d., not detectable. Data are representative of three independent experiments with three to five mice each.

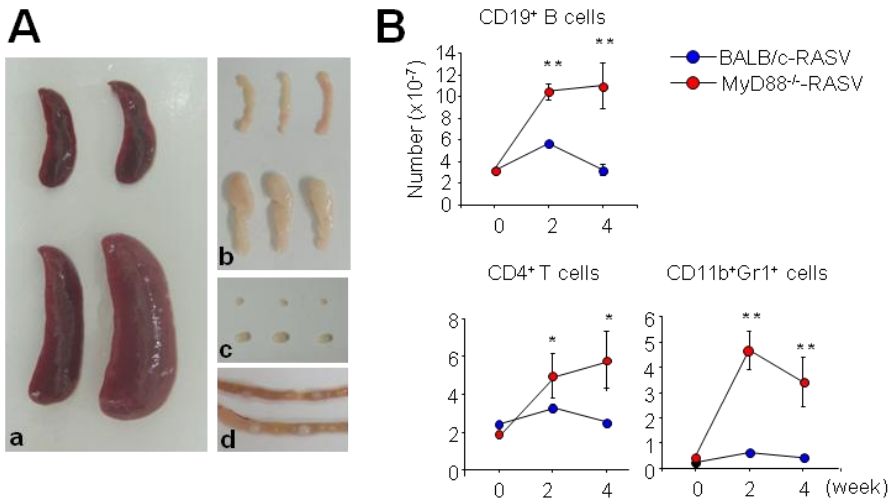

Figure 4. A. Wild-type and MyD88$^{-/-}$ mice were orally administered 1x10^{9} cfu of RASV on day 0 and sacrificed at weeks 2 and 4 (5 mice/group). **A**. Enlarged spleens (a), mesenteric lymph nodes (b), Peyer's patches (c), and inguinal lymph nodes (d) in MyD88$^{-/-}$ mice (bottom) compared with wild-type mice (top) 4 weeks after RASV challenge. Data are representative of five experiments. B. Kinetic analysis of absolute numbers of CD4^{+} T cells, CD19^{+} B cells, and CD11b^{+}Gr-1^{+} myeloid cells in the spleens of wild-type and MyD88$^{-/-}$ mice 2 and 4 weeks after RASV challenge. Data are shown as mean ± SD of n=4-5. *p<0.05, **p<0.01, Student's *t*-test. The data are representative of three independent experiments.

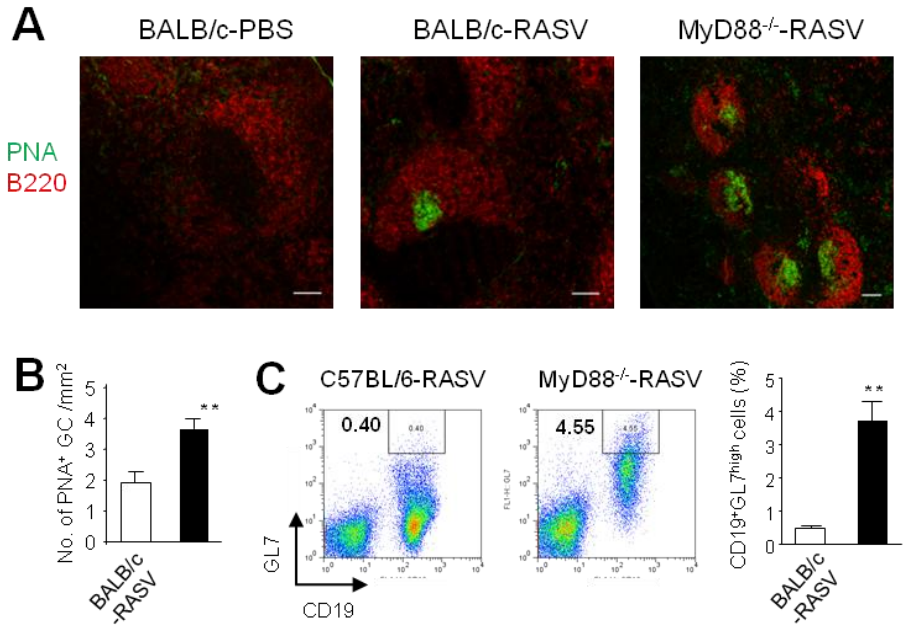

Figure 5. A. Immunofluorescent analysis of spleen sections before and 4 weeks after RASV challenge. Expression patterns of peanut agglutinin (PNA, green) and B220 (red) are shown. Scale bar: 100 μm. B. Number of PNA^+ germinal centers counted in the histologic sections. Data are shown as mean + SD of six independent experiments. C. Flow cytometric analysis of GL7-expressing B cells and statistics for GC B cells. Data are shown as mean + SEM of n=3-4 samples (right). **p<0.01, Student's *t*-test. The data are representative of three independent experiments.

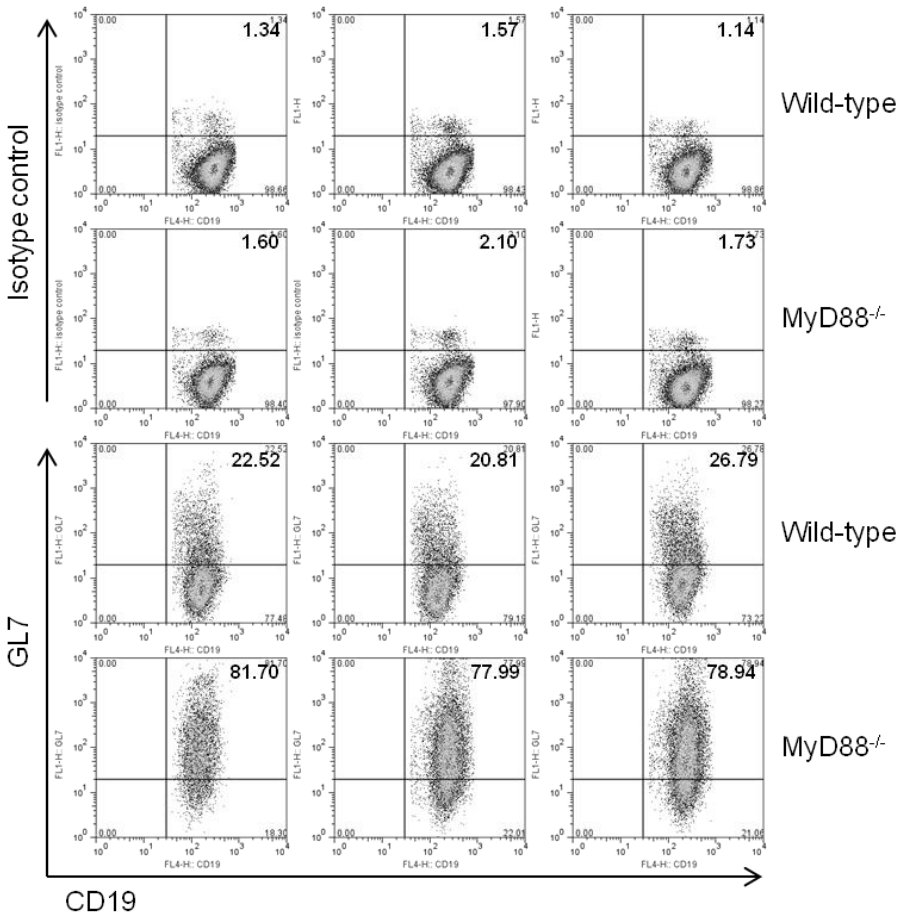

Figure 6. Expression levels of GL7 on $CD19^+$ B cells 4 weeks after oral administration of RASV. Splenocytes from three individual wild-type and $MyD88^{-/-}$ mice were analyzed by FACS to assess GL7 expression, and the percentages of GL7-expressing B cells among total $CD19^+$ B cells were shown.

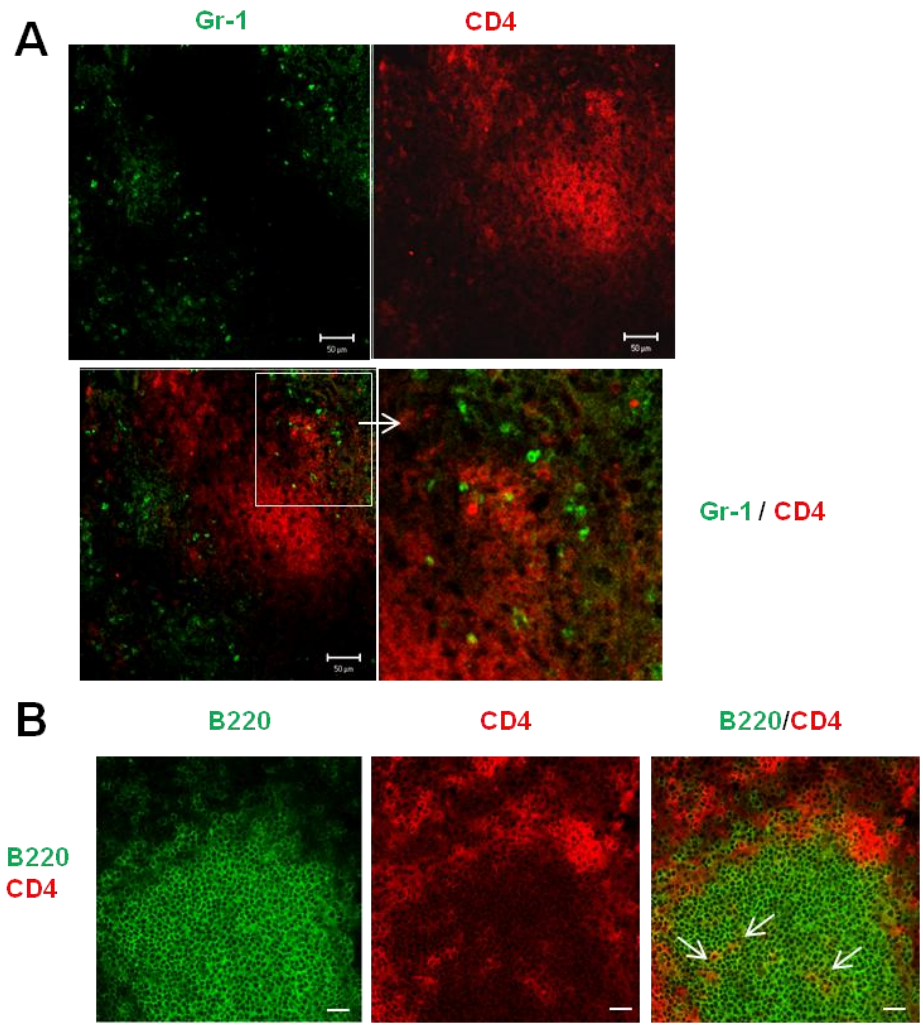

Figure 7. A. Two-color staining with Gr-1 $^{+}$ cells (green) and CD4^{+} T cells (red) in spleens of MyD88$^{-/-}$ mice after oral RASV administration. Scale bar: 50 mm. Data are representative of two independent experiments with at least three mice per group. B. Immunofluorescent analysis of spleen sections from MyD88$^{-/-}$ mice at 4 weeks following oral RASV administration. Expression patterns of B220 (green) and CD4 (red) are shown. Scale bar: 20 μm. Data are representative of five independent experiments.

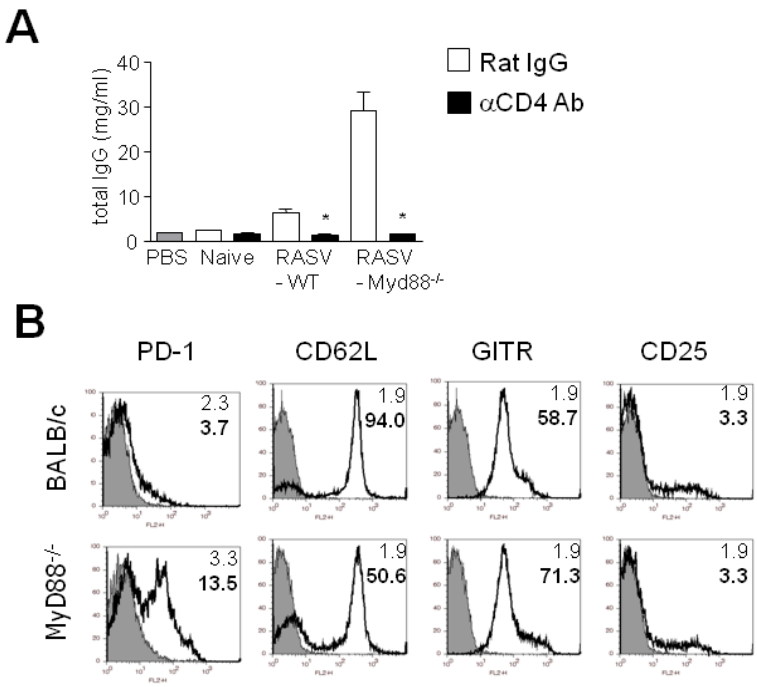

Figure 8. A. Wild-type and MyD88$^{-/-}$ mice were treated with anti-CD4-depleting Ab by i.p. injection at 3-day intervals beginning 1 day before oral RASV administration. Four weeks later, sera were obtained and analyzed for total IgG Ab. Data are shown as mean + SD of n=5 mice from one experiment representative of two. *$p<0.05$ versus control Ab-injected mice, Student's *t*-test. B. Expression levels of PD-1, CD62L, GITR, and CD25 on splenic CD4^{+} T cells in wild-type (WT) and MyD88$^{-/-}$ mice 4 weeks after oral administration of RASV. Data are representative of three independent experiments.

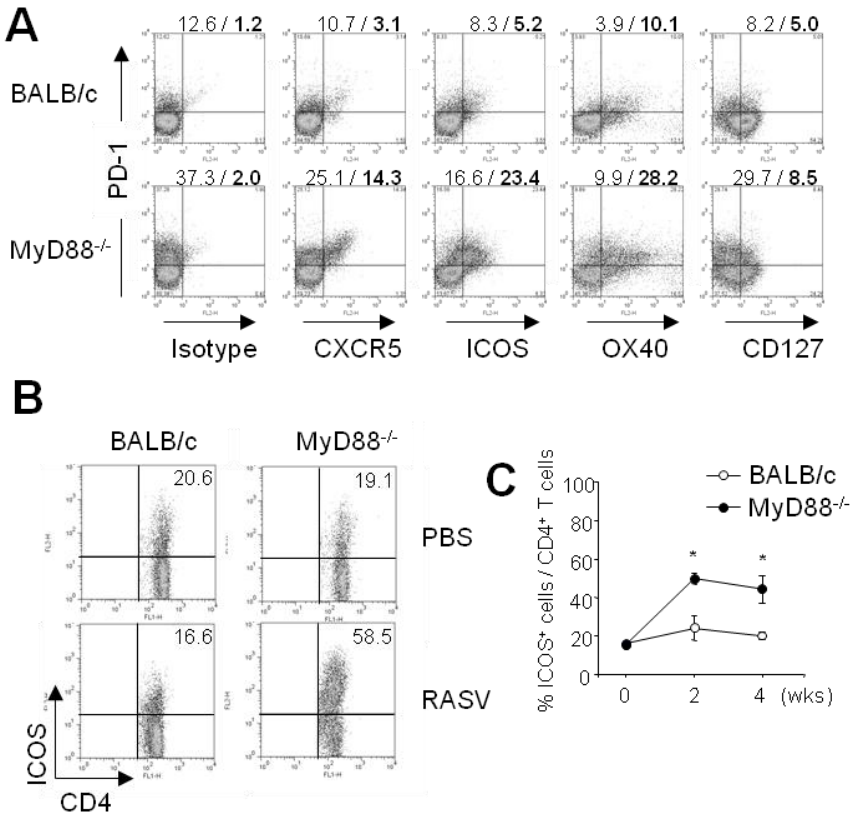

Figure 9. A. Co-expression of Tfh cell markers CXCR5, ICOS, OX40, and CD127 Ab on PD-1-expressing $CD4^+$ T cells was analyzed on splenocytes from WT or $MyD88^{-/-}$ mice 4 weeks after oral RASV administration. Ratios of each negative and positive population among $PD\text{-}1^+$ cell populations are shown in upper left and upper right of each quadrant. Data are representative of three experiments (n=3 mice/group). B. Flow cytometric analysis of ICOS expression on $CD4^+$ T cells from spleens of WT and $MyD88^{-/-}$ mice before and 4 weeks after oral RASV administration. Data are representative of five experiments. C. Kinetic analysis of $ICOS^+$ cells among splenic $CD4^+$ T cells at 0, 2, and 4 weeks after oral RASV challenge. Data are shown as mean ± SD of n=3-4 mice. *$p<0.05$, Student's *t*-test.

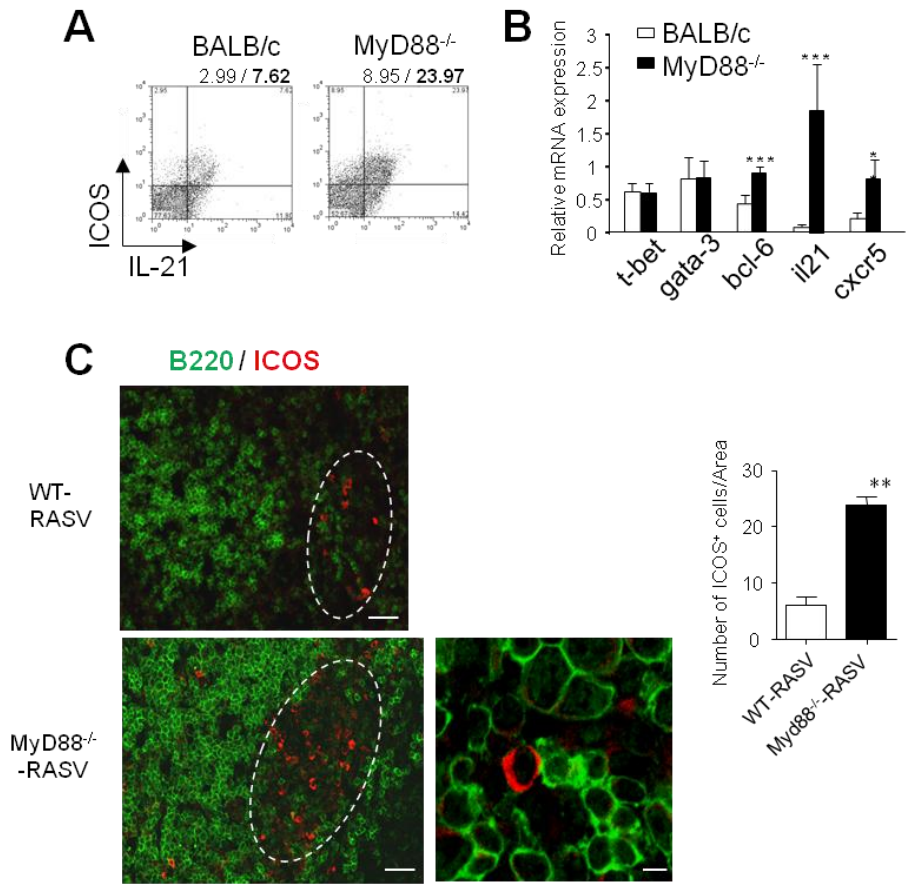

Figure 10. A. IL-21 production of $CD4^+ICOS^+$ cells analyzed by flow cytometry after restimulation with PMA and ionomycin in vitro. The ratio on top of the dot plots represents the percentage of $CD4^+ICOS^+IL\text{-}21^+$ cells in $CD4^+$ cells (n=3 mice/group). B. Relative expression levels of T-bet, Gata-3, Bcl-6, IL-21, and CXCR5 mRNA isolated from splenic $CD4^+$ T cells of BALB/c or $MyD88^{-/-}$ mice 4 weeks after RASV administration analyzed by real-time PCR. Data are mean +SD (n=4) after normalization to β-actin levels. C. Immunohistochemical analyses of spleen sections of BALB/c and $MyD88^{-/-}$ mice. Green; B220, Red; ICOS. Scale bar: 50 mm (left and middle) and 10 mm (right). Data are representative of three independent experiments. Number of $ICOS^+$ cells in indicated areas counted in histologic sections. **p<0.01; ***p<0.001, Student's *t*-test.

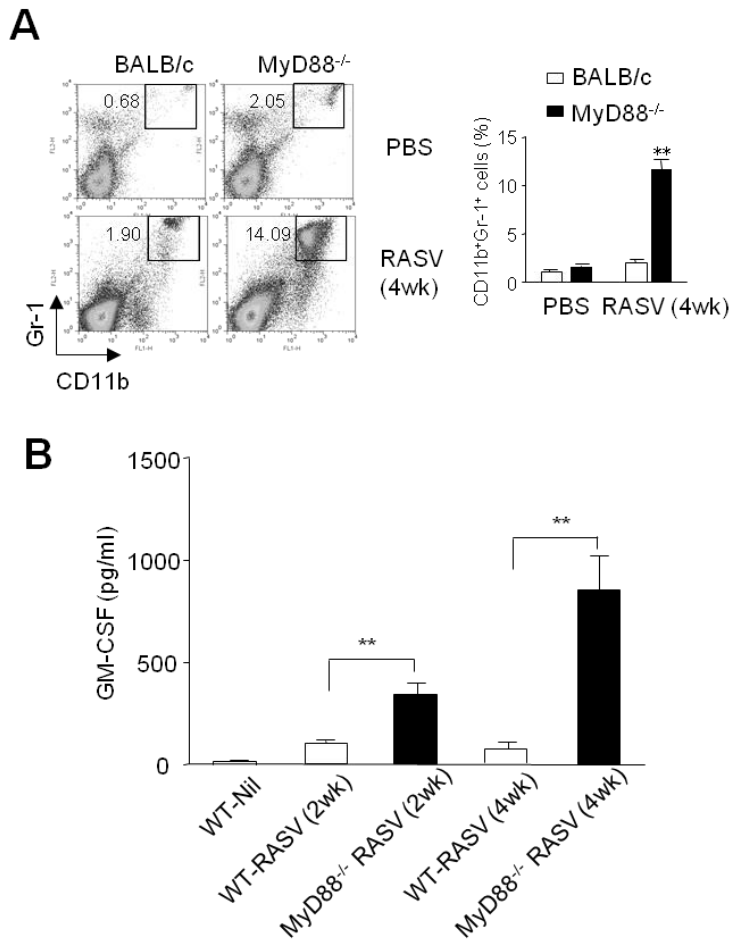

Figure 11. A. Percentages of $CD11b^{+}Gr\text{-}1^{+}$ cells in splenocytes after flow cytometry analysis. Data are shown as mean + SEM of n=2-5 mice/group (right) and are representative of five independent experiments. B. GM-CSF levels in the serum of wild-type or $MyD88^{-/-}$ mice of BALB/c background were determined by ELISA kit (BD Biosciences, San Diego, CA) at 2 or 4 weeks after oral RASV administration. **$p<0.01$, Student's *t*-test. (n=4 or 5 mice/group).

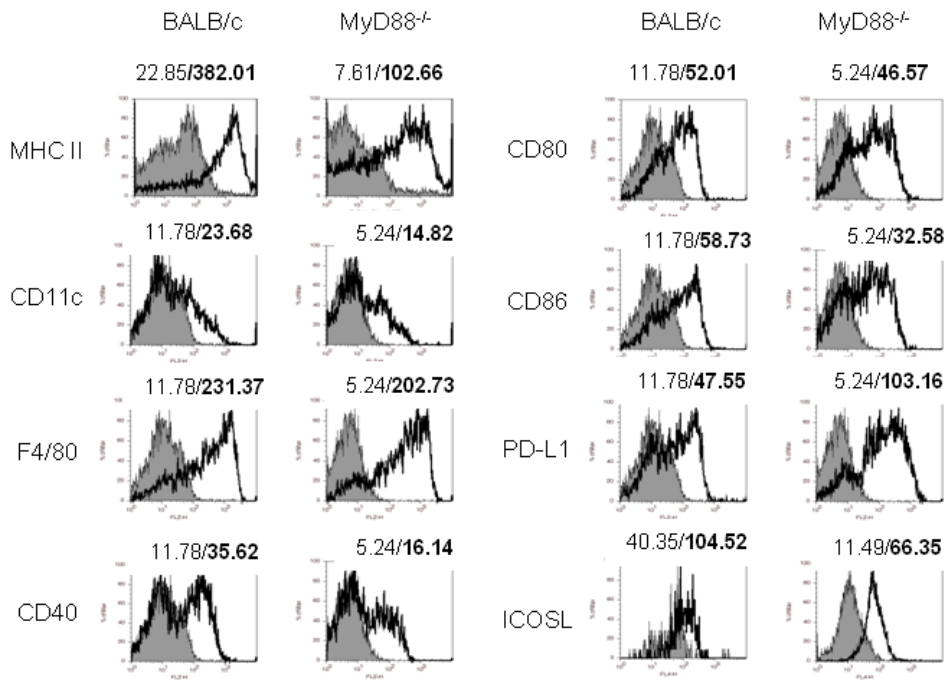

Figure 12. Surface expression of indicated molecules on $CD11b^{+}Gr\text{-}1^{+}$ gated cells from WT and $MyD88^{-/-}$ mice as determined by flow cytometry analysis (gray filled histogram: isotype control). Median fluorescence intensities (MFIs) of gated cells from WT and $MyD88^{-/-}$ mice are indicated at tops of histograms. Data are representative of three independent experiments (n=2–4/group).

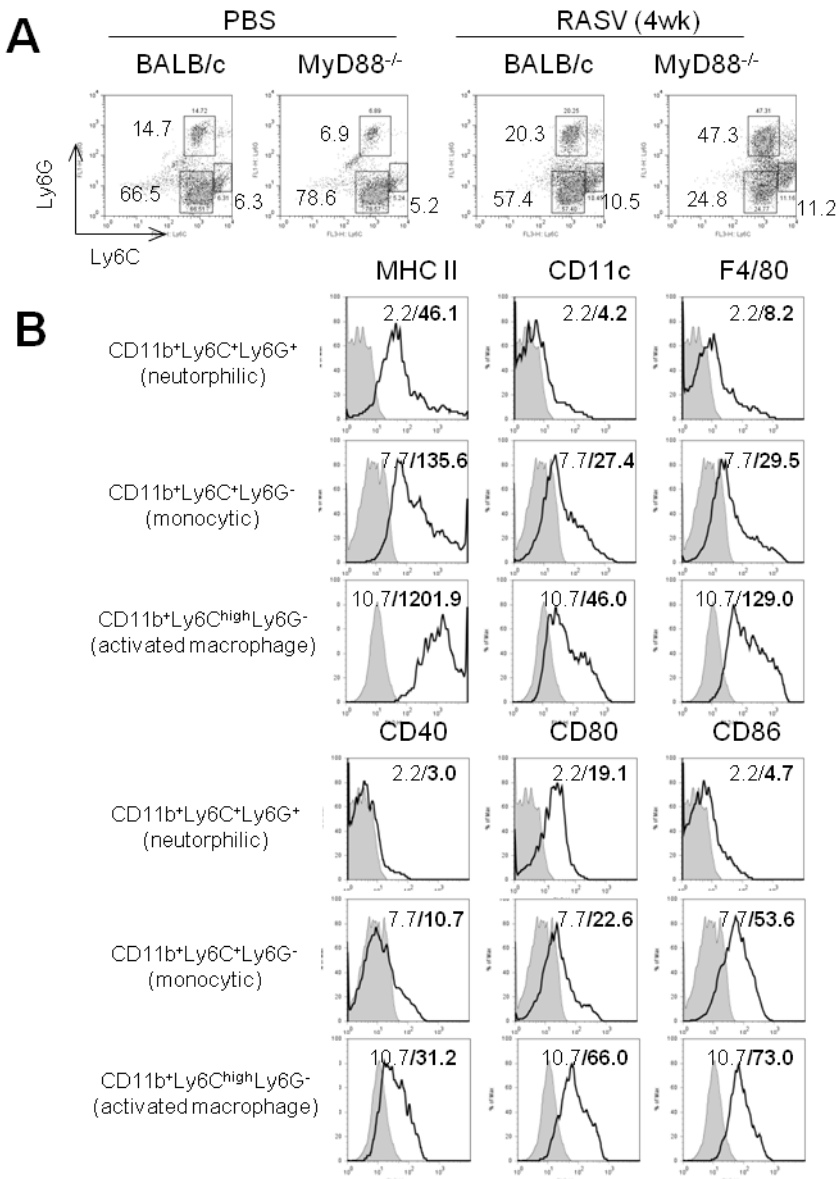

Figure 13. Splenic cell populations in BALB/c and MyD88$^{-/-}$ mice. A. CD11b^{+} Gr-1^{+} cells analyzed by FACS to classify subsets expressing Ly6C and/or Ly6G. B. After gating CD11b^{+}Gr-1^{+} cells into CD11b^{+}Ly6C^{+}Ly6G^{+}, CD11b^{+}Ly6C^{+}Ly6G^{-}, and CD11b^{+}Ly6C^{high}Ly6G^{-} cells, FACS analysis results of surface expression of the indicated molecules on the gated cells. Median fluorescence intensities of gated cells from isotype control (gray) and each specific Ab (bold). Data are representative of three independent experiments with two to four mice per group.

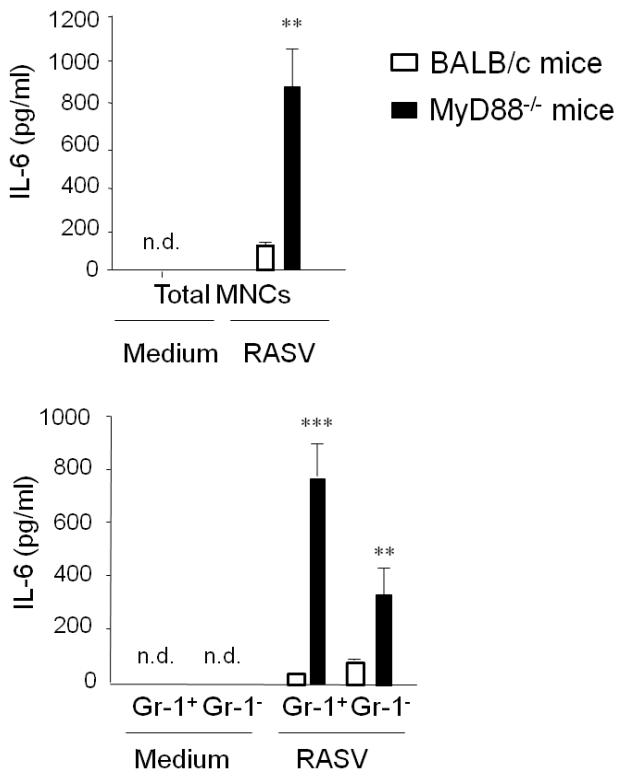

Figure 14. Total mononuclear cells (MNCs), Gr-1^{+}, or Gr-1^{-} cells in spleens of WT (blue bars) and MyD88$^{-/-}$ mice (red bars). MyD88$^{-/-}$ mice were infected with 10 MOI of RASV in vitro for 4 hr before ELISA analysis of IL-6 in supernatant. Data are shown as mean + SD of n=3-5 mice/group and are representative of three independent experiments. **p<0.01 and ***p<0.001 compared with BALB/c-RASV, Student's *t*-test. n.d., not detected.

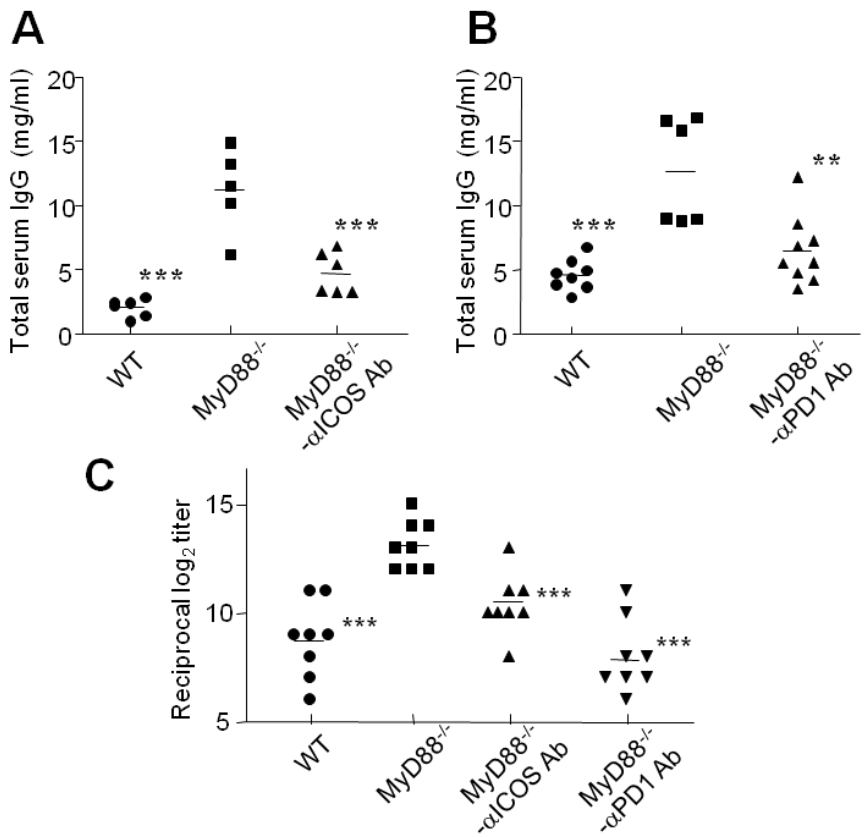

Figure 15. A. MyD88$^{-/-}$ mice (B6 background) were treated i.p. with anti-ICOS Ab (200 μg/mouse) at 3-day intervals beginning 1 day before oral RASV administration (1×10^9 cfu/mouse). Four weeks later, sera were analyzed for total IgG. Data are shown as mean of n=5-6 mice/group. B. MyD88$^{-/-}$ mice (B6 background) were treated i.p. with anti-PD-1 Ab (200 μg/mouse) at 3-day intervals beginning 1 day before oral RASV administration (1×10^9 cfu/mouse). Four weeks later, sera were analyzed for total IgG. Data are shown as mean of n=6-9 mice/group. C. Titers of anti-dsDNA-specific IgG Ab in serum were measured by ELISA. Data are shown as mean of n=8 mice/group. **p<0.01; ***p<0.001 versus MyD88$^{-/-}$ mice, ANOVA. The data are representative of three independent experiments.

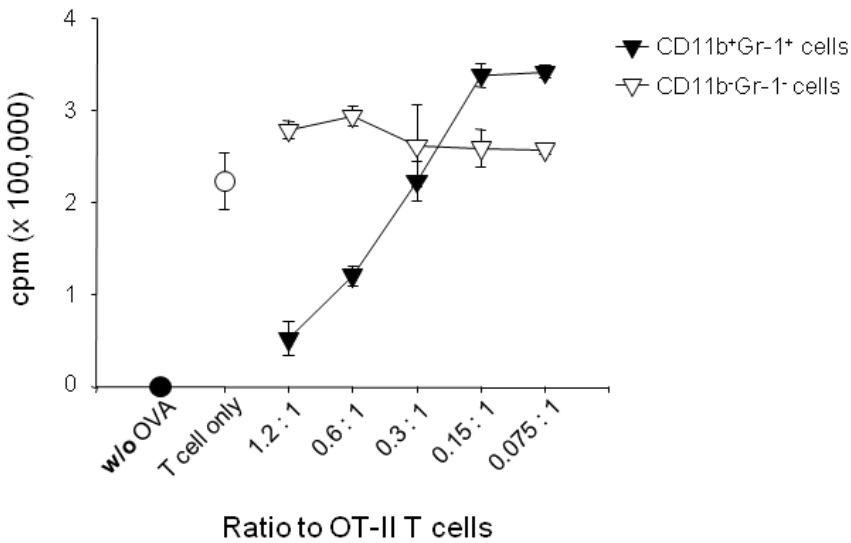

Figure 16. OVA-specific $CD4^+$ T cells from OT-II mice were stimulated with OVA-pulsed splenocytes and co-cultured for 3 days with serially diluted $Gr\text{-}1^+$ or $Gr\text{-}1^-$ cells isolated from RASV-administered $MyD88^{-/-}$ mice. Detection of [^{3}H]thymidine incorporation in divided cells. Data are representative of three independent experiments (n=4).

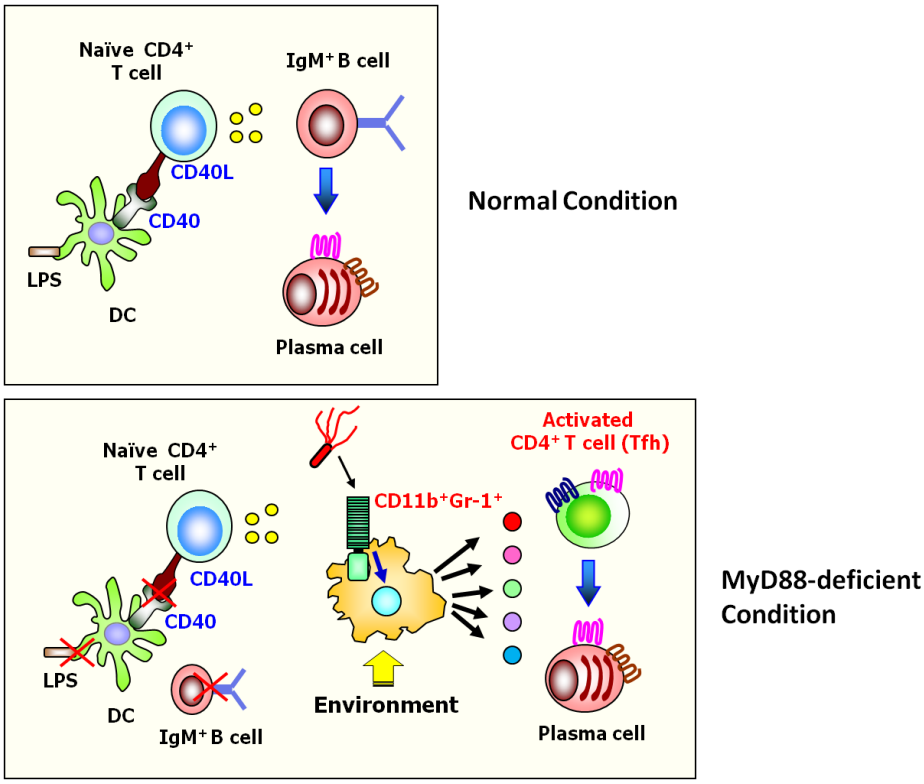

Figure 17. Graphic summary. In normal condition, various TLR ligands such as LPS activate dendritic cells (DC) by the infection of *salmonella*. The activated DC presenting *salmonella* antigens differentiates naïve $CD4^+$ T cells into effector T cells which help the B cell function. In contrast, DC activation may be reduced and normal T and B cell activation also decreases in MyD88-deficient condition. In $MyD88^{-/-}$ mice, chronic *salmonella* exposure causes accumulation of $CD11b^+Gr1^+$ myeloid cells which can produce IL-6. IL-6 rich environment related to the generation of Tfh. Increased Tfh cells activate B cells which produce antibodies including self-specific autoantibodies.

General discussion

In the overall study, the role of innate signals induced by IL-1 and MyD88 were examined in two different bacteria infection models. One was the pulmonary infection of pneumococcus and the other was the systemic infection of the attenuated *salmonella* strain which was administered orally. These two studies were focused on innate and adaptive immune responses, respectively. However, they could be combined in the IL-1R/TLR superfamily and bacterial infection.

The chapter I is entitled "IL-1 promotes coagulation which is necessary for protective immunity in the lung against *S. pneumoniae* infection". The coagulation was proposed as an innate immune response in the respiratory tract. IL-1 was discovered as a fever producer over 60 years ago [146]. The researches about IL-1 were considered as an old-fashioned subject because new cytokines were discovered continuously. However, IL-1 was given attention once again when the focus shifted to finding inflammasome which is important mechanism to produce the active form of IL-1β and IL-18. The study of IL-1 is complicated because it is a very initiative signal and links to various secondary responses. Bacterial proliferation was not controlled in IL-1 deficient condition. Some reports insisted that the recruitment of neutrophils was defective in IL-1R$^{-/-}$ mice. But others claimed the neutrophil trafficking was regulated by several signals and was able to be compensated by other signals [62, 70]. This argument might be influenced by time points after infection, methods to isolate and to count cells and stain of pathogens. In this study, several methods and various time points were employed to count recruited neutrophils in the low respiratory tract. CD11b^{+}Ly6C^{+}Ly6G^{+} neutrophils in the bronchial alveolar lavage fluid (BALF) migrated normally in IL-1R$^{-/-}$ mice at 1 day after the infection. At 3 day post-infection (dpi), more neutrophils were detected in IL-1R$^{-/-}$ mice because of more bacterial burden even though the possibility of the immune regulatory function of IL-1 was concerned. In

contrast, neutrophils were less detected within 1 dpi in the cytospin of BALF from IL-1R$^{-/-}$ mice than wild-type mice (data are not shown). Overall, IL-1 influences the recruitment of neutrophils for which other signals can compensate at early time after infection. IL-1 may impact on the maturation of neutrophils in the tissue to shape the characteristic morphology of nuclei segmentation.

Blood clotting was unexpectedly found as an immune system for pulmonary infection with bacteria. The participation of coagulation in bacterial pneumonia is a unique report in the immunology. Coagulation is highly conserved in vertebrate so that the animal and human might conduct the coagulation pathway for controlling bacterial proliferation although some pathogens also have the escaping properties from clotting for the virulency. In this study, exogenous fibrinogen was treated in vivo to recover the deficiency of IL-1R$^{-/-}$ mice. The treatment was obviously effective but the survival was delayed only one day. The reason of the insufficient rescue of IL-1R$^{-/-}$ mice is the reduced thrombin activity of IL-1R$^{-/-}$ mice. The providing of both active thrombin and fibrinogen can be more effective but the intratracheal administration in the C57BL/6 mice is difficult because of the small capacity of lung compared with BALB/c mice. In addition, the coagulation can occur between treated thrombin and fibrinogen without bacteria trapping. Therefore, the coagulation factors regulated by IL-1 signals in the upstream of thrombin should be identified to develop more efficient treatment for coagulation.

The bacteria killing mechanism of coagulation is not fully elucidated yet. The elevated level of fibrinogen in the lung after the infection is approximately one thousandth less than that of the fibrinogen in the blood. In addition, the clots were hardly observed in the histological study. However, the corelationship between coagulation pathway and bacterial propagation in the lung is evident based on the data in this study. Coagulation can be initiated in the pathogen-specific manner by binding to the surface of bacteria [49]. Coagulation pathway is also linked to complement pathway [99]. Moreover, neutrophils are involved in the activation of

coagulation [64]. Therefore, the complicated relation of coagulation pathway with other compartments manipulates the regulation of bacteria.

The chapter II is entitled “Expansion of Tfh-like cells during chronic *Salmonella* exposure mediates the generation of autoimmune hypergamma-globulinemia in MyD88-deficient mice”. The RASV-administered MyD88$^{-/-}$ mice demonstrated chronic salmonellosis and hypergammaglobulinemia. MyD88 molecule is markedly important to the innate signals. However, MyD88-independent innate signals also exist, for example, TRIF-dependent TLR3 signal. The induction of hyperIgG syndrome in MyD88$^{-/-}$ mice administered with RASV seems to be associated with chronic infection rather than MyD88-deficient signals. Since, MyD88$^{-/-}$ mice showed more severe inflammation than wild-type mice. Furthermore, there is a report in which the chronic infection of virus induces the differentiation of Tfh [131]. Hence, RASV-administered MyD88$^{-/-}$ mice are proposed as a chronic infection model of *salmonella* Typhimurium.

In this study, the detail mechanism for the generation of Tfh is not fully described. Several data support that the CD11b^{+}Gr1^{+} cells can be a candidate to differentiate Tfh cells. CD11b^{+}Gr1^{+} cells express MHC II, PD-L1 and ICOSL and secrete IL-6 after stimulation of *salmonella*. Also, these cells are located and contact with CD4^{+} T cells in the spleen. Several experiments to clarify the role of CD11b^{+}Gr-1^{+} cells are performed. CD11b^{+}Gr-1^{+} cells can induce the activation of the expression of ICOS in naïve CD4^{+} T cells and the proliferation of ICOS^{+}CD4^{+} T cells in antigen-specific manner in vitro (data are not shown). However, CD11b^{+}Gr-1^{+} cells are concerned with myeloid-derived suppressor cells (MDSC) in tumor and chronic infection models [147]. For assertion that CD11b^{+}Gr-1^{+} cells can act as antigen-presenting cells (APC) to produce Tfh cells, the suppressive function of CD11b^{+}Gr-1^{+} cells should be explained.

The role of innate signal in the pathogenic infection was studied. IL-1 encourages a coagulation pathway to restrict the multiplication of pneumococci in the low respiratory tract. The chronic salmonellosis in RASV-administered

MyD88-deficient condition generates the accumulation of Tfh cells in spleen. The increased Tfh cells modulate the production of autoantibody and the induction of hypergammaglobulinemia. Overall, the innate signals through IL-1 and MyD88 have not only a pivotal role in restraining bacteria but also in the induction of adaptive immune responses.

References

1. Hirst RA, Kadioglu A, O'Callaghan C, Andrew PW. The role of pneumolysin in pneumococcal pneumonia and meningitis. Clin Exp Immunol **2004**; 138:195-201.

2. Lanie JA, Ng WL, Kazmierczak KM, et al. Genome sequence of Avery's virulent serotype 2 strain D39 of Streptococcus pneumoniae and comparison with that of unencapsulated laboratory strain R6. J Bacteriol **2007**; 189:38-51.

3. Kadioglu A, Weiser JN, Paton JC, Andrew PW. The role of Streptococcus pneumoniae virulence factors in host respiratory colonization and disease. Nat Rev Microbiol **2008**; 6:288-301.

4. Bogaert D, De Groot R, Hermans PW. Streptococcus pneumoniae colonisation: the key to pneumococcal disease. Lancet Infect Dis **2004**; 4:144-54.

5. Dudley S, Ashe K, Winther B, Hendley JO. Bacterial pathogens of otitis media and sinusitis: detection in the nasopharynx with selective agar media. J Lab Clin Med **2001**; 138:338-42.

6. van der Poll T, Opal SM. Pathogenesis, treatment, and prevention of pneumococcal pneumonia. Lancet **2009**; 374:1543-56.

7. Mogensen TH, Paludan SR, Kilian M, Ostergaard L. Live Streptococcus pneumoniae, Haemophilus influenzae, and Neisseria meningitidis activate the inflammatory response through Toll-like receptors 2, 4, and 9 in species-specific patterns. J Leukoc Biol **2006**; 80:267-77.

8. Akira S, Uematsu S, Takeuchi O. Pathogen recognition and innate immunity. Cell **2006**; 124:783-801.

9. Dockrell DH, Marriott HM, Prince LR, et al. Alveolar macrophage apoptosis contributes to pneumococcal clearance in a resolving model of pulmonary infection. J Immunol **2003**; 171:5380-8.

10. Mizgerd JP, Meek BB, Kutkoski GJ, Bullard DC, Beaudet AL, Doerschuk CM. Selectins and neutrophil traffic: margination and Streptococcus pneumoniae-induced emigration in murine lungs. J Exp Med **1996**; 184:639-45.

11. Crump JA, Luby SP, Mintz ED. The global burden of typhoid fever. Bull World Health Organ **2004**; 82:346-53.

12. Halle S, Bumann D, Herbrand H, et al. Solitary intestinal lymphoid tissue provides a productive port of entry for *Salmonella enterica* serovar Typhimurium. Infect Immun **2007**; 75:1577-85.

13. Jones BD, Ghori N, Falkow S. Salmonella typhimurium initiates murine infection by penetrating and destroying the specialized epithelial M cells of the Peyer's patches. J Exp Med **1994**; 180:15-23.

14. Tam MA, Rydstrom A, Sundquist M, Wick MJ. Early cellular responses to Salmonella infection: dendritic cells, monocytes, and more. Immunol Rev **2008**; 225:140-62.

15. Fujimoto Y, Pradipta AR, Inohara N, Fukase K. Peptidoglycan as Nod1 ligand; fragment structures in the environment, chemical synthesis, and their innate immunostimulation. Nat Prod Rep **2012**; 29:568-79.

16. O'Neill LA, Greene C. Signal transduction pathways activated by the IL-1 receptor family: ancient signaling machinery in mammals, insects, and plants. J Leukoc Biol **1998**; 63:650-7.

17. Dunne A, O'Neill LA. The interleukin-1 receptor/Toll-like receptor superfamily: signal transduction during inflammation and host defense. Sci STKE **2003**; 2003:re3.

18. Brikos C, Wait R, Begum S, O'Neill LA, Saklatvala J. Mass spectrometric analysis of the endogenous type I interleukin-1 (IL-1) receptor signaling complex formed after IL-1 binding identifies IL-1RAcP, MyD88, and IRAK-4 as the stable components. Mol Cell Proteomics **2007**; 6:1551-9.

19. March CJ, Mosley B, Larsen A, et al. Cloning, sequence and expression of two distinct human interleukin-1 complementary DNAs. Nature **1985**; 315:641-7.

20. Eisenbarth SC, Colegio OR, O'Connor W, Sutterwala FS, Flavell RA. Crucial role for the Nalp3 inflammasome in the immunostimulatory properties of aluminium adjuvants. Nature **2008**; 453:1122-6.

21. Dinarello CA. Blocking IL-1 in systemic inflammation. J Exp Med **2005**; 201:1355-9.

22. Greenfeder SA, Nunes P, Kwee L, Labow M, Chizzonite RA, Ju G. Molecular cloning and characterization of a second subunit of the interleukin 1 receptor complex. J Biol Chem **1995**; 270:13757-65.

23. Sims JE. IL-1 and IL-18 receptors, and their extended family. Curr Opin Immunol **2002**; 14:117-22.

24. Dinarello CA. Immunological and inflammatory functions of the interleukin-1 family. Annu Rev Immunol **2009**; 27:519-50.

25. Lohning M, Stroehmann A, Coyle AJ, et al. T1/ST2 is preferentially expressed on murine Th2 cells, independent of interleukin 4, interleukin 5, and interleukin 10, and important for Th2 effector function. Proc Natl Acad Sci U S A **1998**; 95:6930-5.

26. Kobayashi M, Saitoh S, Tanimura N, et al. Regulatory roles for MD-2 and TLR4 in ligand-induced receptor clustering. J Immunol **2006**; 176:6211-8.

27. Sioud M. Innate sensing of self and non-self RNAs by Toll-like receptors. Trends Mol Med **2006**; 12:167-76.

28. Paul WE, Seder RA. Lymphocyte responses and cytokines. Cell **1994**; 76:241-51.

29. Szabo SJ, Sullivan BM, Peng SL, Glimcher LH. Molecular mechanisms regulating Th1 immune responses. Annu Rev Immunol **2003**; 21:713-58.

30. Zheng W, Flavell RA. The transcription factor GATA-3 is necessary and sufficient for Th2 cytokine gene expression in CD4 T cells. Cell **1997**; 89:587-96.

31. Fazilleau N, Mark L, McHeyzer-Williams LJ, McHeyzer-Williams MG. Follicular helper T cells: lineage and location. Immunity **2009**; 30:324-35.

32. Harrington LE, Hatton RD, Mangan PR, et al. Interleukin 17-producing $CD4^+$ effector T cells develop via a lineage distinct from the T helper type 1 and 2 lineages. Nat Immunol **2005**; 6:1123-32.

33. Ivanov, II, McKenzie BS, Zhou L, et al. The orphan nuclear receptor RORgammat directs the differentiation program of proinflammatory $IL\text{-}17^+$ T helper cells. Cell **2006**; 126:1121-33.

34. Yang XO, Pappu BP, Nurieva R, et al. T helper 17 lineage differentiation is programmed by orphan nuclear receptors ROR alpha and ROR gamma. Immunity **2008**; 28:29-39.

35. Zhou L, Lopes JE, Chong MM, et al. TGF-beta-induced Foxp3 inhibits T(H)17 cell differentiation by antagonizing RORgammat function. Nature **2008**; 453:236-40.

36. Zhu J, Paul WE. CD4 T cells: fates, functions, and faults. Blood **2008**; 112:1557-69.

37. Ansel KM, Ngo VN, Hyman PL, et al. A chemokine-driven positive feedback loop organizes lymphoid follicles. Nature **2000**; 406:309-14.

38. Zhou L, Ivanov, II, Spolski R, et al. IL-6 programs T(H)-17 cell differentiation by promoting sequential engagement of the IL-21 and IL-23 pathways. Nat Immunol **2007**; 8:967-74.

39. Nurieva RI, Chung Y, Hwang D, et al. Generation of T follicular helper cells is mediated by interleukin-21 but independent of T helper 1, 2, or 17 cell lineages. Immunity **2008**; 29:138-49.

40. Vogelzang A, McGuire HM, Yu D, Sprent J, Mackay CR, King C. A fundamental role for interleukin-21 in the generation of T follicular helper cells. Immunity **2008**; 29:127-37.

41. Chtanova T, Tangye SG, Newton R, et al. T follicular helper cells express a distinctive transcriptional profile, reflecting their role as non-Th1/Th2 effector cells that provide help for B cells. J Immunol **2004**; 173:68-78.

42. Bauquet AT, Jin H, Paterson AM, et al. The costimulatory molecule ICOS regulates the expression of c-Maf and IL-21 in the development of follicular T helper cells and TH-17 cells. Nat Immunol **2009**; 10:167-75.

43. Good-Jacobson KL, Szumilas CG, Chen L, Sharpe AH, Tomayko MM, Shlomchik MJ. PD-1 regulates germinal center B cell survival and the formation and affinity of long-lived plasma cells. Nat Immunol **2010**; 11:535-42.

44. Kim MY, Gaspal FM, Wiggett HE, et al. $CD4^{+}CD3^{-}$ accessory cells costimulate primed CD4 T cells through OX40 and CD30 at sites where T cells collaborate with B cells. Immunity **2003**; 18:643-54.

45. Rasheed AU, Rahn HP, Sallusto F, Lipp M, Muller G. Follicular B helper T cell activity is confined to $CXCR5^{hi}ICOS^{hi}$ CD4 T cells and is independent of CD57 expression. Eur J Immunol **2006**; 36:1892-903.

46. Arnold CN, Campbell DJ, Lipp M, Butcher EC. The germinal center response is impaired in the absence of T cell-expressed CXCR5. Eur J Immunol **2007**; 37:100-9.

47. Qi H, Cannons JL, Klauschen F, Schwartzberg PL, Germain RN. SAP-controlled T-B cell interactions underlie germinal centre formation. Nature **2008**; 455:764-9.

48. Sun H. The interaction between pathogens and the host coagulation system. Physiology (Bethesda) **2006**; 21:281-8.

49. Loof TG, Morgelin M, Johansson L, et al. Coagulation, an ancestral serine protease cascade, exerts a novel function in early immune defense. Blood **2011**; 118:2589-98.

50. Flick MJ, Du X, Witte DP, et al. Leukocyte engagement of fibrin(ogen) via the integrin receptor alphaMbeta2/Mac-1 is critical for host inflammatory response in vivo. J Clin Invest **2004**; 113:1596-606.

51. Herwald H, Cramer H, Morgelin M, et al. M protein, a classical bacterial virulence determinant, forms complexes with fibrinogen that induce vascular leakage. Cell **2004**; 116:367-79.

52. Nowicki ST, Minning-Wenz D, Johnston KH, Lottenberg R. Characterization of a novel streptokinase produced by Streptococcus equisimilis of non-human origin. Thromb Haemost **1994**; 72:595-603.

53. Schroeder B, Boyle MD, Sheerin BR, Asbury AC, Lottenberg R. Species specificity of plasminogen activation and acquisition of surface-associated proteolytic activity by group C streptococci grown in plasma. Infect Immun **1999**; 67:6487-95.

54. Ringdahl U, Svensson HG, Kotarsky H, Gustafsson M, Weineisen M, Sjobring U. A role for the fibrinogen-binding regions of streptococcal M proteins in phagocytosis resistance. Mol Microbiol **2000**; 37:1318-26.

55. Esmon CT, Mather T. Switching serine protease specificity. Nat Struct Biol **1998**; 5:933-7.

56. Lahteenmaki K, Westerlund B, Kuusela P, Korhonen TK. Immobilization of plasminogen on Escherichia coli flagella. FEMS Microbiol Lett **1993**; 106:309-14.

57. Hollingshead SK, Briles DE. Streptococcus pneumoniae: new tools for an old pathogen. Curr Opin Microbiol **2001**; 4:71-7.

58. O'Brien KL, Walters MI, Sellman J, et al. Severe pneumococcal pneumonia in previously healthy children: the role of preceding influenza infection. Clin Infect Dis **2000**; 30:784-9.

59. Morens DM, Taubenberger JK, Harvey HA, Memoli MJ. The 1918 influenza pandemic: lessons for 2009 and the future. Crit Care Med **2010**; 38:e10-20.

60. McCullers JA. Effect of antiviral treatment on the outcome of secondary bacterial pneumonia after influenza. J Infect Dis **2004**; 190:519-26.

61. Malley R, Henneke P, Morse SC, et al. Recognition of pneumolysin by Toll-like receptor 4 confers resistance to pneumococcal infection. Proc Natl Acad Sci USA **2003**; 100:1966-71.

62. Jones MR, Simms BT, Lupa MM, Kogan MS, Mizgerd JP. Lung NF-kappaB activation and neutrophil recruitment require IL-1 and TNF receptor signaling during pneumococcal pneumonia. J Immunol **2005**; 175:7530-5.

63. Tennent GA, Brennan SO, Stangou AJ, O'Grady J, Hawkins PN, Pepys MB. Human plasma fibrinogen is synthesized in the liver. Blood **2007**; 109:1971-4.

64. Massberg S, Grahl L, von Bruehl ML, et al. Reciprocal coupling of coagulation and innate immunity via neutrophil serine proteases. Nat Med **2010**; 16:887-96.

65. Park SM, Ko HJ, Shim DH, et al. MyD88 signaling is not essential for induction of antigen-specific B cell responses but is indispensable for protection against Streptococcus pneumoniae infection following oral vaccination with attenuated Salmonella expressing PspA antigen. J Immunol **2008**; 181:6447-55.

66. Hava DL, Camilli A. Large-scale identification of serotype 4 Streptococcus pneumoniae virulence factors. Mol Microbiol **2002**; 45:1389-406.

67. Seo SU, Kwon HJ, Ko HJ, et al. Type I interferon signaling regulates Ly6C^{hi} monocytes and neutrophils during acute viral pneumonia in mice. PLoS Pathog **2011**; 7:e1001304.

68. Shim DH, Chang SY, Park SM, et al. Immunogenicity and protective efficacy offered by a ribosomal-based vaccine from Shigella flexneri 2a. Vaccine **2007**; 25:4828-36.

69. Hsu LC, Enzler T, Seita J, et al. IL-1beta-driven neutrophilia preserves antibacterial defense in the absence of the kinase IKKbeta. Nat Immunol **2011**; 12:144-50.

70. Mijares LA, Wangdi T, Sokol C, Homer R, Medzhitov R, Kazmierczak BI. Airway epithelial MyD88 restores control of Pseudomonas aeruginosa murine infection via an IL-1-dependent pathway. J Immunol **2011**; 186:7080-8.

71. Ray CA, Lasbury ME, Durant PJ, et al. Transforming growth factor-beta activation and signaling in the alveolar environment during Pneumocystis pneumonia. J Eukaryot Microbiol **2006**; 53 Suppl 1:S127-9.

72. Mahavadi P, Korfei M, Henneke I, et al. Epithelial stress and apoptosis underlie Hermansky-Pudlak syndrome-associated interstitial pneumonia. Am J Respir Crit Care Med **2010**; 182:207-19.

73. Marriott HM, Dockrell DH. Streptococcus pneumoniae: the role of apoptosis in host defense and pathogenesis. Int J Biochem Cell Biol **2006**; 38:1848-54.

74. Duan HO, Simpson-Haidaris PJ. Cell type-specific differential induction of the human gamma-fibrinogen promoter by interleukin-6. J Biol Chem **2006**; 281:12451-7.

75. Yamamoto M, Yamazaki S, Uematsu S, et al. Regulation of Toll/IL-1-receptor-mediated gene expression by the inducible nuclear protein IkappaBzeta. Nature **2004**; 430:218-22.

76. Duan HO, Simpson-Haidaris PJ. Functional analysis of interleukin 6 response elements (IL-6REs) on the human gamma-fibrinogen promoter: binding of hepatic Stat3 correlates negatively with transactivation potential of type II IL-6REs. J Biol Chem **2003**; 278:41270-81.

77. Lin L, Amin R, Gallicano GI, et al. The STAT3 inhibitor NSC 74859 is effective in hepatocellular cancers with disrupted TGF-beta signaling. Oncogene **2009**; 28:961-72.

78. Fong Y, Lowry SF. Tumor necrosis factor in the pathophysiology of infection and sepsis. Clin Immunol Immunopathol **1990**; 55:157-70.

79. Calbo E, Garau J. Of mice and men: innate immunity in pneumococcal pneumonia. Int J Antimicrob Agents **2010**; 35:107-13.

80. Bergeron Y, Ouellet N, Deslauriers AM, Simard M, Olivier M, Bergeron MG. Cytokine kinetics and other host factors in response to pneumococcal pulmonary infection in mice. Infect Immun **1998**; 66:912-22.

81. O'Neill LA. The interleukin-1 receptor/Toll-like receptor superfamily: 10 years of progress. Immunol Rev **2008**; 226:10-8.

82. Zwijnenburg PJ, van der Poll T, Florquin S, Roord JJ, Van Furth AM. IL-1 receptor type 1 gene-deficient mice demonstrate an impaired host defense against pneumococcal meningitis. J Immunol **2003**; 170:4724-30.

83. Kafka D, Ling E, Feldman G, et al. Contribution of IL-1 to resistance to Streptococcus pneumoniae infection. Int Immunol **2008**; 20:1139-46.

84. Mayer-Barber KD, Barber DL, Shenderov K, et al. Caspase-1 independent IL-1beta production is critical for host resistance to mycobacterium tuberculosis and does not require TLR signaling in vivo. J Immunol **2010**; 184:3326-30.

85. He X, Mekasha S, Mavrogiorgos N, Fitzgerald KA, Lien E, Ingalls RR. Inflammation and fibrosis during Chlamydia pneumoniae infection is regulated by IL-1 and the NLRP3/ASC inflammasome. J Immunol **2010**; 184:5743-54.

86. Brinkmann V, Reichard U, Goosmann C, et al. Neutrophil extracellular traps kill bacteria. Science **2004**; 303:1532-5.

87. Mednick AJ, Feldmesser M, Rivera J, Casadevall A. Neutropenia alters lung cytokine production in mice and reduces their susceptibility to pulmonary cryptococcosis. Eur J Immunol **2003**; 33:1744-53.

88. Herbold W, Maus R, Hahn I, et al. Importance of CXC chemokine receptor 2 in alveolar neutrophil and exudate macrophage recruitment in response to pneumococcal lung infection. Infect Immun **2010**; 78:2620-30.

89. Stokes CA, Ismail S, Dick EP, et al. Role of interleukin-1 and MyD88-dependent signaling in rhinovirus infection. J Virol **2011**; 85:7912-21.

90. Wajant H, Scheurich P. TNFR1-induced activation of the classical NF-kappaB pathway. FEBS J **2011**; 278:862-76.

91. Rijneveld AW, Florquin S, Branger J, Speelman P, Van Deventer SJ, van der Poll T. TNF-alpha compensates for the impaired host defense of IL-1 type I receptor-deficient mice during pneumococcal pneumonia. J Immunol **2001**; 167:5240-6.

92. Doolittle RF. Fibrinogen and fibrin. Annu Rev Biochem **1984**; 53:195-229.

93. Vasse M, Paysant J, Soria J, Collet JP, Vannier JP, Soria C. Regulation of fibrinogen biosynthesis by cytokines, consequences on the vascular risk. Haemostasis **1996**; 26 Suppl 4:331-9.

94. Haidaris PJ. Induction of fibrinogen biosynthesis and secretion from cultured pulmonary epithelial cells. Blood **1997**; 89:873-82.

95. Simpson-Haidaris PJ, Courtney MA, Wright TW, Goss R, Harmsen A, Gigliotti F. Induction of fibrinogen expression in the lung epithelium during Pneumocystis carinii pneumonia. Infect Immun **1998**; 66:4431-9.

96. Bode JG, Albrecht U, Haussinger D, Heinrich PC, Schaper F. Hepatic acute phase proteins--regulation by IL-6- and IL-1-type cytokines involving STAT3 and its crosstalk with NF-kappaB-dependent signaling. Eur J Cell Biol **2012**; 91:496-505.

97. Skovgaard K, Mortensen S, Boye M, Hedegaard J, Heegaard PM. Hepatic gene expression changes in pigs experimentally infected with the lung pathogen Actinobacillus pleuropneumoniae as analysed with an innate immunity focused microarray. Innate Immun **2010**; 16:343-53.

98. Duan J, Chung H, Troy E, Kasper DL. Microbial colonization drives expansion of IL-1 receptor 1-expressing and IL-17-producing gamma/delta T cells. Cell Host Microbe **2010**; 7:140-50.

99. Amara U, Rittirsch D, Flierl M, et al. Interaction between the coagulation and complement system. Adv Exp Med Biol **2008**; 632:71-9.

100. McAdow M, Kim HK, Dedent AC, Hendrickx AP, Schneewind O, Missiakas DM. Preventing Staphylococcus aureus sepsis through the inhibition of its agglutination in blood. PLoS Pathog **2011**; 7:e1002307.

101. Mullarky IK, Szaba FM, Berggren KN, et al. Infection-stimulated fibrin deposition controls hemorrhage and limits hepatic bacterial growth during listeriosis. Infect Immun **2005**; 73:3888-95.

102. Johnson LL, Berggren KN, Szaba FM, Chen W, Smiley ST. Fibrin-mediated protection against infection-stimulated immunopathology. J Exp Med **2003**; 197:801-6.

103. Jansen PM, Boermeester MA, Fischer E, et al. Contribution of interleukin-1 to activation of coagulation and fibrinolysis, neutrophil degranulation, and the release of secretory-type phospholipase A2 in sepsis: studies in nonhuman primates after

interleukin-1 alpha administration and during lethal bacteremia. Blood **1995**; 86:1027-34.

104. Henderson C, Goldbach-Mansky R. Monogenic IL-1 mediated autoinflammatory and immunodeficiency syndromes: finding the right balance in response to danger signals. Clin Immunol **2010**; 135:210-22.

105. Soulas P, Woods A, Jaulhac B, et al. Autoantigen, innate immunity, and T cells cooperate to break B cell tolerance during bacterial infection. J Clin Invest **2005**; 115:2257-67.

106. Bach JF. The effect of infections on susceptibility to autoimmune and allergic diseases. N Engl J Med **2002**; 347:911-20.

107. Hunziker L, Recher M, Macpherson AJ, et al. Hypergammaglobulinemia and autoantibody induction mechanisms in viral infections. Nat Immunol **2003**; 4:343-9.

108. Groom JR, Fletcher CA, Walters SN, et al. BAFF and MyD88 signals promote a lupuslike disease independent of T cells. J Exp Med **2007**; 204:1959-71.

109. Herlands RA, Christensen SR, Sweet RA, Hershberg U, Shlomchik MJ. T cell-independent and toll-like receptor-dependent antigen-driven activation of autoreactive B cells. Immunity **2008**; 29:249-60.

110. Woods A, Soulas-Sprauel P, Jaulhac B, et al. MyD88 negatively controls hypergammaglobulinemia with autoantibody production during bacterial infection. Infect Immun **2008**; 76:1657-67.

111. Vinuesa CG, Tangye SG, Moser B, Mackay CR. Follicular B helper T cells in antibody responses and autoimmunity. Nat Rev Immunol **2005**; 5:853-65.

112. Liu YJ, Joshua DE, Williams GT, Smith CA, Gordon J, MacLennan IC. Mechanism of antigen-driven selection in germinal centres. Nature **1989**; 342:929-31.

113. Crotty S. Follicular Helper CD4 T Cells (T(FH)). Annu Rev Immunol **2011**; 29:621-63.

114. Branger CG, Fetherston JD, Perry RD, Curtiss R, 3rd. Oral vaccination with different antigens from Yersinia pestis KIM delivered by live attenuated

Salmonella typhimurium elicits a protective immune response against plague. Adv Exp Med Biol **2007**; 603:387-99.

115. Ko HJ, Yang JY, Shim DH, et al. Innate immunity mediated by MyD88 signal is not essential for induction of lipopolysaccharide-specific B cell responses but is indispensable for protection against *Salmonella enterica* serovar *Typhimurium* infection. J Immunol **2009**; 182:2305-12.

116. Mackay F, Woodcock SA, Lawton P, et al. Mice transgenic for BAFF develop lymphocytic disorders along with autoimmune manifestations. J Exp Med **1999**; 190:1697-710.

117. Cimmino L, Martins GA, Liao J, et al. Blimp-1 attenuates Th1 differentiation by repression of ifng, tbx21, and bcl6 gene expression. J Immunol **2008**; 181:2338-47.

118. Reinhardt RL, Liang HE, Locksley RM. Cytokine-secreting follicular T cells shape the antibody repertoire. Nat Immunol **2009**; 10:385-93.

119. Cunningham AF, Gaspal F, Serre K, et al. Salmonella induces a switched antibody response without germinal centers that impedes the extracellular spread of infection. J Immunol **2007**; 178:6200-7.

120. Linterman MA, Beaton L, Yu D, et al. IL-21 acts directly on B cells to regulate Bcl-6 expression and germinal center responses. J Exp Med **2010**; 207:353-63.

121. Zotos D, Coquet JM, Zhang Y, et al. IL-21 regulates germinal center B cell differentiation and proliferation through a B cell-intrinsic mechanism. J Exp Med **2010**; 207:365-78.

122. Guay HM, Andreyeva TA, Garcea RL, Welsh RM, Szomolanyi-Tsuda E. MyD88 is required for the formation of long-term humoral immunity to virus infection. J Immunol **2007**; 178:5124-31.

123. Odegard JM, Marks BR, DiPlacido LD, et al. ICOS-dependent extrafollicular helper T cells elicit IgG production via IL-21 in systemic autoimmunity. J Exp Med **2008**; 205:2873-86.

124. Bentebibel SE, Schmitt N, Banchereau J, Ueno H. Human tonsil B-cell lymphoma 6 (BCL6)-expressing $CD4^+$ T-cell subset specialized for B-cell help outside germinal centers. Proc Natl Acad Sci USA **2011**; 108:E488-97.

125. Morales JK, Kmieciak M, Knutson KL, Bear HD, Manjili MH. GM-CSF is one of the main breast tumor-derived soluble factors involved in the differentiation of $CD11b^-Gr1^-$ bone marrow progenitor cells into myeloid-derived suppressor cells. Breast Cancer Res Treat **2010**; 123:39-49.

126. Dunay IR, Damatta RA, Fux B, et al. $Gr1^+$ inflammatory monocytes are required for mucosal resistance to the pathogen Toxoplasma gondii. Immunity **2008**; 29:306-17.

127. Kaisho T, Hoshino K, Iwabe T, Takeuchi O, Yasui T, Akira S. Endotoxin can induce MyD88-deficient dendritic cells to support Th2 cell differentiation. Int Immunol **2002**; 14:695-700.

128. Sun J, Walsh M, Villarino AV, et al. TLR ligands can activate dendritic cells to provide a MyD88-dependent negative signal for Th2 cell development. J Immunol **2005**; 174:742-51.

129. Delano MJ, Scumpia PO, Weinstein JS, et al. MyD88-dependent expansion of an immature $GR\text{-}1^+CD11b^+$ population induces T cell suppression and Th2 polarization in sepsis. J Exp Med **2007**; 204:1463-74.

130. Bessa J, Kopf M, Bachmann MF. Cutting edge: IL-21 and TLR signaling regulate germinal center responses in a B cell-intrinsic manner. J Immunol **2010**; 184:4615-9.

131. Fahey LM, Wilson EB, Elsaesser H, Fistonich CD, McGavern DB, Brooks DG. Viral persistence redirects CD4 T cell differentiation toward T follicular helper cells. J Exp Med **2011**; 208:987-99.

132. King C, Tangye SG, Mackay CR. T follicular helper (TFH) cells in normal and dysregulated immune responses. Annu Rev Immunol **2008**; 26:741-66.

133. McAdam AJ, Greenwald RJ, Levin MA, et al. ICOS is critical for CD40-mediated antibody class switching. Nature **2001**; 409:102-5.

134. Yu D, Tan AH, Hu X, et al. Roquin represses autoimmunity by limiting inducible T-cell co-stimulator messenger RNA. Nature **2007**; 450:299-303.

135. Platt AM, Gibson VB, Patakas A, et al. Abatacept limits breach of self-tolerance in a murine model of arthritis via effects on the generation of T follicular helper cells. J Immunol **2010**; 185:1558-67.

136. Akiba H, Takeda K, Kojima Y, et al. The role of ICOS in the $CXCR5^+$ follicular B helper T cell maintenance in vivo. J Immunol **2005**; 175:2340-8.

137. Barber DL, Wherry EJ, Masopust D, et al. Restoring function in exhausted CD8 T cells during chronic viral infection. Nature **2006**; 439:682-7.

138. Hams E, McCarron MJ, Amu S, et al. Blockade of b7-h1 (programmed death ligand 1) enhances humoral immunity by positively regulating the generation of T follicular helper cells. J Immunol **2011**; 186:5648-55.

139. Kremer JM, Westhovens R, Leon M, et al. Treatment of rheumatoid arthritis by selective inhibition of T-cell activation with fusion protein CTLA4Ig. N Engl J Med **2003**; 349:1907-15.

140. Dienz O, Eaton SM, Bond JP, et al. The induction of antibody production by IL-6 is indirectly mediated by IL-21 produced by $CD4^+$ T cells. J Exp Med **2009**; 206:69-78.

141. Poholek AC, Hansen K, Hernandez SG, et al. In vivo regulation of Bcl6 and T follicular helper cell development. J Immunol **2010**; 185:313-26.

142. Heithoff DM, Enioutina EY, Bareyan D, Daynes RA, Mahan MJ. Conditions that diminish myeloid-derived suppressor cell activities stimulate cross-protective immunity. Infect Immun **2008**; 76:5191-9.

143. Johansson C, Ingman M, Jo Wick M. Elevated neutrophil, macrophage and dendritic cell numbers characterize immune cell populations in mice chronically infected with Salmonella. Microb Pathog **2006**; 41:49-58.

144. Pelletier N, McHeyzer-Williams LJ, Wong KA, Urich E, Fazilleau N, McHeyzer-Williams MG. Plasma cells negatively regulate the follicular helper T cell program. Nat Immunol **2010**; 11:1110-8.

145. McHeyzer-Williams LJ, Pelletier N, Mark L, Fazilleau N, McHeyzer-Williams MG. Follicular helper T cells as cognate regulators of B cell immunity. Curr Opin Immunol **2009**; 21:266-73.

146. Dinarello CA, Cannon JG, Wolff SM, et al. Tumor necrosis factor (cachectin) is an endogenous pyrogen and induces production of interleukin 1. J Exp Med **1986**; 163:1433-50.

147. Gabrilovich DI, Nagaraj S. Myeloid-derived suppressor cells as regulators of the immune system. Nat Rev Immunol **2009**; 9:162-74.

병원성 세균 감염 시 방어면역을 위한 IL-1과 MyD88 신호의 역할

국문 초록

서울대학교 대학원

수의학과 해부세포생물학 전공

양형준

(지도교수: 성제경)

모든 생명체는 다양한 병원균의 침입에 대한 방어기제로 면역체계를 가지고 있다. 이 면역체계를 발동시키기 위해서는 먼저 개체 자신과 구별하여 병원체들만이 특이적으로 가지고 있는 분자 패턴을 인지하기 위한 수용체들이 필요하다. 이러한 수용체들 중 대표적인 것으로 인터류킨 1 수용체/ 톨유사 수용체 슈퍼패밀리가 있다. 이 수용체들은 다양한 병원균들의 감염에 대해 면역반응을 유도하는 초기 신호체계이다. 본 연구에서는 병원성 세균의 감염에 있어서 개체가 가진 선천성 면역 신호들의 역할을 규명하고자 한다.

본 논문의 첫번째 부분에서는, 세균감염시 TNF-α와 함께 선천성 면역반응을 유도하는 것으로 잘 알려진 인터류킨 1 (IL-1)에 대해 연구하였다. IL-1 은 알려진 시간에 비해 호흡기 감염에 있어서 그 기작이

충분히 밝혀지지 않았다. 따라서 본 연구에서는 마우스 모델에서 폐렴균 (*Streptococcus pneumoniae*) 감염시 인터류킨 1 의 신호가 어떻게 개체의 방어기제에 작용하는 지를 연구하였다. 인터류킨 1 수용체 결손 마우스 ($IL-1R^{-/-}$)는 폐렴균의 감염시 높은 사망률을 보이며, 동시에 폐부에서 대량의 사이토카인의 분비와 침습물이 관찰된다. 또한 인터류킨 1 의 신호가 결손되었을때 폐부에서 세균의 분열이 억제되지 않는 것이 관찰되었다. 하지만 이러한 세균의 확산이 억제되지 않는 것이 $CD11b^{+}Ly6C^{+}Ly6G^{+}$ 한 호중구의 유입이나 살균작용이 정상인 마우스보다 결핍되어 일어나는 현상은 아니었다. 놀랍게도 폐렴균 감염시 인터류킨 1 수용체 결손마우스에서 정상 마우스에서는 감염후 증가하는 피브리노겐 알파와 감마의 전사가 저하되어 있는 것을 발견하였다. 피브리노겐은 혈액응고의 중요한 인자로서 피브리노겐의 합성이 인터류킨 1, 인터류킨 6, Stat 3 의 신호전달 체계에 의존적이라는 결과를 얻었다. 또한 인터류킨 1 수용체 결손마우스에서 피브리노겐을 투여하였을때 생존율과 세균의 증식이 억제되었고, 정상 마우스에서 혈액응고를 억제하는 약물을 투여하였을 때에 폐렴균 감염에 대한 감수성이 증가하는 것을 확인하였다. 이러한 결과를 토대로 인터류킨 1 의 신호가 폐렴균 감염시 폐조직 내에서 혈액응고에 관여하는 피브리노겐의 합성을 증가시키고 이를 통해서 폐렴균의 증식을 억제할 수 있다는 결론을 도출하였다.

본 논문의 두번째 부분으로, 만성 살모넬라균 감염시 Myeloid Differentiation factor 88 (MyD88)에 의존적인 톨유사 수용체의 신호가 B 세포 반응의 생성에 어떠한 역할을 하는 지에 관해 연구하였다. MyD88 결손 마우스에 약독화한 살모넬라 백신균주 (Recombinant attenuated *Salmonella* Typhimurium vaccine; RASV)를 구강투여하였을 때에 감염의 만성화가 나타났다. 그 결과로 germinal

center 가 증가하고, 혈액 내에 항 이중나선 DNA 에 특이적인 항체를 포함하는 고감마글로불린혈증이 관찰되었다. 또한 자가면역질환의 특징으로 나타나는 신장에 면역복합체의 침착이 관찰되었다. 만성 감염화된 마우스에서는 PD-1, CXCR5, ICOS, IL-21 을 발현하는 CD4 양성인 T 세포가 특히 증가하였고, 이러한 T 세포의 증식은 Follicular helper T (Tfh)와 유사한 특징을 가지고 있다. T 세포를 결핍시켰을때에는 혈액 내에 다클론성 항체의 생성이 완전히 억제되었다. RASV 를 구강투여한 MyD88 결손 마우스의 또 다른 특징으로는 비장에서 많은 양의 CD11b 와 Gr-1 을 발현하는 염증성 골수세포가 축적되었음을 관찰하였다. 흥미롭게도 PD-1 이나 ICOS 의 신호를 방해하였을때에 고감마글로불린혈증과 항이중나선 DNA 에 대한 항체가 감소하였음을 확인하였다. 따라서 만성 살모넬라균의 감염시 PD-1 과 ICOS 에 의존적으로 Tfh 유사 세포의 작용에 의해 자가면역성의 고감마글로불린혈증이 나타나는 것으로 결론지을 수 있다.

주요어: 인터류킨 1, 페렴균, 페렴, 선천면역, 혈액응고, MyD88, 살모넬라, Tfh, 적응면역, 만성감염, 자가항체, 고감마글로불린혈증

학번: 2010 - 30458